The Fiber Society

Annual Fall Technical Meeting

October 16-18, 2002

Natick Crowne Plaza Hotel
Natick, Massachusetts

Conference Chairs
Heidi Schreuder-Gibson and Phil Gibson
U.S. Army Soldier Systems Center
Natick, Massachusetts

Book of Abstracts - Presentations

Organized by:
U.S. Army Soldier Systems Center

Sponsored by:
U.S. Army Soldier Systems Center
Albany International

the fiber society
for the advancement of scientific knowledge
pertaining to fibers, fiber products, and fibrous materials.

Functionalized Nanofibers by Electrospinning

Andreas Greiner
Philipps-Universität Marburg, FB Chemie, Institut für Physikalische Chemie, Kernchemie und Makromolekulare Chemie, Hans-Meerwein-Str., D-35032 Marburg, Germany

The preparation and design of fibers with average fiber diameters in the nanometer range gain considerable attention for academic as well as commercial purposes. Major driving forces are promising perspectives for new materials for a broad range of applications in electronics, optics, medicine, sensors, controlled release technology, and for bionic design, just to name a few. Nanoshaped fibers are available by electrospinning technique, which is based on fiber spinning from polymer melts or solutions in an electrical field. A wide variety of polymers can be processed by electrospinning. However, the shape of the fibers obtained by electrospinning is controlled by numerous parameters including polymer related parameters (glass transition temperature, molecular weight, molecular weight distribution, crystallinity, solubility), solution/melt related parameters (vapor pressure of solvent, solution/melt viscosity, conductivity, surface tension, phase diagram of polymer/solvent), and apparatus related parameters (electrical field, electrode design, gap between electrodes, charge of substrate, velocity of solution/melt). In view of these numerous parameters it is obvious control of fiber shape is mostly based on empirical results. Consequently, systematic testing of various spinning parameters, which will addressed in our contribution, is still of major importance for progress in the field of electrospinning of polymers.

Another important aspect for progress of electrospinning is functionalization of electrospun fibers. We will present in our contribution the functionalization of electrospun fibers by various techniques including cospinnning with various reactive and unreactive compounds for modification of fiber properties as well as postprocessing coating of electrospun by various materials.

In view of potential applications of electrospun fibers we will present the usage of electrospun fibers as templates for the preparation of novel nanotubes following the so-called TUFT-process (tubes by fiber templates)[1-3]. TUFT-polymer and polymer/metal nanotubes will be presented with inner diameters < 10 nm and outer diameters in the range of 40 – 200 nm, which is clearly in the range of multi-walled carbon nanotubes. This breakthrough in the preparation of polymer-based nanotubes by the TUFT-process opens the field for a completely new class of materials based on accomplishments in electrospun polymer template fibers.

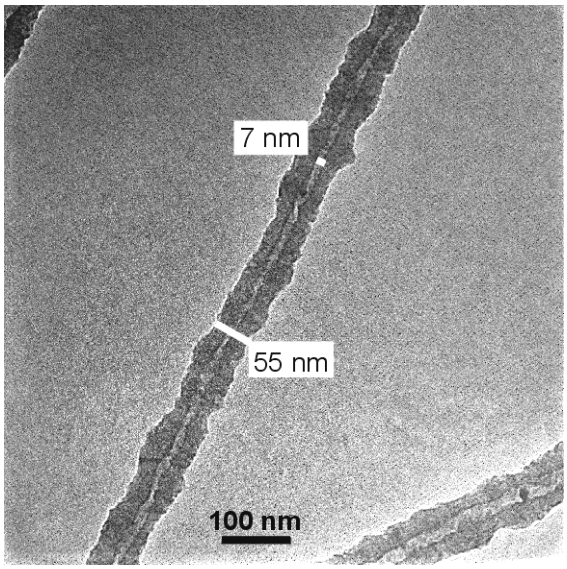

A

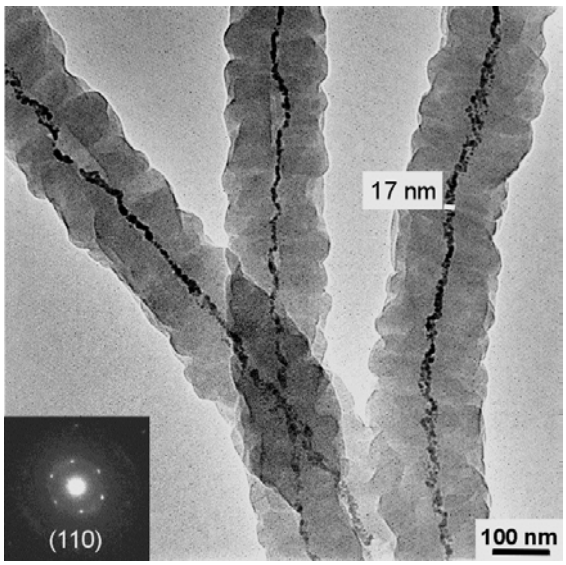

B

Figure 1. Poly(p-xylyene) (PPX) TUFT-nanotubes obtained by coating of electrospun poly-L-lactide (PLA) nanofibers and subsequent removal of PLA template fibers (A); PPX/Pd TUFT nanotubes obtained by coating of electrospun PLA/$Pd(OAc)_2$ followed by pyrolysis of PLA fibers and conversion of $Pd(OAc)_2$ to Pd.

Acknowledgements: Financial support by DFG, BMBF, Stiftung des Deutschen Volkes, and Creavis is kindly acknowledged.

1) M. Bognitzki, H. Hou, M. Ishaque, T. Frese, M. Hellwig, C. Schwarte, A. Schaper, J.. H. Wendorff, A. Greiner, Adv. Mater. **12**, 637 (2000)

2) R. A. Caruso, J. H. Schattka, A. Greiner, Adv. Mat. **13**, 1577 (2001)

3) H. Hou, Jun Zeng, A. Schaper, J. H. Wendorff, A. Greiner, Macromolecules **35**, 2429 (2002).

Numerical Modeling of an Electrostatically Driven Liquid Meniscus in the Cone-jet Mode

Bakhtier Farouk, Fang Yan, and Frank Ko*
Department of Mechanical Engineering and Mechanics,* Department of Materials Engineering, Drexel University, Philadelphia, PA 19104

When a conducting liquid is supplied to a capillary nozzle at a low flow rate and when the interface between air and the liquid is charged to a sufficiently high electrical potential, the liquid meniscus takes the form of a stable cone, whose apex emits a microscopic jet. In the present paper, we describe an axisymmetric formulation of the flow and electric fields of the electrostatically driven meniscus through a capillary nozzle. Based on the governing equations, a numerical model has been developed to calculate the shape of the liquid cone and the resulting jet, the electric fields, and the surface charge density along the liquid surface. The liquid properties, liquid flow rate and electrode configuration are needed as input parameters. Two-dimensional axi-symmetric equations of continuity, momentum and Gauss' law are solved numerically. The simulation results are compared with experimental data.

The configuration for an electrostatically driven meniscus is depicted in Figure 1. A dielectric liquid with electrical conductivity K and permittivity β is issuing in the form of a steady capillary jet from an injection nozzle of length L and diameter d_{nozzle}. A high voltage Φ_0 is applied on the top electrode and the nozzle so that an external electric field is formed between the nozzle and the ground along the jet direction. The liquid flow rate Q is an input parameter to the model. Other physically relevant parameters of the problem are the liquid-gas surface tension γ, liquid density ρ, and liquid viscosity μ. As a result of the electric charge carried by the jet, there will be a net electric current I flowing from the injecting nozzle towards the ground. There are two possibilities depending on the flow rate and the strength of the electrostatic field: (i) the jet is continuous and strikes the ground before breaking up into droplets (ii) the jet breaks up into charged droplets which travel towards the ground under the external electrostatic field force. In the present paper, only the first situation (the cone-jet mode) is considered.

The model is able to calculate the shape of the liquid cone and the resulting jet, the velocity fields inside the liquid cone-jet, the electric fields in and outside the cone-jet, and the surface charge density at the liquid surface. The equations of continuity, momentum and electric potential are solved numerically with an iterative procedure developed for the model. The results of the present model fit well with experimental observations of the cone shape and jet formation.

The cone-jet shape depends on the liquid flow rate, the applied electric potential and the liquid properties such as density, viscosity, conductivity, permittivity and surface tension. Also, the electrode configuration has some influence on the process.

---

[1] Submitted for presentation, Fall 2002 Annual Technical Conference, The Fiber Society.

[2] To whom correspondence should be addressed
Tel : 215-895-2287 Fax : 215-895-1478 e-mail : bfarouk@coe.drexel.edu

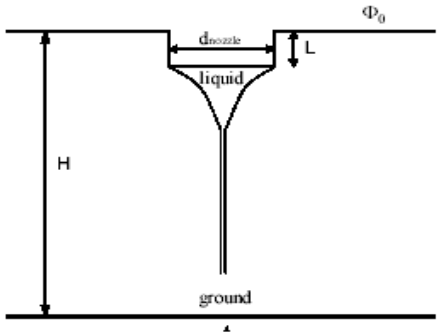

Figure 1. Configuration of the physical model

Table 1 lists the cases studied. The cases are characterized by the type of liquid and the flow rate. The cases were simulated with different values of applied voltage. Figure 2 gives the comparison between the cone shape predicted by the model for case 1 and measurements reported under similar conditions (Hartman et al., 1999). The numerical solution agrees very well with the experimental measurements.

Table 1. Cases considered for simulation

Case	Liquid	Nozzle dia. (mm)	Distance between electrodes (mm)	Flow rate (10^{-10} m^3/s)
1	Ethylene glycol	8.0	34.0	14
2	1-octanol	1.2	38.5	44.5
3	Ethylene glycol	1.0	9.0	1.1
4	Ethylene glycol	1.0	9.0	5.5
5	1-octanol	1.0	9.0	1.1

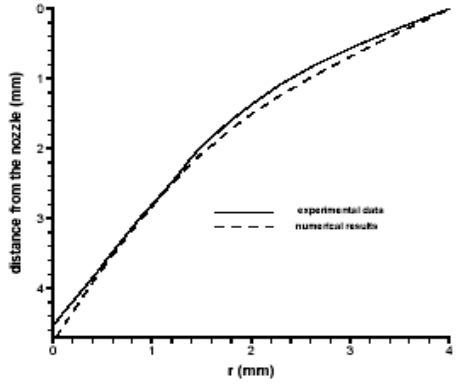

Figure 2. Comparison of numerical results of the cone-jet radius with experimental data (Hartman et al., 1999) for ethylene glycol

With the present model, the cone-jet mode can be predicted without any fitting parameters, given the liquid properties, liquid flow rate and the electrode configurations. This model calculates the cone-jet shape and the velocity field within the meniscus. This model can also estimate the electric field inside and outside the liquid. The charge density, the tangential electric field along the interface and the normal electrical field inside the liquid are found to change sharply near the cone apex and all reach the maximum values at the cone apex where the stable jet emerges.

Reference:

Hartman, R.P.A., Brunner, D.J., Camelot, D.M.A., Marijnissen, J.C.M. and Scarlett, B., (1999). Electrohydrodynamic atomization in the cone-jet mode physical modeling of the liquid cone and jet. Journal of Aerosol Science, 30(7): 823-849

Bakhtier Farouk

Brief biography

Professor Bakhtier Farouk received his BS degree in Mechanical Engineering from the Bangladesh University of Engineering and Technology in 1975. He received his MS and Ph.D. degrees in 1978 and 1981 respectively from the University of Delaware and thereafter joined the Mechanical Engineering and Mechanics department in Drexel University. His research and teaching interests include transport processes in materials processing, convective and radiative heat transfer, combustion and fires, multi-phase flows, plasma processing, microfluidics and computational fluid dynamics. He is a registered Professional Engineer and a Fellow of the American Society of Mechanical Engineers. He was awarded the SAE Ralph Teetor Educational Award in 1986 and the American Society of Metals Henry Marion Howe Medal in 1989. He served as a Summer Faculty Research Associate at the Naval Research Laboratory in Washington, D. C. in 1988 and 1997. He also served as a Guest Researcher at Air Products and Chemicals Inc. and the National Institute of Standards and Technology, Gaithersburg, MD on sabbatical leaves during 1991-92 and 1999-00 respectively. He was awarded the Presidential Citation for outstanding achievement by the University of Delaware in 1999.

Electrospun Molecular Sieve and Composite Fibers

Kenneth J. Balkus, Jr., Sudha Madhugri and John P. Ferraris
University of Texas at Dallas, Department of Chemistry and the UTD NanoTech Institute, Richardson, TX 75083-0688, USA

Introduction

Electrospinning involves the application of electrical forces to produce fibers with diameters in the nanometer to micron range. This is a nonmechanical process for spinning fibers which has been well studied for various polymers and textiles. The application of this technique to inorganic materials such as porous metal oxides is unknown. We now report a method of electrospinning mesoporous silica molecular sieve fibers. Additionally, we have extended this effort to include a novel dual electrospinning setup that allows formation of interwoven networks of inorganic molecular sieve and polymer fibers. The interest in mesoporous molecular sieves continues to grow as applications emerge. Catalysis, separations, sensors, optical waveguides, lasers and drug delivery are just a few of the areas that could benefit form a fibrous configuration. Surfactant templated mesoporous materials are known to form interesting shaped particles including rods and fibers. In the present work electrospinning is applied to form fibers of mesoporous molecular sieves SBA-15 and DAM-1. The application of these brittle metal oxides in papers and textiles will rely on the ability to form composites with polymers. Therefore, the nanoporous silicas were also electrospun with a variety of polymers including the semiconducting poly[2-methoxy-5-(2-ethylhexyloxy)-1,4-phenylene-vinylene] (MEH-PPV) which results in some interesting luminescent fibrous networks. This may represent the first example of an electrospun mesh of organic and inorganic fibers of this type.

Experimental

Polymer solutions used for electrospinning are usually made in volatile solvents and when fibers are spun using these solutions, drying of polymer fibers is quick and effective. However, in the case of molecular sieve materials, the solvents that could be used were limited to water and alcohol because of the necessity to hydrolyze the silica source and for it to condense around the micelles. In a basic gel preparation, the surfactant was first dissolved in ethanol under constant stirring and the required amount of water and 2M HCl were added to this solution followed by the silica source. In the case of MEH-PPV polymers the solvent was 1,2-dichloroethane. Details of the silica and polymer gel preparations will be reported elsewhere. The final viscosity of the synthesis gels were~14000 cP. The gels were transferred to a 3mL syringe or dual syringes, which is part of a fluid dispensing system (EFD 1500 XL). One electrode was attached to the 22 gauge syringe needle(s) and the other was attached to the target at a distance of 22-25 cm. A voltage of 20kV was then applied to the gel. Upon application of current, the gel forms a fine jet and produces very thin fibers. Different types of targets were employed including aluminum foil, acid treated glass and various Anapore filters.

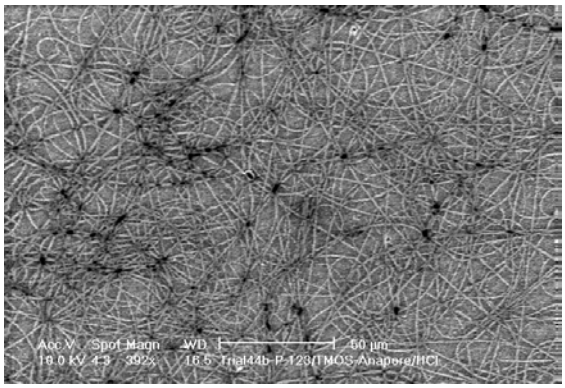

Figure 1 Electrospun Fibers of SBA-15 on a 200 nm Anapore filter

Results and Discussion

The SEM images of SBA-15 fibers electrospun onto Anapore filters with ~200 nm holes are shown in Figure 1. The fibers exhibit and XRD pattern with the main reflection at 97Å which correlates well with the d-spacing reported for this mesoporous material. The macromolecular templates such as the block polymer Pluronic 123 sieves is a key component in the gel chemistry and will be discussed in more detail. The template can be removed by calcination or by extraction without damaging the fibers. Figure 2 shows a SEM image of DAM-1 electrostatically deposited onto a glass cover slip. The XRD pattern of these fibers reveals a low angle 100 reflection at 65Å. Further characterization of these molecular sieve fibers including FT-IR, Raman and TEM results will be presented. Figure 3 shows an SEM image of a composite mesh of SBA-15 and the conducting polymer MEH-PPV. This photoluminescent polymer glows bright red in the case of the bulk polymer and as the electrospun nanofibers. However, when a composite mesh is prepared with SBA-15, the emission shifts dramatically to higher energy. Figure 4 shows the change in color from red to orange with SBA-15 and green with SBA-15 functionalized with phenylsilanes. These reversible changes are ascribed to a reduction in conjugation length with in the polymer fibers. Additionally, the molecular sieve fibers may serve as nanospacers at contact points and prevent polymer aggregation. Details of the fluoresence as well as IR and Raman spectroscopy will be presented.

There is enormous potential for these inorganic fibers, which can be prepared in a variety of compositions and pore architectures. The molecular sieve fibers prepared to date were found to be well ordered and stable to calcination or template extraction. These fibers and related composites are currently be evaluated for a variety of applications ranging from scaffolds for cell growth to solar cells.

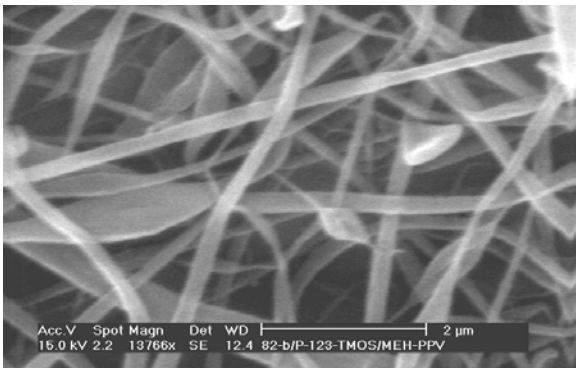

Figure 3 Electrospun composite mesh of MEH-PPV and SBA-15 after 5 minutes

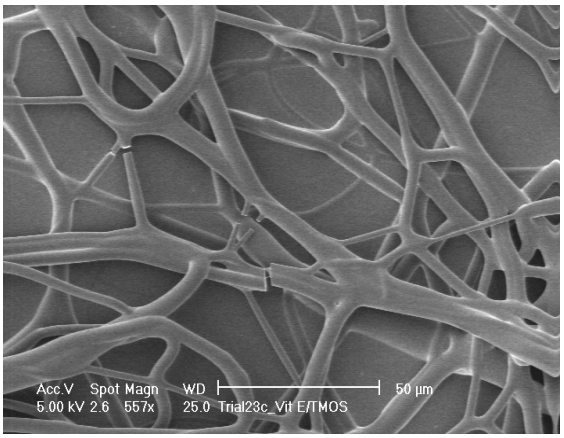

Figure 2 Electrospun DAM-1 fibers on glass

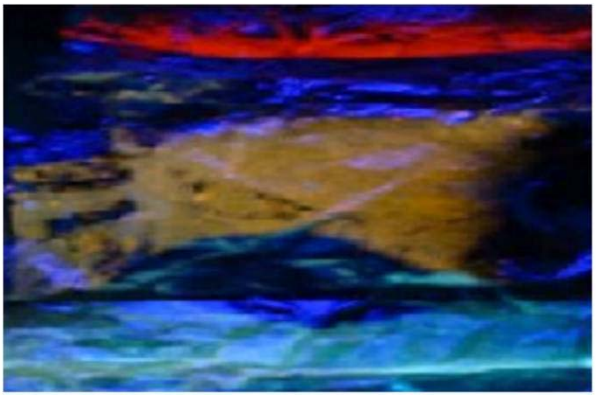

Figure 4 Digital images of MEH-PPV fibers and composites with SBA-15 upon exposure to a blacklight.

Pore Structure and Wetting Properties of Carbon Nanotube Fibers

Alexander V. Neimark[1], Sigrid Ruetch[1], Konstantin G. Kornev[1], Peter I. Ravikovitch[1], Stéphane Badaire[2], Maryse Maugey[2] and Philippe Poulin[2]
[1]Center for Modeling and Characterization of Nanoporous Materials TRI/Princeton, P.O. Box 625, Princeton, New Jersey 08542
[2] Centre de Recherche Paul Pascal/CNRS, Université Bordeaux I, Avenue Schweitzer, 33600 Pessac, France

Recent discovery of a process of spinning of fibers from single wall carbon nanotubes open new horizons in nanofiber technology [1]. Nanotube fibers with diameters ranging between 10 and 30 nm were produced and studied by various techniques including SEM, gas adsorption, and droplet absorption. We show that nanotube fibers are highly porous, capable of absorbing liquids and vapors in significant amounts. Nanotube fibers, which primary blocks are single wall nanotubes of ca. 1-2 nm in diameter, possess a hierarchical structure with three levels of structural organization. Primary nanotubes form bundles referred to as fibrils of 10-30 nm in diameter. Fibrils preferentially oriented along the fiber axis are packed into straight cylindrical filaments of 0.1-1 nm in diameter. These filaments with a hairy surface are aligned in a close packing forming a fiber of 10-30 nm in diameter. Unlike classical carbon fibers, the nanotube fibers can be strongly bent without breaking. Their elastic modulus is 10 times higher than the modulus of high-quality bucky paper.

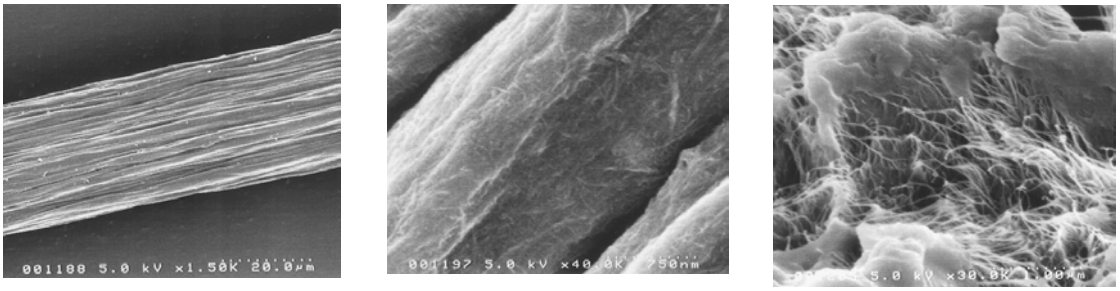

Fig.1 SEM images of a nanotube fiber. Three hierarchical levels (left to right): fiber (10-30 nm) composed of aligned filaments; straight cylindrical filament (0.1-1 nm) built of packed fibrils, nanofelt of fibrils (10-30 nm) which represent bundles of single wall nanotubes (1-2 nm).

Porosity of nanotube fibers ranges from 1 to 100 nm. The pore size distribution was obtained by capillary condensation of nitrogen at 77 K. The isotherms of nitrogen vapor sorption and desorption form a hysteresis loop typical for mesoporous solids.

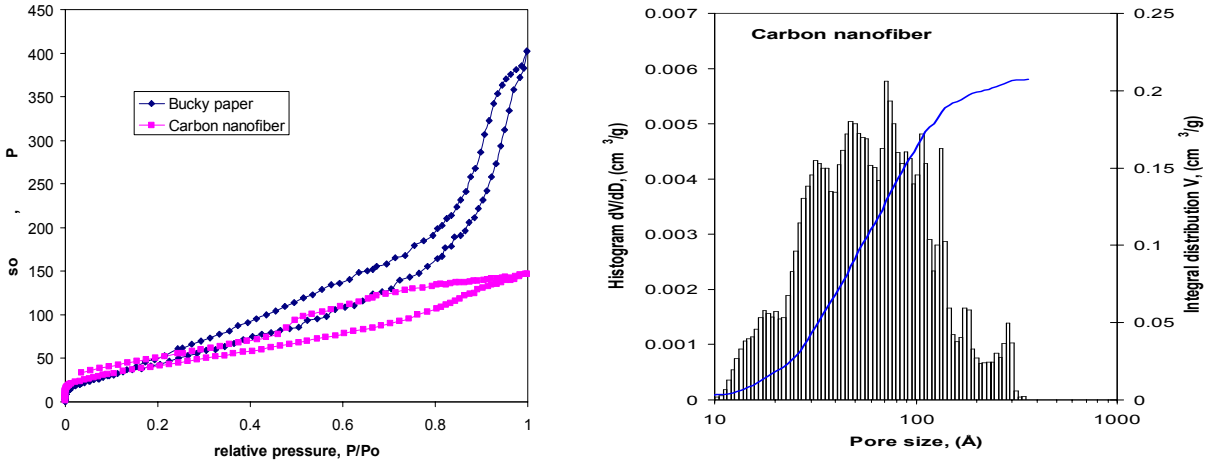

Fig.2. Capillary condensation and desorption of nitrogen on nanotube fibers and bucky paper (right). Pore size distribution in nanotube fibers in the range 10 –500 angstroms.

Fluid absorption by nanotube fibers was studied by monitoring spreading and uptake of single droplets. We found that the absorption of droplets of wetting fluids (hexadecane) proceeds in two stages: within a relatively long period the droplet rests on the fiber without visible changes and then swiftly penetrates into the pores.

Fig.3 Absorption of a hexadecane droplet by a nanotube fiber of ~30 nm in diameter.

The results presented show that fibers produced by spinning of single wall carbon nanotubes can be used as absorbing/adsorbing and reinforcing components of composite materials, membranes and other nanostructures.

References.

1. Vigolo B, Penicaud A, Coulon C, et al.Macroscopic fibers and ribbons of oriented carbon nanotubes. SCIENCE 290 (5495): 1331-1334 NOV 17 2000

Biographical Information

Professor Alexander V. Neimark is a Research Director at TRI/Princeton. Dr. Neimark received M.S. in Mechanical Engineering, Ph.D. in Chemical Engineering, and D.Sc. in Physical Chemistry, at Moscow State University. He is a recipient of a number of national and international awards and honored appointments. Dr. Neimark is a renowned expert in theoretical foundations of porous materials characterization and modeling of adsorption, fluid flow and capillary phenomena. He is the author of the monograph "Multiphase Processes in Porous Media" and 130+ research papers. The TRI/Princeton Center for Modeling and Characterization of Nanoporous Materials, which he has established and directs, is recognized as a leading international center for fundamental research, technology transfer, and professional education in porous and particulate materials. His current research program focuses on interactions of fluids with nanomaterials., including fibers and fibrous materials, permselective membranes, adsorbents, catalysts, and other nanostructured porous solids.

Image Processing Technology in Textile Applications

B.K. Behera
Department of Textile Technology, Indian Institute of Technology, Hauz Khas, New Delhi-110016

Modern Textile Industries have been facing difficult challenges for creating a high productivity and high quality manufacturing environment. Such an environment requires improving quality, increasing production and flexibility, reducing inventory and cycle time and minimizing the cost. For this purpose the textile manufacturing processes essentially need on-line, real time, and dynamic controls. Many textile properties when being assessed require a subjective assessment by trained personnel. The reproduction of results by this method is often a problem, howsoever good may be the training of the personnel. For a number of reasons the subjective approach and manual handling of measurement process yield erratic results. In this context digital image analysis is discussed which offers the most promising avenue to the future development of a rapid and reliable instrumental method for measurement, analysis and real time dynamic controls of numerous textile process and product characteristics.

Image analysis technology, which has rapidly developed since 1960s is especially useful in textile manufacturing and inspections, including texture evaluation and inspection of textile surface characteristics. Computerized image capture and image analysis offers promising applications and very rapid, accurate and objective measurements of a wide range of textile material properties. In recent research it is demonstrated that how a simulation model can be built to predict the 3D behaviour of a garment during wear. The research method tries to put forward a new concept in which textile materials can be created in the virtual world by specifying fundamental properties.

While the human vision system evolves in a self-programming fashion from the birth on, with a prior knowledge acquired by trial-and-error, computer vision requires individual programming of each particular task.

Image processing is basically the technique of manipulating and improving grey scale video images using mathematical functions. Image analysis involves calculations on a final image to produce numerical results. In general a typical image processing system contains three fundamental elements: an image acquisition element, an image processing element, and an image display element.

A continuous scene is converted to a digital image and stored in a memory by the image acquisition element. This image is displayed in some form by the image-display element for human viewing. This image processing element is designed to carry out various tasks, which generally fall into three main groups: image enhancement, image analysis, and image-coding.

The objective of image analysis in general is to extract, from the very large amount of data in an image, that small set of measurements containing the information of interest. The standard strategy to achieve this is to break the whole task into a sequence of smaller, independent steps. The object of each step is to achieve a limited but significant reduction in the amount of data by discarding irrelevant information. The result after each stage is a new representation of the image. Objects in an image have to be separated from each other and from their background before any measurements of object properties can take place. This strategy is analogous to the way in which human visual system works, as one sees an object in a scene only because that object is different and thus separable from its surroundings in some manner.

Image Processing has been used as an established technique in many areas of research such Digital Aerial Video Recording, High capacity image archiving, Medical imaging, Motion analysis, Flow studies, Spurious event capture, Video playback on demand, Process monitoring/analysis, Security, On-line transaction processing, Hyper spectral imaging, Human brain development analysis, printed circuit board part presence, placement, and alignment, printed circuit board pin and connector gauging, assembly verification, semiconductor inspection, automated or , interactive measurement, on-line inspection and gauging (cast part, extruded plastic part, etc.) , part counting and sorting, product packaging inspection, real-time process, monitoring, web process inspection, printing process inspection, food and perishables, inspection, bar code reading, template matching, color analysis, defect and failure analysis, etc. Imaging technique has also already started making in – road into the textile field. Research work have been carried out for the investigation of fiber cross section analysis, maturity measurement of cotton, estimation of trash in cotton, measurement of pore size distribution, assessment of warp stripeness, analysis of fibre crimp, fibre blend, yarn structure i.e. yarn thickness, yarn twist, yarn hairiness, determination of weave type, detection of fabric defects, measurement of Shrinkage, fabric wrinkle, carpet appearance, seam pucker, Rotary Screen Print Inspection etc. In this paper only few developments such as objective measurement of fabric pilling, drape and wrinkle properties have been briefly discussed for which Textile Department, IIT, Delhi has developed Digital Image Processing Systems.

The pilled fabric image is processed to obtain the various pilling parameters like number of pills, total pilled area, mean pill area, and the number of pills per unit area. To eliminate the basic weave structure and the color patterns the image is Fast Fourier Transformed and the spikes formed in the spectrum is filtered. After filtering the image is again reconstructed by Inverse Fourier Transformation of the spectrum; the reconstructed image has only the required information i.e. the pills, which is converted to binary form. The group of white pixels represents a pill, and the total number of such groups are searched and counted. The result is compared with the standards like ASTM, EMPA and IWS and assigned a suitable grade.

In another development to assess the drapability of a fabric, the draped fabric image is converted to binary and then separated from the background and processed to find the center of the image. The distances from the center to the edge of the fabric is found by rotating the image by one degree and all the drape parameters like Drape coefficient, Drape Distance Ratio, Fold Depth Index, Amplitude to Radius Ratio, Number of Nodes, were found out. The drape parameters of the fabric is also found out by Fourier series and compared with the results of the DIP method and conventional method.

Similarly for wrinkled fabrics, images are compared with standard replicas to ensure an objective evaluation of wrinkle behavior of a fabric with the help of image processing technique.

Air Particulate Filtration Through Parallel Fiber Alignment

Kyung-Ju Choi
AAF Intenational, 10300 Ormsby Park Place, Suite 600, Louisville, KY, USA
Tel: (502) 637-0773, Fax: (502) 637-0676, email: kchoi@aafintl.com

This study relates to the fibrous structure of air filtration media and its particulate removing performance in the ambient air. It is particularly related to its construction where the fibers of the medium are oriented with respect to the air stream to be passed through.

Following the implementation of the $PM_{2.5}$ standards, people pay much attention to the fine particles. Some fine particles may have a strong correlation between indoors and in the ambient. Since there are much more particles indoors than in the ambient, an effective filtration system is needed to remove these fine particles. There are numerous fibrous filtration media available in the market place. Most of air filtration media used in HVAC is a nonwoven material which contains filaments oriented approximately perpendicular to the incoming air direction. The pressure drop across the filtration medium is a crucial factor because of the capability of the fan motor to draw air through the medium to the room. The desirable filtration medium should have better particle capture efficiency at the lower pressure drop through the filtration medium. Hence, the present research had been carried out by preparing nonwoven fibrous material where the majority of fibers are oriented with respect to the air stream to be passed through (Choi, 2000).

THEORETICAL BACKGROUND

In 1959, Sinzi Kuwabara and John Happel derived the equations for the pressure drop using the single fiber theory with different boundary conditions.

Kuwabara (Kuwabara, 1959) theory for flow perpendicular to fiber axis is

$$\Delta P_K = \frac{4\eta chU}{R^2\left[-\frac{1}{2}\ln(c) - 0.75 + c - \frac{c^2}{4}\right]} \quad (1)$$

Happel (Happel, 1959) theory for flow parallel to fiber axis is

$$\Delta P_H = \frac{2\eta chU}{R^2\left[-\frac{1}{2}\ln(c) - 0.75 + c - \frac{c^2}{4}\right]} \quad (2)$$

where c: packing density, η: viscosity, h: thickness of media, U: air velocity, R: radius of fiber and P: pressure.

Here clearly the pressure drop of the flow parallel to the fiber axis is half of the pressure drop of the flow perpendicular fiber axis, i.e. $\Delta P_H/\Delta P_K = 0.5$.

EXPERIMENT

Two non-woven materials were prepared with equal amount of 6 denier polyester fibers and low melt fibers. One made by a conventional way and the other was a vertically lapped nonwoven material cut top and bottom parts in order to make the same thickness as that of a conventional one (0.4 cm). The basis weight of both samples was 122 g/m^2.

The fractional efficiency test stand was used. Polydispersed KCl particles were generated by a collision Nebulizer. Test is performed at the air velocity of 61 m/min (200 ft/min) and 152.4 m/min (500 ft/min).

CONCLUSION

The experimental results show that the efficiency increases with increasing air velocity indicating inertial mechanism is dominant. The medium with a majority of the fibers aligned with the direction of fluid stream provides a unique filter and fibrous medium arrangement having an increased filtration efficiencies and a reduced resistance to the fluid streams to be filtered. This medium can be used in many air filter applications in HVAC system in order to improve IAQ.

REFERENCES

Choi K., 2000, Filter media with fluid stream positioned fibers, US Patent 6165244

Kuwabara S., 1959, The forces experienced by randomly distributed parallel circular cylinders or spheres in a viscous flow at small Raynolds Numbers, J of Physical Society of Japan, Vol 14, pp 527-532.

Happel J., 1959, Viscous flow relative to arrays of cylinders, AIChE J. Vol 5, pp. 174-177.

A Blending of Thai Hybrid Silk Wastes and Cotton in The Cotton's Spinning System

Chollakup, R., Sinoimeri, A., and Dréan, J-Y.
Laboratoire de Physique et Mécanique Textiles
Ecole Nationale Supérieure des Industries Textiles de Mulhouse
Université de Haute-Alsace, 11 rue Alfred Werner
68093 MULHOUSE CEDEX, FRANCE

Thai hybrid silk is a special variety which is famous for its luster in bright yellow and Thai style in knobby texture. In the industry of reeling silk, the waste remains almost 15-20% including the defected cocoon. One of the use of these wastes, besides spinning of silk yarn, is to blend them with other fibers, to develop a new yarn with functional properties and to improve the properties of yarn and fabric in recent times.

The present study has to be considered as a first step in this direction. Three types of silk wastes; inferior knubbs, filature gum waste and pierced cocoon using in this study are hybridization between Thai hybrid (native polyvoltine) and bivoltine. The three waste represent the outer, middle and mixed portion of filaments of the cocoon, respectively. All wastes are prepared following the main processes which are degumming and bleaching, opening, carding and cutting into 35 mm length. All types of wastes after preparation process have proved to have similar contents of impurities (sericin and oil content). After carding and cutting, the filaments from all parts are well mixed and individualised (Figure 1).

The physical properties such as length, fineness, tenacity and elongation of these fibers are studied and presented in Table 1. It is found that the inferior knubbs fibers are finer than the filature gum waste and the pierced cocoon fiber. Strength of the inferior knubbs fiber is quite similar to the pierced cocoon and both lower than that of the filature gum waste.
In this study the pierced cocoon is chosen to be blended with cotton fiber at different percentages of silk fibers (25, 50 and 75%) in order to obtain further data concerning the blended processing in the short staple spinning system. Blending has been carried out either before carding or in drawing frame. Physical and mechanical properties of blending slivers and yarns have been studies and compared with those of pure components. These results will be discuss in the presentation. This study indicates that there is potential for making the silk and cotton blended yarn in the cotton's spinning.

Table 1. Physical properties of the silk waste and cotton fibres before carding.

		Silk fibre[1]			Cotton fibre
		Inferior knubbs	Filature gum waste	Pierced cocoon	HVI
Length	Mean Length, ML (mm)	21.1 ± 0.6 b	19.4 ± 1.6 c	24.8 ± 1.2 a	23.9 ± 0.6
	Upper Half Mean Length, UHML (mm)	37.0 ± 1.6 b	36.2 ± 2.8 b	46.0 ± 1.2 a	28.6 ± 0.5
Fineness	Fineness (mtex)	136	165	156	166
Strength	Tenacity (cN/tex)	23.9 ± 1.8 b	25.6 ± 1.4 a	23.2 ± 1.5 b	27.3 ± 1.0
	Elongation at peak (%)	14.0 ± 0.9 ns	13.6 ± 0.7 ns	13.3 ± 0.9 ns	5.4 ± 0.2
	Elongation at break (%)	24.7 ± 1.5 ns	25.7 ± 2.1 ns	25.8 ± 2.3 ns	-

[1]All values with different letters (a, b, c) in the same row are significantly different at $p \leq 0.05$, ns means non significantly different, NA means non appropriated method

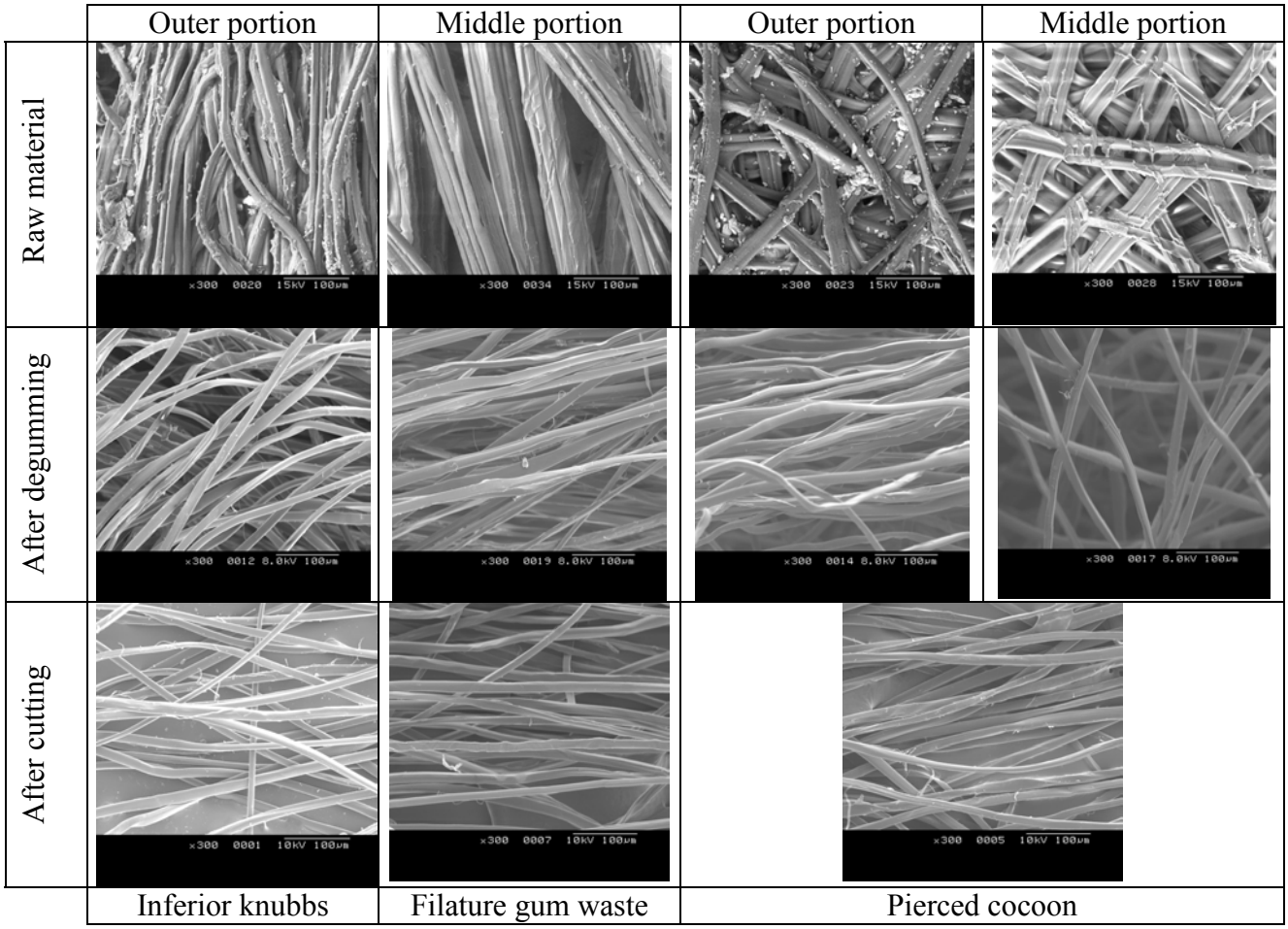

Figure 1. SEM images of the raw material and the materials after preparing processes of silk waste at 300 x magnifications.

Biography

Rungsima Chollakup, she was born in 1970, Thailand. After obtaining my master degree in Food Technology at Chulalongkorn University, Thailand in 1995, she worked as researcher at Kastsart Agricultural and Agro-Industrial Product Improvement Institute, Kasetsart University for 5 years. During that period, she trained and researched in subject polymer blends for biodegradable plastics for 3 months at National Institute of Bioscience and Human Technology, Japan in 1996 and 1997. Now she is the second year Phd student in Ecole Nationale Supérieure des Industries Textiles de Mulhouse, France under Prof J-Y Dréan. The topic in her thesis is Blending Thai silk and Thai cotton

Evaluation of Pore Structure Characteristics of Nanofiber Nonwovens

Akshaya Jena and Krishna Gupta
Porous Materials, Inc., 83 Brown Road, Ithaca, NY 14850 USA

Nano-fiber nonwovens are finding innovative applications in many areas of modern technology such as healthcare, power sources, biotechnology and protective devices. The pore structure characteristics of nanofiber nonwovens are very important in determining their performance in applications. The important pore characteristics are the diameter of a pore at its most constricted part, the largest pore diameter, the mean pore diameter, pore distribution, pore volume, surface area of through pores, liquid permeability and gas permeability. Mercury intrusion porosimetry is often used to examine pore structure. This technique is limited to the determination of only the pore volume, pore volume distribution and total surface area. No other pore structure characteristic can be measured by this technique. Also, this technique uses mercury, which is hazardous to health and pollutes the environment. The high pressures often required for mercury intrusion may drastically alter the pore structure of nanofiber nonwovens. Therefore, mercury intrusion porosimetry is not a very desirable technique for pore structure analysis of nanofiber nonwovens.

In this paper two innovative techniques based on liquid extrusion for pore structure analysis of nanofiber nonwovens will be discussed and results obtained using these techniques will be presented.

Capillary Flow Porometry is one of the techniques. In this technique the pores of the sample are filled with a wetting liquid and a non-reacting gas under pressure is used to displace the liquid from pores and permit gas flow. Differential pressures and gas flow rates through wet and dry samples are measured. The results are used to obtain characteristics of through pores. The diameter of a pore at its most constricted part, the largest constricted pore diameter, mean flow pore diameter, flow distribution over pore diameter, surface area of through pores, gas permeability and liquid permeability are computed.

Liquid Extrusion Porosimetry is the second technique. In this technique, the pores of the sample are filled with a wetting liquid. The sample is placed on a membrane. The membrane is such that the largest pore of the membrane is smaller than the smallest pore of the sample and the liquid used to fill the pores of the sample spontaneously fills the pores of the membrane. The pressure of a nonreacting gas is increased on the sample. The liquid extruded from the pores of the sample pass through the pores of the membrane while the pores of the membrane remain filled with the liquid and do not permit gas to pass through. The pressure of the gas and the volume of displaced liquid are measured. Pore volume, pore diameter, pore volume distribution and through pore surface area are computed from these data. If the permeability of the membrane is much higher than that of the sample, measurement of volume of liquid flowing out of the sample as a function of pressure on excess liquid on the sample yields liquid permeability. If the permeability of the membrane is not much higher than the sample, experiment carried out with the membrane removed gives liquid permeability.

These two techniques can measure all the required pore structure characteristics. In addition, these two techniques do not use any toxic material or high pressures that may distort the pore structure. The tests are also faster and much simpler to execute.

Presenting Author

Krishna Gupta
Porous Materials, Inc.
83 Brown Road, Ithaca, NY 14850
Phone: (607) 257 5544
Fax: (607) 257 5639
e-mail: info@pmiapp.com

Krishna Gupta has a Sc.D. in Materials Science and Engineering from the Massachusetts Institute of Technology. He is the founder, President and Technical Director of Porous Materials, Inc. For over two decades, he has been developing methodology and technology to convert many concepts in to designs and commercial instruments for characterization of pore structure of materials. Some of the instruments like Capillary Flow Porometers, Liquid Extrusion Porosimters, Compression Porometers, On-Line Porometers, QC Porometers, and QBET are used in industries all over the globe. He is the author of many patents and a large number of technical papers.

Water Vapor Permeability of Hydrophilic Polyurethane Membrane With Melting Point as Switch Temperature

X. M. Ding [1], J. L. Hu [1], C. P. Hu [2], and X. M. Tao [1]

[1] Institute of Textiles and Clothing, The Hong Kong Polytechnic University,Hong Kong, P. R. China, [2]Institute of Material Science and Engineering, East China University of Science and Technology, Shanghai, P. R. China

Hydrophilic polyurethane (HPU) with temperature sensitivity is one type of intelligent polymers that can react to environmental temperature. This intelligent property could be applied to many fields. For example, the water vapor permeability (WVP) of such dense PU membrane undergoing a large change within a specified temperature range, can be applied to textiles by incorporating into the textile structure, which can respond to temperature and provide variable breathability. In 1992, Hayashi prepared the HPU samples with their Tg at the room temperature range, and explained the phenomena that WVP changes significantly at Tg using the micro-brown theory [1]. They used this kind of HPU membrane to have developed an intelligent fabric, namely, Diaplex™. Jeong in 2000 also reported that the abrupt increase of WVP at the melting temperature of the crystalline PU could be enhanced by modification with hydrophilic segments [2].

Based on Jeong's report and our preliminary study on the Diaplex™, a hypothesis was put forward that the significant increase in WVP of HPU membrane may be related to the increase in free volume of its membrane at crystal melting point (Tm) [3]. Accordingly HPU for variable WVP was prepared in our project with its Tm as switch temperature. That is, when the temperature rises near or higher than the Tm, the free volume of its membrane can increase obviously, and then leads to the significant increase in WVP. For this purpose, five series of HPU were prepared with five different polyols and three hydrophilic segment contents, in which their Tm were specified at the room temperature range. Then their crystalline structure and properties were investigated using Fourier Transform Infra Red Spectroscopy (FT-IR), Polarizing microscopy (POM), Transmission Electron Microscopy (TEM), Differential Scanning Calorimetry (DSC), Dynamic mechanical analysis (DMA) and Wide Angle X-way (WAXR). Their fraction free-volume (FFV) of the PU membranes at the specified temperature range were investigated using Positron Annihilation Lifetime Techniques (PALS).

Some of DSC results of these HPU samples are shown as in Fig. 1 and Table 1 where the crystal melting of the PUs took place at the specified temperature range, for example, for recipe B1, 36°C.

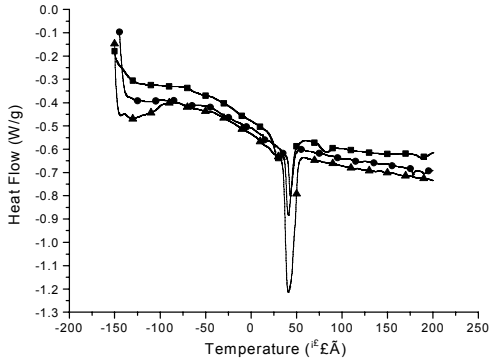

Figure 1 DSC curves of B1/B9/B14

Table 1 Thermal property of the polyurethanes

Sample	Tm (°C)	ΔH_m (J/g)
B1	36.02	26.81
B9	40.25	8.28
B14	35.43	39.19

Using the POM with heating stage, the crystalline structure and crystal melting behavior of the HPU could be observed as in Fig. 2. At different temperatures such as 25°C, 40°C and 45°C, there are significant changes in the crystalline structure, namely, crystal domain decreases with temperature rising.

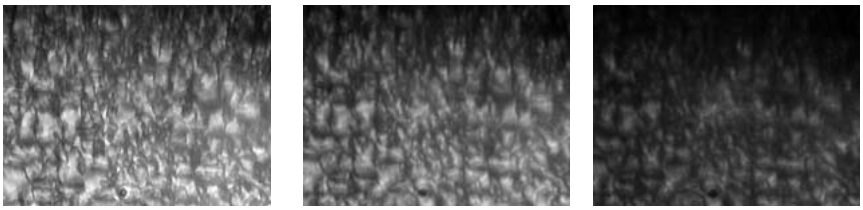

B14-25°C B14-40°C B14-45°C

Figure 2 POM pictures of B14

According to the above observations, is it anticipated that the significant increase in WVP of the HPU membrane will be triggered at the crystal melting point (Tm) because the enhanced chain mobility of the crystalline segment leads to the obvious increase in the free volume. The WVP values of membranes using the synthesized HPU mentioned above will be reported and the relationship between the WVP and the temperature as well as the crystal structure changes will be presented to validate this statement.

Keywords: Free volume, water vapor permeability, PALS, crystalline structure

Reference:

1. Hayashi, S., Ishikawa, N., and Giordano, C., *High moisture permeability polyurethane for textile application.* J. Coated Fabrics, 1993.**23**(7)?p.74-83.
2. Jeong, H.M., Ahn, B. K., and Kim, B. K., *Temperature sensitive water vapour permeability and shape memory effect of polyurethane with crystalline reversible phase and hydrophilic segments.* Polym. International, 2000.**49**(12)?p.1714-1721.
3. Ding, X.M., Hu, J. L., Tao, X. M., and Hayashi, S. *Effect of crystal structure of shape memory polyurethane film on water vapour permeability*.in?*The 6th Asia textile conference*.2001.Hong Kong.

Electrospinning of Nylons, Poly(ethylene terepthalate) and Their Blends

Kevin M. Kit and Sudhakar Jagannathan
Department of Material Science and Engineering
University of Tennessee, Knoxville

A polymer blend, a combination of two or more polymers developed for superior properties to suit specific applications, is produced by mixing the individual polymers in melt phase or by casting from a common solvent. The desired properties of the blend are obtained only when the two parent polymers are completely miscible. However most of the polymers commercially used for making polymer blends are not compatible with each other in solid and liquid state.

Electrospinning is a process by which fibers with diameters as small as 10 nanometers are produced when a polymer solution is accelerated from a capillary towards a grounded target by an electric field. When two different polymers are spun from a common solvent using this method, a nano-size fiber of the blend results whose final morphology is determined by the processing conditions and the properties of individual polymers. Hence this method is suitable to produce a homogenous phase for almost any polymer pair that is melt immiscible but soluble in a common solvent.

This process has been used to spin nylon 6, nylon 66 fibers and their blends from a solution of formic acid and poly(ethyleneterepthalate) from triflouroacetic acid. The solution concentration of the polymer and the composition of the individual polymers are varied and its effect on the structure, morphology and properties are studied using scanning electron microscopy, x-ray diffraction and dynamic mechanical analysis. We find that the polarity and viscosity are correlated with the formation of bead defects in the fibers of polystyrene and polycarbonate produce beads in the fibers. The nylon, having higher polarity, yields fibers of smaller diameters without any beads. The solution concentration has been found to strongly affect the fiber size, with 5% solution of nylon 66 produced fibers as small as 15nm, which increases to size greater than 100nm as the concentration is increased to 20%. On the other hand, the variation in target distance and applied voltage does not have much effect on the dimensions of the fibers. The mass throughput of the fiber, however, is found to be a function of spinning voltage.

The orientation of the as spun and wound nylon and poly(ethyleneterepthalate) fibers and its effects on the morphology and mechanical properties of the spun blends will also be presented.

SEM Pictures

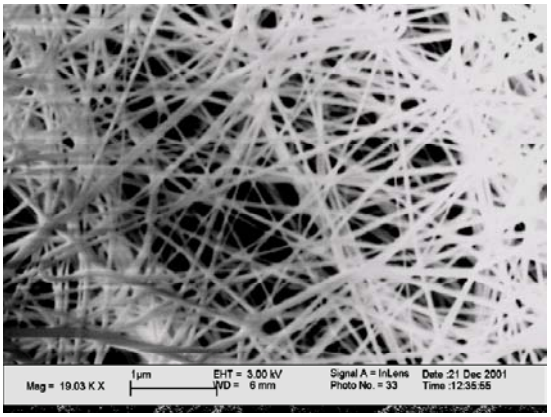

Fig 1. Nylon 66 fibers spun from formic acid (avg. diameter 50nm)

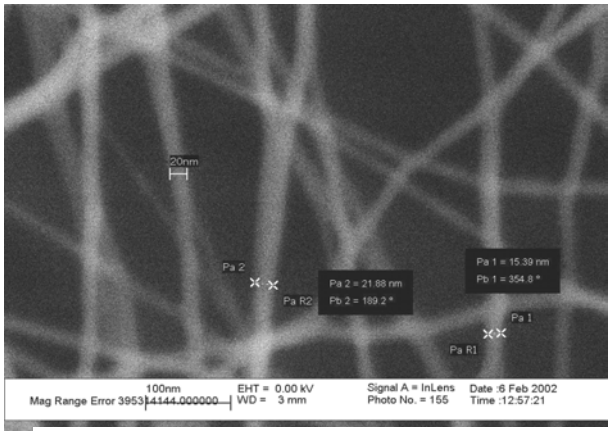

Fig 2. Smallest Nylon 66 fiber diameter obtained ~15nm

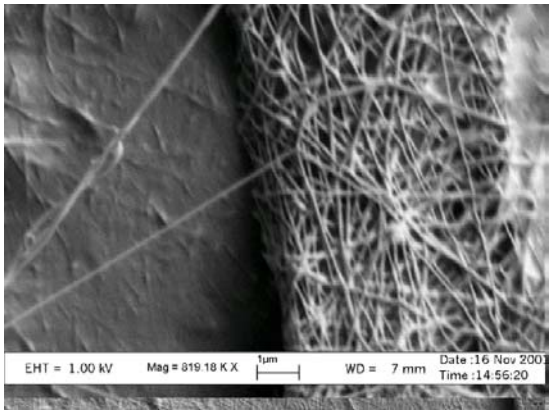

Fig 3. Nylon 6 –66 blend spun from formic acid.

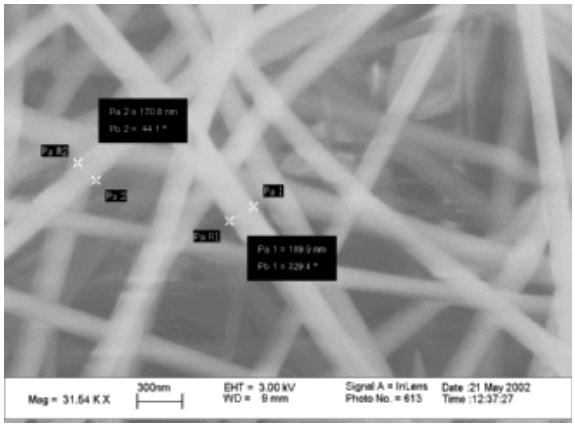

Fig 4. Poly(ethyleneterepthalate) fibers spun from triflouro acetic acid (avg. diameter 150nm)

Presenting author:

Sudhakar Jagannathan is a graduate student in polymer engineering from University of Tennessee in Knoxville working in a area of electrospinning of polymer blends. He is also president for the Society of Plastics Engineers for the UT student chapter. He has obtained a Bachelor of Technology degree from University of Madras in India in polymer technology discipline.

Carbon Nanotube Based Nanocomposite Fibrils by Electrospinning

Frank K. Ko, Ashraf Ali, Yury Gogotsi, Guoliang Yang and Christopher Li
Drexel University, Philadelphia, PA, 19104

Carbon nanotube (CNT) possess many unique characteristics that promise to revolutionize the world of structural materials resulting in significant impact on our capability to build lighter, smaller and higher performance structures for aerospace and many other industrial applications. When the CNT are aligned, micro-mechanical studies showed an order of magnitude increase in mechanical properties comparing to the state of the art carbon fiber reinforced composites. The co-electrospinning process (Fig. 1) is introduced as a means to align and deliver the CNT in the form of nanocomposite fibrils; thus forming the precursor for linear, planar and 3D fiber assemblies for macrocomposites. In this study, SWNT were purified and dispersed in polyacrylonitrile (PAN) solution for co-electrospinning into nanocomposite fibrils. The structure, composition and physical properties of these composite fibrils were characterized by Raman spectroscopy, TEM, (Fig. 2) AFM (Fig. 3) and X-ray diffraction A multiscale, hierarchical fiber architecture based model is offered to account for the contribution of these nanocomposite fibril building blocks over the entire structure length scales from the CNT level to the macrostructural level.

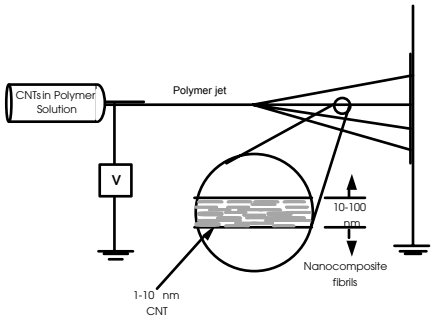

Figure 1

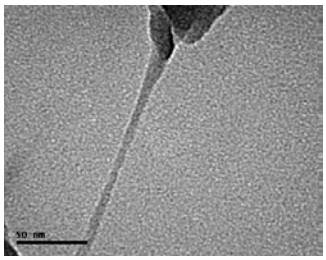

Figure 2

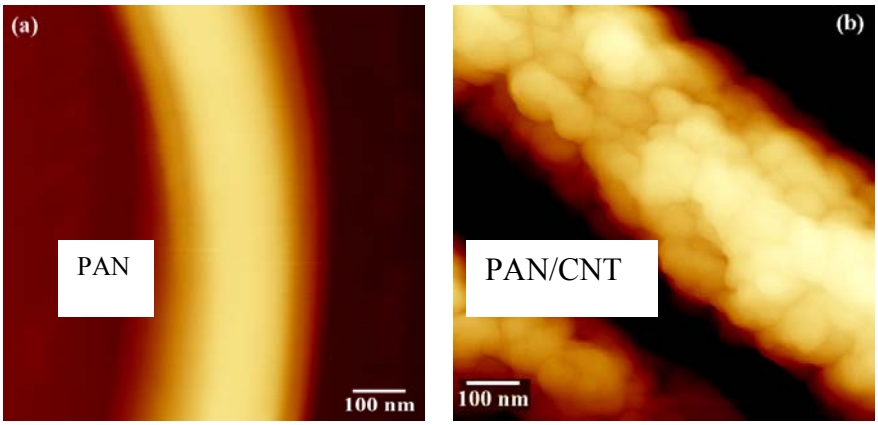

Figure 3 AFM Image of Electrospun Fibrils

A battery of characterization methods were established for the characterization of nanocomposites in this study. For example, the AFM was used to measure the mechanical properties of the SWNT/PAN fibers. In such an experiment, the fibers are first imaged, and the AFM tip is then positioned on top of the fiber at the point of interest, and the sample surface is then raised as shown in figure 4(a). The force is obtained from the deflection of the cantilever Δd, the amount of fiber indentation/deformation Δz can be obtained from the difference of the sample height increase Δh and Δd: Δz=Δh - Δd. The elastic modulus of the fiber can be evaluated from the load-deformation curves shown in Figure 4b and 4c. based on the approach of Kracke and Damaschke.

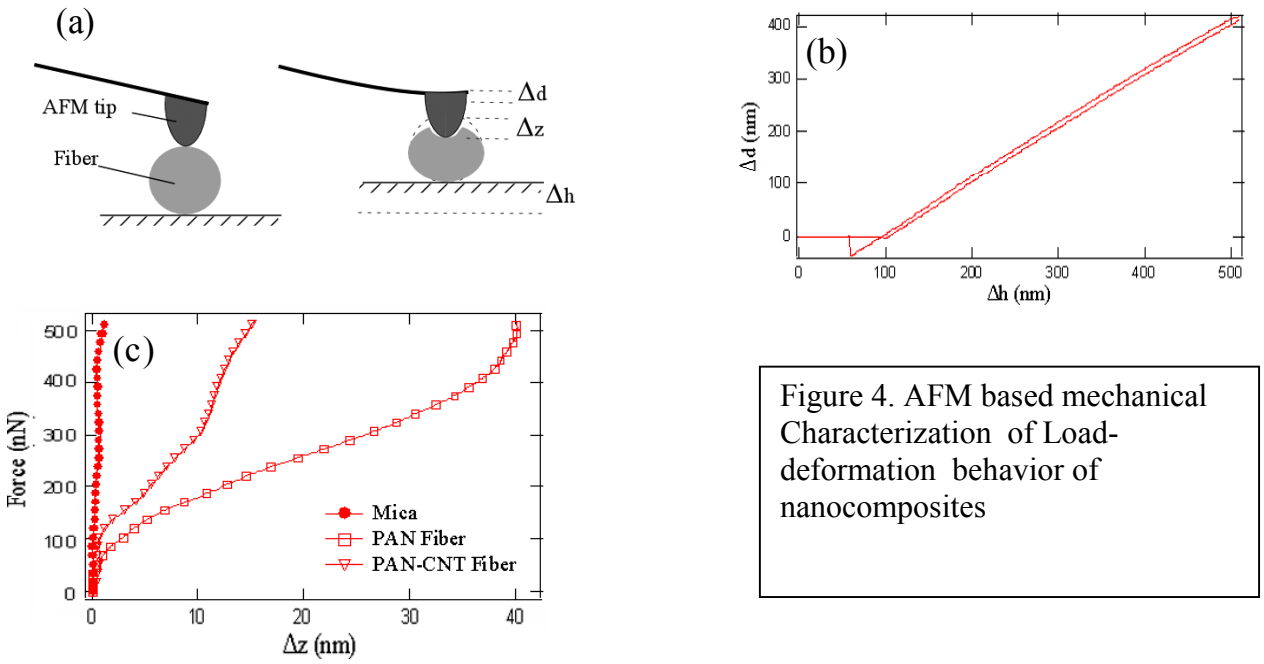

Figure 4. AFM based mechanical Characterization of Load-deformation behavior of nanocomposites

This study showed that co-electrospinning process is a viable means to produce continuous polymeric filaments filled with SWNT. Purified HiPco SWNT were dispersed in PAN solution and co-electrospun, achieving a weight fraction approaching 10%. Raman spectroscopy and TEM images showed convincingly the presence of SWNT in the electrospun PAN fibrils. AFM images showed a rough surface of the SWNT/PAN fibril as compared to the smooth surface appearance of the PAN fibrils. TEM images further confirm the presence of SWNT along the length of the fibrils revealing a diamond pattern of the SWNTsThe thermal stability of the SWNT/PAN was demonstrated by TGA showing greater than 15°C increase in decomposition temperature comparing to PAN. Load-deformation relationship of single SWNT/PAN fibril was characterized showing a ductile mode of failure and a strong reinforcement effect by doubling the tensile modulus with less than 10% reinforcement by weight.

* This study is supported by NASA under grant no. NRA 99-OSS-05.

Experimental Analysis on Thermal Insulation and Thermal Contact Properties of Animal Furs with Biomimetic Objectives

Lubos Hes
Technical University of Liberec, Faculty of Textiles, Czech Republic
e-mail: luboshes@hotmail.com

Abstract

In the study, thermal-resistance, thermal conductivity and warm-cool feeling characteristics of 16 various animal overcoat furs were determined and the effect of hair length and diameter was analyzed. It was found, that warm feeling of furs generally decreases with the ratio of hair diameter / hair length. Thermal resistance, as expected, increases linerarly with the fur thickness.

Interesting results were found, when analyzing the reason, why thermal resistance of silver fox fur is higher than that of red fox fur of similar fur thickness. All the results can be used for design of advanced synthetic furs with enhanced thermal insulation and thermal contact properties.

1. Introduction

Properties of textile fabrics and garments embrace both purely mechanical properties and heat/moisture transfer properties. Complex effect of these properties characterise comfort properties of fabrics. Properties, which involve the effect of fabric humidity on selected mechanical parameters along with the effect of deformation properties and contact force of garments on the user's perception during the garment wearing we call sensorial properties. As regards the fabric hand or handle, this is perceived by hands and involves purely mechanical (tactile) properties and thermal.contact properties characterising warm-cool feeling of fabrics [1]. It was just Prof. Kawabata, who in his work [2] emphasised the importance of the last fabric parameter. Whereas the tactile properties of fabrics are largely studied, warm-cool feeling characteristics of fabrics and furs are still published vary rarely.

Warm-cool feeling means the feeling which we get when the human skin touches shortly textile fabric, leather or any polymer used in clothing, furniture or carpets, especially in wet state. Since this feeling strongly affects the choice of people when buying the clothes or garments, the objective assessment of this feeling became very important in the last decade.

Study on thermal insulation and thermal contact properties of 16 natural furs are the main objective of this paper. No similar study was found in literature, in spite of the importance of the so called „biomimetic approach" for the next development of new fabrics and synthetic furs with improved comfort properties.

2. Description of the ALAMBETA instrument used for testing of thermal properties of furs

This commercial computer controlled instrument works in the semi-automatic regime, calculates all the statistic parameters of the measurement and exhibits the instrument auto-diagnostics, which checks the measurement precision and avoids any faulty instrument operation. The whole measurement procedure, including the measurement of thermal conductivity λ, thermal resistance R, q_{max}, sample thickness and the results evaluation, lasts less than 3 -5 min. As the objective measure of warm-cool feeling of fabrics, so called thermal absorbtivity b [$Ws^{1/2}/m^2K$] was introduced [3].

This characteristic can be used for the calculation of the initial level of heat flow q passing between the skin (characterised by a constant temperature t_1) and textile fabric with temperature t_2 according to the next equation, whose derivation is explained in [4]:

$$\mathbf{q_{dyn} = b\,(t_1 - t_2)/(\pi\,\tau)^{1/2}\ ,\ where\ b = (\lambda\rho c)^{1/2}} \qquad (1)$$

As it can be seen, the level of thermal absorbtivity depends neither on the temperature gradient between the fabric and skin, nor on the measurement time. It depends on the contact pressure, which also corresponds to real situation. The validity of thermal absorbtivity as a new parameter expressing the warm-cool feeling of fabrics was confirmed by tests where the results of subjective feeling of nearly 100 persons were compared with the values of thermal absorbtivity determined by means of the ALAMBETA instrument [5].

Typical levels of thermal absorbtivity of dry textiles fabrics range from 20 to 400 and exceed 800 for wet fabrics - see in [6], [7]. The higher is this value, the cooler feeling represents. As results from extended measurements, thermal contact feeling of fabrics is strongly affected by their structure and composition. Which feeling is better, depends on customer: for hot summer garments cooler feeling is demanded, whereas in the north of Europe warmer (wool) clothing is preferred.

Since the thermal absorbtivity is mainly the superficial property, its level can be changed by finishing treatment like raising, brushing and coating [6]. Due to the dependence of thermal absorbtivity on the real contact area between the object and hand, the surface geometry of furs, given by lenght and bending stiffness of fur hairs, effects substantially thermal absorbtivity of furs.

3. Analysis of the effect of hair parameters on thermal contact area and evaluation of results

When touching a skin, the contact force **F** causes bending deformation **y** of a hair, whose component perpendicular to the skin surface indicates the fur compression. The deformation **y** then depends on the hair length **l** and hair diameter **d** according to the generally known relationship, where **E** means the Youngs modulus and **J** is the momentum of inertia:

$$y_{\max} = y_B = \frac{F.l^3}{3.E.J} = \frac{64.F.l^3}{3.E.\pi.d^4} = \mathbf{C \,.\, l^3/d^4} \qquad (2)$$

From this relationship follows, that the hair deformation (and the fur compressibility as well) is proportional to the ratio $\mathbf{l^3/d^4}$. It can be concluded, that long and fine hairs will create (under pressure) larger contact area, which results in cooler contact feeling then in the case of short and coarse hairs.

Professional furriers distinguish the hand feeling of various furs by means of the **fineness coefficient**, **given by the ratio d/l.** As follows from the previous simple analysis, the application of such empirical coefficient is quite well justified. Due to this observation, thermal absorbtivity and conductivity of the analyzed furs will be in this study also correlated with this empirical coefficient.

Tab. 1. The effect of hair geometry (hair fineness coefficient d/l) on thermal properties of furs

Average value (CV in %) / Type of fur	***l*** [mm]	***D*** [μm]	***d/l*** [μm/mm]	***λ*** [mW/m.K]	***B*** [$Ws^{1/2}/m^2K$]
Silver fox	91,6	77,77	0,85	32,76 (2,14)	49,55(14,11)
Red fox	70	71,44	1,02	42,06(2,78)	83,25(10,56)
Chinchilla	31	32,53	1,05	39,02(2,00)	87,83(4,09)
Opossum(north American)	90	109,49	1,22	41,04(4,17)	74,93(7,03)
Raccoon	66	93,70	1,42	41,03(1,36)	78,18(3,12)
Rabbit skin, long hairs, dyed	45,8	86,38	1,89	37,31(3,48)	62,46(8,87)
American muskrat, ridge	34	76,16	2,24	42,25(2,34)	116,10(7,04)
Amer. muskrat, dyed belly	32	73,92	2,31	38,14(1,63)	69,38(4,09)
Stone marten	33	86,57	2,62	37,78(3,23)	69,56(12,58)
Lambskin merino, velour fin.	12,1	33,06	2,73	40,96(1,81)	59,01(2,46)
English sheepskin, velour fin.	15	41,64	2,78	44,06(1,36)	68,12(3,78)
American muskrat, belly	26	78,14	3,01	39,00(1,63)	107,20(4,09)
Rabbit skin, natural, cut	20,6	62,72	3,04	35,33(1,40)	69,28(4,32)
Rabbit skin, dyed and cut	16	53,38	3,34	38,79(1,03)	98,42(7,85)
Nutria dyed	42	152,21	3,62	42,88(2,15)	104,45(12,2)
Mink	19	82,27	4,33	47,87(1,19)	133,90(2,79)

From this Tab. 1 follows, that thermal resistance of furs, as expected, increases with the thickness. But this thermal resistance, given by the relation R = h / λ, depends also on thermal conductivity λ. When comparing values of λ of various furs mentioned in Tab.1, we find, that λ of silver fox fur is incredibly low. The reason of this „natural miracle" results from special structure of hairs of this animal, which lives in severe arctic climate: the hairs are hollow (confirmed by microscopic technique at TU Liberec [7]), but the cavity is separated into individual cells, in order to prevent even very low heat transfer by natural convection. Deeper analysis of this fur is recommended for the future biomimetic development of synthetic furs.

Fig. 3 **The effect of hair geometry on thermal absorbtivity of furs**

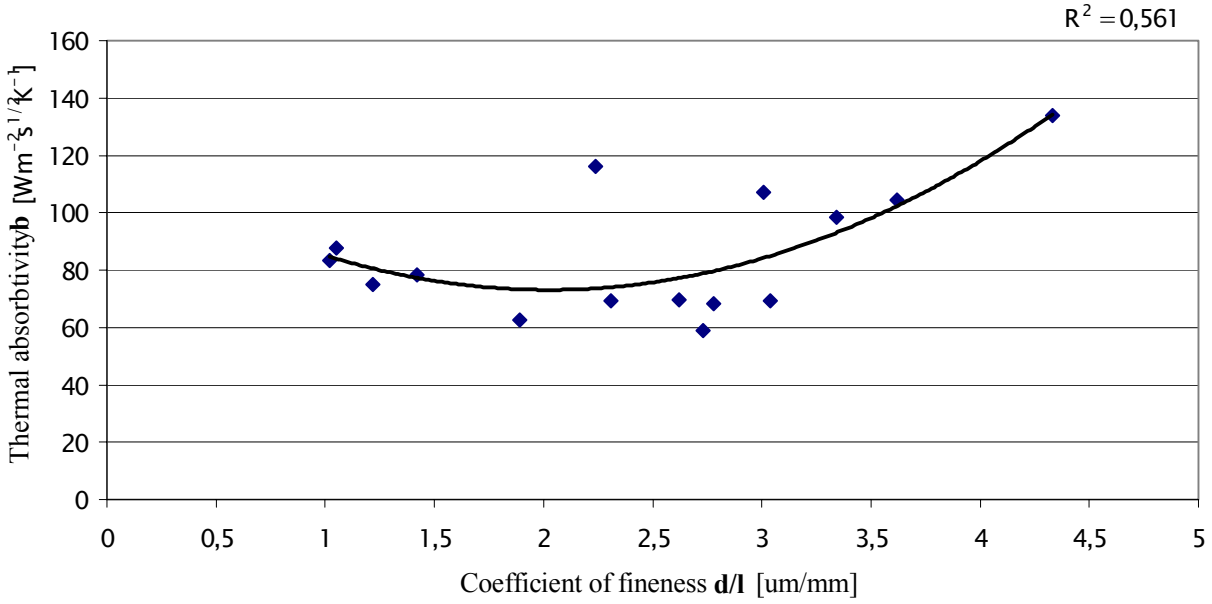

From the study of the effect of hair parameters on thermal absorbtivity of furs results, that the warmest feeling is achieved when the ratio **d/l** ranges between 2 and 2,5. This result can be applied in design of synthetic furs characterized by warmest contact felling.

Acknowledgement

Completing and presentation of this paper was partially supported by a grant No. LN00B090 offered by the Ministry of Education of Czech Republic.

Literature cited

[1] Yoneda M., Kawabata S., Analysis of Transient Heat Conduction in Textiles and Its Applications, Part II, *J. Text. Mach. Soc. Jpn* **31** (1983) 73-81
[2] Barker R.: From Fabric Hand to Thermal Comfort…in: Textile Res. Symp. at Mt. Fuji (2001)
[3] Hes L.: Thermal Properties of Nonwovens, in: Proc. INDEX 1987 Congress, Section B1, Genf (1987)
[4] Hes L., Dolezal I., New Method and Equipment for Measuring Thermal Properties of Textiles, *J. Text. Mach. Soc. Jpn* **42** (1989) T124-128
[5] Hes L., Prommerova M., The Effect of Thermal Resistance and Absorptivity of Various Fabrics on Their Thermal Contact Characteristics. In: 21st Textile Res. Symp. at Mt. Fuji (1992)
[6] Hes L., Araujo M., Djulay, V., Effect of Mutual Bonding of Textile Layers on Thermal Insulation and Thermal-Contact properties of Fabric Assemblies, *Textile Res.J.* **66** (1996) 245-250
[7] Hes L., A New Indirect Method For Fast Evaluation of the Surface Moisture Absorbtivity of Engineered Garments: In: "Internat. Conference on Engineered Textiles", MIST, May 20-22nd (1998)
[8] Vorlova L., Dimensional characteristics of furs, MSc Thesis, Tech. Univ. of Liberec (2001)

Plasma deposition of a durable, water repellent coating on aramid fabric

D. Tessier*, M. Filteau
CTT Group, Center for Textile Technologies, 3000 Boullé, Saint-Hyacinthe, Quebec, Canada, J2S 1H9.

Cold plasma technology is a versatile, environmentally friendly, energy cost effective, and promising tool for surface modification. Plasma treatments allow the tailoring of many surface properties for technical textiles such as : wettability, adhesion, wear or wash resistance, capillarity, moisture absorption, colorfastness, water and oil repellency, solvent/chemical resistance, anti-soiling, barrier to liquids, gas permselectivity, electrostatic dissipation and so forth.

Still environmentally hazardous fluoropolymer emulsions are applied for the preparation of so called conventional water repellent (WR) technical textiles. However, our work demonstrates that cold plasma process is very effective to obtain excellent WR ratings and durability to domestic washing. Aramid fabric, used in fire-fighter clothing, was treated in a semi-continuous low pressure plasma pilot line to obtain a durable WR treatment.

Effectively, we used a roll to roll plasma process to deposit a thin WR coating onto individual fibers, by way of plasma polmerization. At the **Figure 1**, SEM analysis revealed that a very thin, pinhole free coating was deposited, with thickness further evaluated to range between 0.2 –0.4 micron. Spray test results were compared to conventional WR treated fabric and, as a result, after several washes ratings remains much higher for the plasma treated fabric. No change of rating is observed for the plasma treated fabric from initial to 5 washes; WR ratings remain excellent. Moreover, after 10 washes, WR rating stands relatively high even if some fabric degradation or fiber damage is observed.

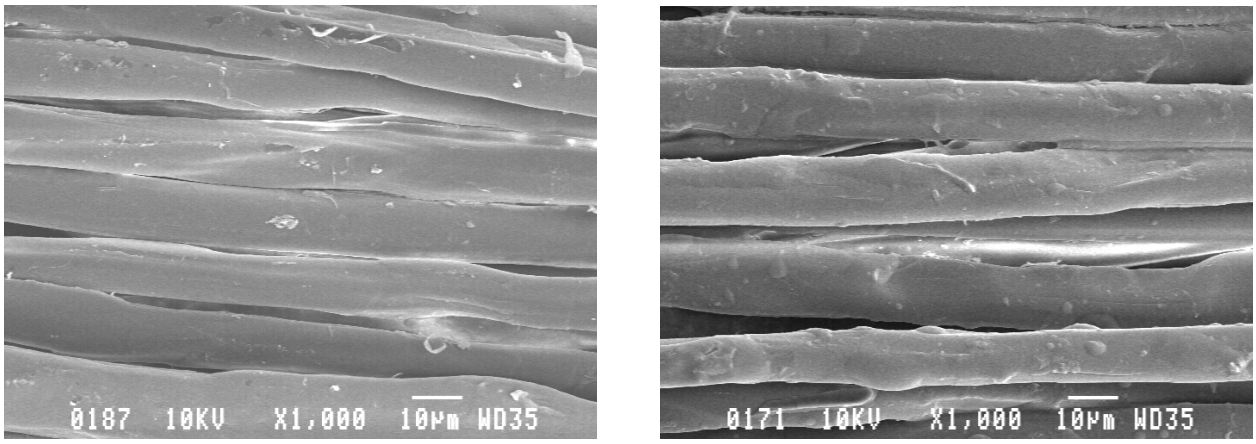

A) Virgin fabric B) Fabric with plasma coating

Figure 1. Virgin (A) and plasma treated (B) aramid fabric.

Plasma treated fabric does not exhibit significant morphological difference from the original, non-treated fabric. Therefore, the hand feel is not changed and the breathability remains high after plasma treatment, which is important for the general comfort of the wearer.

---

* Corresponding author : Dominic Tessier, Ph.D., M.Sc,.
dtessier@ctt.ca.

Dr Dominic Tessier joined the Center for Textile Technologies, a division of the CTT Group at St-Hyacinthe in Canada, from year 2000 as a Project Leader. Presently, Dr Tessier is Researcher and Industrial Research Fellow of NSERC (Natural Sciences and Engineering Research Council of Canada). Dr Tessier holds a Ph.D. in material sciences from Université du Québec (Canada) as well as a M.Sc. in polymer chemistry from Université Laval (Canada). He better defines himself as a plasma and polymer chemist. Dr Tessier is responsible of the development of cold plasma technology, R&D and technology transfert at TTC. His current interests focus on the plasma surface modification of technical textiles and fabrics for medical, military and protection applications.

Evolutionary Design of Barriers and Filters Using Genetic Intelligence

E. Unsal[1], P. Schwartz[1] and G. Dozier[2]
[1]Department of Textile Engineering, Auburn University, AL 36849-5327
[2] Department of Computer Science and Engineering, Auburn University, AL 36849-5347
unsalev@eng.auburn.edu, schwartz@eng.auburn.edu, gvdozier@eng.auburn.edu

A model for flow through porous media is presented. A porous medium may be described as a solid containing many holes and tortuous passages. A textile fabric material is a good example for porous media. Each yarn has been formed by combining fibers or filaments; and there are air gaps and spaces between these fibers. Fabrics are usually constructed by weaving and knitting yarns, or formed as nonwoven structures. There are also air gaps and spaces between these yarns. These gaps and spaces can be considered as the pores, and the fabric can be considered as the porous medium. The pore sizes, shapes and their orientations are all different. This situation makes it all impossible to model an actual porous structure. To overcome this problem a universal pore structure that consists of straight, nonintersecting cylindrical capillary tubes, the diameters of which are distributed according to some distribution function is used. In this paper, both protective barrier textiles and filters are considered. Protective barrier clothing material is any material or combination of materials used in an item of clothing for the purpose of isolating parts of the body from contact with a potential hazard. Barrier materials have applications in medicine, civil engineering, geology etc. Medical textiles are used as barriers in this model. Separation of suspended particles from a fluid media by passing the solution through the porous media is called filtration. As the fluid or suspension is forced through the pores of the filter medium, the solid particles are retained on the medium's surface or, in some cases, on the walls of the pores, while the fluid, which is referred as the filtrate, passes through. In this model, oil filter media is used as filtration material.

The liquid transports through the fabric pores formed between fibers and yarns once it wets the fabric surface. The flow through porous medium can be explained by several fluid mechanics approaches. Laplace Equation is used for filling the pore and Poiseuille's Equation is used for fluid flow through the pore. The fabric is composed of pores, which are assumed to have capillary structures. As the liquid comes in contact with fabric's bottom surface, the liquid pressure required to enter the pore is measured by Laplace Equation (filling the pore). Once the pressure is strong enough, the fluid flows into the pore (flow through the pore). Here the Poiseuille Equation is used to measure the flow rate.

The process is modeled by using First-Passage Percolation Theory, which is a time-dependent model for the passage of fluid through porous medium. In its most general form, a percolation process is mathematical model of the random spread of a fluid through a medium, where the term 'fluid' and 'medium' are to be broadly interpreted. The physical processes to be modeled might include the penetration of a porous solid by a liquid. The fabric material is assumed to have a lattice shape structure, in which each square represents a fabric pore. Each pore might be either closed or open. The closed ones, which represented by '0', do not admit the liquid enter while the open ones, which represented by '1', do. The liquid is forced to penetrate into fabric under constant pressure from the bottom of the fabric.

The current model is designed to measure the penetration time for different liquids through a certain type of fabric. Genetic Algorithms, which invented to mimic some of the processes observed in natural evolution, were used in the model. The Genetic Algorithm searches for the best liquid, which will give the maximum time for barrier applications and minimum time for filtration applications, once the fabric parameters are known. The fabric parameters are lower bound and upper bound for pore diameter, fabric porosity; and the liquid parameters are lower and upper bound for liquid density, lower and upper bound for liquid viscosity and liquid pressure. The initial population of individuals (different liquids in this case) need not be very good. In fact, each individual of an initial population usually represents a randomly generated candidate solution. By repeatedly applying selection and reproduction, GAs evolve satisfactory solutions quickly and efficiently. The user is able to select the application type: if barrier application is selected, then the GA searches for the liquid that will give the maximum time. If the user asks for filtration application, then the GA searches for the liquid that will give the minimum time. If the best liquid found cannot give the desired time for selected application type, then the user is able create and test another fabric by changing the fabric parameters.

The main target is to design a tool, which will allow the user search for different fabric-liquid combinations depending on the application type. This will reduce the need for testing, testing costs and help to save time.

Biography:

Evren Unsal has a BSc. Degree in Textile Engineering from Istanbul Technical University, and an MSc. Degree in Textile Engineering from Auburn University. She is currently a PhD student at Auburn University, Textile Engineering Department. Her research interests are protective textiles, filters, evolutionary computation and genetic algorithms.

Numerical Simulation of Hydroentangling Orifice Flow

H. Vahedi Tafreshi and B. Pourdeyhimi
Nonwovens Cooperative Research Center, North Carolina State University, Raleigh, NC 27695-8301 hvtafres@unity.ncsu.edu

Hydroentanglement is a process for entangling and mechanically bonding a web of loose fibers to form a uniform sheet or fabric. The underlying mechanism in hydroentanglement is exposing the fibers to a non-uniform pressure field created by a successive bank of high velocity waterjets. The impact of the waterjets with the fibers, while they are in contact with their neighbors, displaces and rotates them with respect to the neighbors and entangles them with each other.

Typical hydroentangling nozzles are made up of two sections; a cylindrical section (capillary part) with a typical diameter of about 120 micron, connected to a slim cone with an angle of about 18 degrees. They are usually made from a stainless steal strip with a thickness of about 1 millimeter. This work deals with simulating the water flow inside the above-mentioned nozzles. Particular attention has been paid to the effects of orifice shape on the waterjet properties. Axi-symmetric steady state model is considered for simulating the two-phase orifice flow in different configurations. Flow is considered to be turbulent and its turbulence features are captured with Realizable k-ε model.

This work has made a close comparison between the characteristics of the waterjets issued from cone-up (conical section as inlet) and cone-down (capillary section as inlet) configurations. We discuss the role of cavitation (referred to the condition where vapor bubbles form in a liquid flow because of the local pressure drop) in the above configurations and highlight their effect on the characteristics of the waterjets. Briefly, cavitation gives rise to the production of a large amount of turbulence that causes the waterjet to break up soon after discharge. Therefore, the lower the cavitation, the higher is the stability of the waterjet. On the contrary, extensive cavitation may results in the formation of a constricted jet wherein the water is separated from the nozzle walls by an air gap enveloping the water flow (hydraulic flip). At this point the cavitation stops because the low-pressure separated region is filled with the downstream ambient air. This results in a significant reduction in the wall friction, and its subsequent turbulence. The constricted jets are known for having a smooth surface and a long intact length.

Our simulation (performed for a manifold pressure of 120 atm) revealed that the waterjets produced by the cone-up orifice keep contact with the nozzle wall all the way through the orifice and undergo cavitation. In contrast, the cone-down geometry can form a constricted waterjet suitable for hydroentangling purposes. The reason for this different behavior is believed to be attributed to the inability of the water flow to follow the orifice wall at the sudden ninety-degree turn in the cone-down condition (vena contracta). The vena contracta is not likely to form in a cone-up configuration having a small cone angle due to the fact that the flow is turning a mild angle when it enters the capillary. However, changing the cone angle in the cone-up configuration, we observed the formation of constricted waterjet.

To investigate the effect of the cone angle and the nozzle aspect ratio (ratio between the capillary diameter to its length) in the cone-down configuration, we simulated different cones having angles smaller that 18 and different capillaries having aspect ratios greater than one. Within the framework of steady state simulation no effects on the constricted waterjet have been observed.

Simulations show almost equal mean axial velocity in both cone-up and cone-down cases implying negligible energy loss associated with the cone direction. Maximum axial velocity is seen to be about 157 m/s.

Discharge coefficient (defined as the ratio of the flow rates obtained from viscous turbulent flow numerical simulation to that obtained by the simple one-dimensional inviscid theory) in the cone-down orifice is considerably lower than that in its the cone-up counterpart. However, the velocity coefficients (ratio of the axial velocities in viscous and inviscid theories) are almost the same in both cases. Comparing our discharge and velocity coefficient with the available experimental data, we observed an excellent agreement verifying the reliability of our simulations.

Presenting author's biography:

Hooman received his BS and MS in Mechanical Engineering in Tehran, Iran. He then moved to Lappeenranta, Finland where he obtained his PhD in Energy Technology. He served as Research Associate at the University of Milan, Italy for two years after his graduation. Hooman has joined Nonwovens Cooperative Research Center, North Carolina State University since October 2001 and is involved with simulation and experiment on the hydroentangling waterjets.

Fiber-to-Fiber Load Transfer in the Extension of Twisted Yarns

Thomas A. Godfrey[1], John N. Rossettos[2], Sinan Müftü[2]
[1]Natick Soldier Center, US Army Soldier & Biological Chemical Command,Natick, MA 01760-5020, U.S.A.
[2]Department of Mechanical Engineering, Northeastern University, Boston, MA 02115-5096, U.S.A.

Fiber-to-fiber load transfer plays a crucial role in the mechanical behavior of fibrous assemblies. In staple fiber yarns, load transfer between the short fibers is essential for the yarn to have any degree of structural integrity. In continuous filament yarns, fiber-to-fiber load transfer becomes important in the tensile failure process. As isolated fiber breaks develop, load transfer mechanisms act to redistribute tension around breaks and the resulting load sharing patterns influence the progression of fiber breakage leading up to complete yarn rupture. The load transfer phenomenon is complex, involving friction between abutting fiber surfaces that may or may not be slipping. The magnitude of the inter-fiber frictional forces is strongly dependent on the current deformed state of the yarn, where lateral compression, due to twist, increases with increasing yarn tension.

Recently, fragmentation processes occurring in yarn extension have been recognized as having an important influence on overall mechanical behavior [1, 2]. In blended yarns composed of fibers with significantly different breaking elongations, the low-elongation-to-break (LE) fibers undergo a successive fragmentation process, where the LE fibers develop multiple breaks along their lengths. First, a series of isolated breaks develop along the LE fibers. As the nominal strain in the neighborhood of an LE fiber is increased, intermediate breaks occur, such that the LE fibers are broken into fragments with an identifiable average length. With continued extension, the fragments develop additional breaks, and so the fragment size becomes progressively smaller. Clearly, fiber-to-fiber load transfer makes LE fiber fragmentation possible by allowing short lengths of the fiber to build up a sufficient load to break the fiber. As in fibrous composites, where fiber fragmentation is used to investigate the shear strength of the fiber-matrix interface [3, 4], fragmentation provides a means to quantify fiber-to-fiber load transfer experimentally.

We have begun a series of experiments to investigate fiber-to-fiber frictional interactions in twisted fibrous structures. In one approach, we embed an LE component (which may itself be a twisted structure, such as cotton sewing thread) within a parallel bundle of HE components. The LE/HE bundle is then helically wrapped with a sheath of fairly stiff yarn or cord. As the entire assembly is extended, the helically wound outer sheath produces lateral compression in the inner bundle, simulating the internal stresses within large twisted yarns or cords. The LE component undergoes fragmentation, and the fragment lengths at given nominal strains in the LE/HE bundle can be used to reveal aspects of the component interactions. In addition, attempts are being made to directly observe the extents over which slip is occurring near the broken ends of the LE component.

In this paper, we review a previously developed micromechanical model [5] for the interactions in a mixed array of elastic fibers representing the microstructure of a blended yarn undergoing LE fiber fragmentation. We discuss the use of the model as an analytical framework to interpret fiber-to-fiber load transfer in yarn fragmentation experiments. Our ongoing experiments with LE/HE bundles are presented to illustrate the fragmentation process and the results of these experiments are discussed in the context of the model.

References:

1. Pan, N., Hua, T. and Qui, Yiping, *Textile Res. J.* **71**(11), 960-964 (2001).
2. Realff, M.L., Pan, N., Seo, M., Boyce, M.C., and Backer, S., *Textile Res. J.* **70**(5), 415-430 (2000).
3. Drzal, L.T., Rich, M.J., and Lloyd, P.F., *J. Adhes.* **16**, 1 (1982).
4. Drzal, L.T., Rich, M.J., and Lloyd, P.F., *J. Adhes.* **16**, 133 (1983).
5. Godfrey, T.A. and Rossettos, J.N., *Textile Res. J.* **71**(10), 845-854 (2001).

Biographical Sketch

Thomas A. Godfrey is a research engineer with the US Army Natick Soldier Center in Natick, Massachusetts. Dr. Godfrey's research interest is in the structural mechanics of textile materials with applications to individual protection, inflatable structures, and airdrop systems. He received master's and doctoral degrees in mechanical engineering from Northeastern University and a BSME from Rensselaer Polytechnic Institute.

Liquid Interactions in Electrospun Fibrous Membranes - Effects of Electrospinning and Chemical Reactions

You-Lo Hsieh
Fiber and Polymer Science, University of California at Davis, Davis, CA 95616, (530) 752-0843; ylhsieh@ucdavis.edu

Electrospun fibrous membranes are unique in many respects. Geometrically, the fiber diameters can range from a few μm down to ~ 40 nm and their pore sizes and porosity can be equally variable. Due to these unique dimensional characteristics and their potential technical applications, there is great value in understanding the surface characteristics as well as overall structure and properties of electrospun fibers. This paper examines surface and liquid wetting properties of electrospun fibers both natural and synthetic polymers. The varying fiber dimensions and pore structures could be achieved by controlling the properties of the polymer solutions as well as the electrospinning processes (Figure 1). In-situ as well as postelectrospinning chemical reactions and modifications further alter fiber chemistry and, if desired, morphology (Figure 2). The effects of these geometric variations and chemical alterations on the liquid wetting and absorption behaviors will be presented.

Figure 1. Varying fiber sizes and packing as well as pore structure of same chemical composition

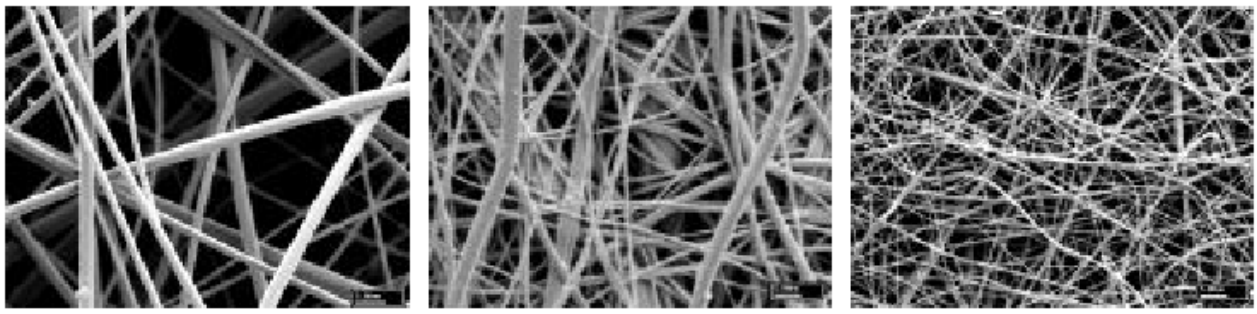

a b c

Figure 2. Chemically modification to polar, reactive and grafted surfaces from 1a.

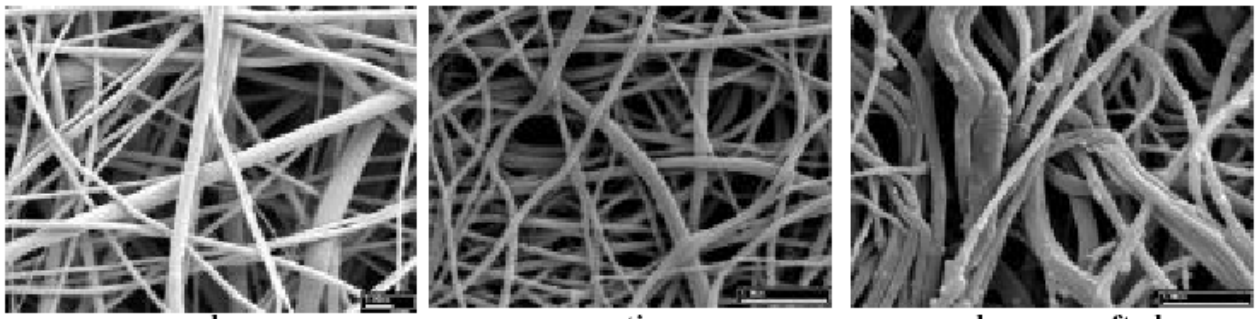

polar reactive polymer grafted

Comfort, Muscle Tension & UV Protection

Malgorzata Zimniewska, Ryszard Kozlowski, Michal Rawluk
The Institute of Natural Fibres, Poznan, Poland

Present studies were undertaken to determine the influence of natural and synthetic fibres, which were covering transiently the forearm muscles on activity of motor units of these muscles. These have been studied in resting conditions of the volunteers and during movements as well. Additionally, assessment of the motor fibres transmission within the nerves supplying the investigated muscles was performed.

The results of electromyographical studies of two groups of subjects, wearing the natural and synthetics shirts, shown:

1. Temporary covering of tested forearm muscles with the synthetic clothing changes the pattern of motor unit activity. It is expressed with the low –frequency spontaneous activity of the muscle fibres during the resting state or diminished high-frequency activity of the motor units during the movement. These phenomena are correlated to the slight changes in the motor conduction velocities of the nerve fibres supplying the muscles.
2. Covering the forearm with the natural clothing doesn't evoke the phenomenon described in conclusion 1.
3. Comparison of the results obtained in both groups of subjects with the controls ones, leads to the conclusion, that slight changes in the activity of the muscle motor units observed in group of synthetic clothing are not pathological.
4. Fluctuations are the reason of desynchronization in muscle motor units that may lead towards higher tendency to fatigue during using the synthetic garments.
5. The electric charges gathered on the polyester cloth surface creating an electrostatic field at the skin-cloth zone as well as the increase of the body temperature in case of the polyester cloth might be a cause for the observed changes.

Another factor influencing the safety of clothing is its protection against hazardous UV radiation. In every culture sun is the symbol of life, living and joy. But sun has not only good influence on human's life. Very often we do not realize that staying outside for a long period we are often exposed to UV radiation and its overdose. This can cause erythema, sun allergies, faster skin ageing and skin cancers, especially melanoma, which is caused by damage to the chromosomes in the cells of our body.

That's why there is a need for efficient protection against harmful radiation. And this should be an aim for textiler's activities: to work up the production of apparels with high Sun Protection Factor (SPF). That can be ensured with production on base of such bast fibres like linen and hemp that also give high use comfort thanks to high hygroscopicity and air permeability. Fabrics made of yarns based on bast fibres have "cool touch" and do not have the ability for gathering electric particles on their surface. The fibres are a perfect absorbent for UV radiation thanks to lignin that are one of their components.
Second part of the paper introduces research results on Ultraviolet Protection Factor (UPF) of weaved and knitted fabrics made of linen and hemp and their blends with other fibres. It also describes the influence of fabric's structure, its density, weight, surface mass and color on level of UV protection.

Determination of the UVR transmission of a dry textile was done in accordance to Australian/New Zealand Standard for sun protection clothing.

A Stochastic Simulation of Interfacial Failure in Fiber Reinforced Polymer Composites

Wen Zhong and Ning Pan
Division of Textiles and Clothing
Biological & Agricultural Engineering
University of California at Davis, CA 95616

A stochastic approach, Ising model combined with Monte Carlo simulation, is employed to study the process of interfacial failure in fiber reinforced polymer composites. The complicated mechanisms involved during the failure can be realistically simulated with a simple algorithm generating robotically predictive results. Specifically, the properties of the materials are statistical variables, the interfaces between fibers and matrix could hardly be viewed as perfect, and the debonding and failure behaviors show a stochastic nature, justifying the use and power of such stochastic approaches as Monte Carlo simulation in predicting polymer-fiber interfacial behavior in composite studies.

In such a method, the target system is treated as being made up from such subsystems as fiber cells and matrix cells that are interacting with each other, including both cohesive interactions within fiber and matrix respectively, and adhesive interactions between fiber and matrix. The interfacial debonding, fiber breaking and/or matrix yielding processes are the results of such interactions.

To demonstrate the validity and usefulness of the approach, two popular experimental techniques, single fiber pull out and single fiber peel tests, are chosen as the subjects for simulation. The examples shown in the parametric studies are in good accord with the experimental results reported in existing literature.

All the factors contributing to these phenomena can be represented in the internal energy expression of the system, where the characteristics of the media involved are reflected by the corresponding coefficients. Accordingly, parametric studies can be performed by adjusting these coefficients to investigate their effects on the system behaviors.

Strain Sensitivity of Polypyrrole-Coated Fabrics under Unidirectional Tensile Deformation

M.Y. Leung, X.M. Tao and M.C.W. Yuen
Institute of Textiles and Clothing, The Hong Kong Polytechnic University, Hung Hom, Kowloon, Hong Kong, E-mail: tclens@inet.polyu.edu.hk, Tele: 852-27666487, Fax: 852-27731432

INTRODUCTION

Sensitivity of textile substrates coated with conducting polymer towards various stimuli like temperature, strains, humidity and recently chemical gases etc. has attracted great interests [1-4]. The polypyrrole-coated fabrics have been demonstrated to possess sensing capacity of strain and temperature. It is most interesting that the gauge factor, i.e. the strain sensitivity factor, varies drastically from the polymer film (0.4 to 0.9) to the coated fabric (-12.5 to –13.3), highlighting the importance of the effects of textile structures [4]. However, the mechanisms on the influence of textile structures to the gauge factor is still very unclear. It is most interesting to investigate the relationships between the electrical conductivity and structures of conducting textile fabrics under repeated large deformation. In the present paper, an attempt is made to develop theoretical treatments for conducting textile structures. The gauge factor or strain sensitivity factor of textile sensor in relation to various degrees of deformation are studied and reported. An example will be given on a plain weave fabric made from 100% of spandex yarns.

THEORETICAL ANALYSIS

Conductive textile structures of either plain weave or a plain knitted structure can be generally represented by an electrical network. The resultant resistance of the structure can be calculated as $V/\sum I_{i(\varepsilon)}$. V: voltage applied, $I_{i(\varepsilon)}$ is the current flows through each part of conductive yarn.

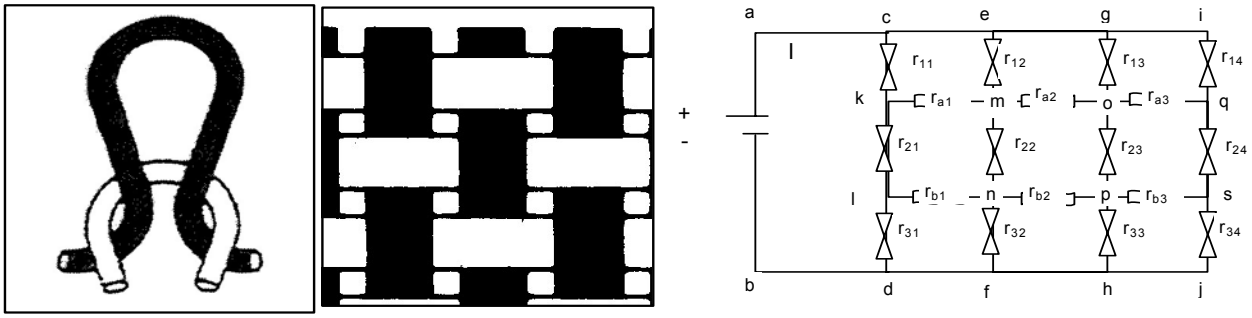

Figure 1. (a) Common textile structures, plain weave and a plain knitted fabric. (b) Electrical network represents the conductive textile structure.

By, using a plain weave fabric as an example and assuming that all resistance in each vertical lines are of the same values and resistance of all horizontal lines are equal. According to the resultant resistance approach, the resultant total resistance of the textile structure (Rt) can be simply expressed by the following equation:

Eq. 1. $$Rt = \frac{(Np - 1) \times R_f}{Ne}$$

Rt: is the resultant total resistance of the structure; Np is the no.s of picks/ gauge length; Ne is the no.s of ends/ width; Rf is the resistance of individual filament per unit pick of the structure.

In this calculation, only DC current is applied on the material so that the effect of capacitance can be assumed to be minimized. During large tensile deformation up to 50% extension, resistance change depends highly on extension (ε), gauge factor or strain sensitivity factor can be illustrated as:

Eq. 2 $$\frac{\partial Rt}{\partial \varepsilon} = \frac{(Np_o - 1)\,\partial R_f/\partial \varepsilon}{Ne_o} + \frac{R_f\,(\partial Np_o)}{Ne_o\,(\partial \varepsilon)} - \frac{(Np_o-1)R_f\,(\partial Ne_o)}{Ne_o^2\,(\partial \varepsilon)}$$

∂Rt: change of resultant resistance of the structure; Npo is the original no.s of picks/ gauge length; Neo is the original no.s of ends/width; ∂Rf is change of resistance of filament.

It is illustrated by the above equation, gauge factor is dependent on the variables: $\partial R_f/\partial\varepsilon$, $\partial Np_o/\partial\varepsilon$ and $\partial Ne_o/\partial\varepsilon$. According to the large edging effect for short gauge length, it can be assumed that there is no change of ends/width for a short gauge length (e.g. 1 inch) is used during extension. Thus ∂Neo/∂ε = 0.

Assume that the change of spacing between picks are evenly distributed, change of picks density during extension can be expressed as:

Eq. 3 $$\partial Np_o/\partial\varepsilon = (1/1+\varepsilon)' Np_o, \text{ thus } \partial Np_o/\partial\varepsilon = -Np_o/(1+\varepsilon)^2$$

Experiment is made to determine the variable $\partial R_f/\partial\varepsilon$. Polypyrrole-coated textile fabrics and filaments is prepared by vapor deposition in vacuum at 20°C for 24 hours, 10 wt% FeCl3 is used as oxidizing agent. Conductivity is measured in line with extension. It is given by figure 2 that the relationship between the electrical resistance of filament and extension is almost linear in all cases for the1st, 5th and 10th cycle of extension. The slopes of equations range from 0.43 to 0.47. Thus, it can be assumed that in the equation $R_f = a\varepsilon + b\varepsilon^2 + c$, the constant "b" is approximately equal to zero and $R_f = a\varepsilon + c$. Therefore, resistance change for filament during extension is constant ($\partial R_f/\partial\varepsilon = a$):

Eq. 4 $$\partial R_f/\partial\varepsilon = a$$

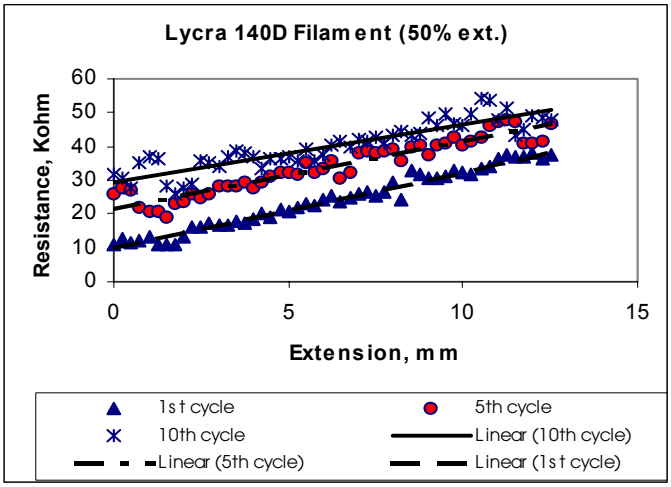

Figure 2: Resistance of filaments R_f against Extension ε.

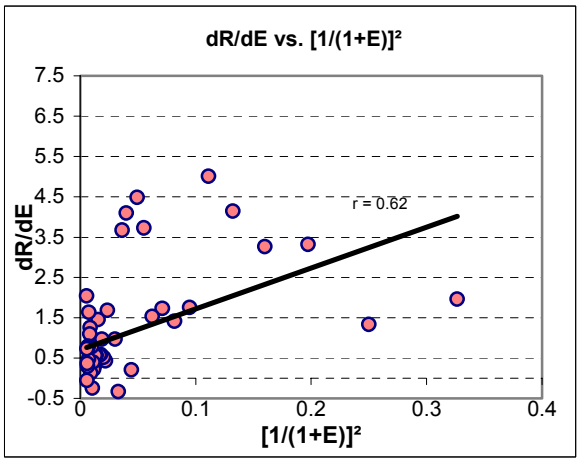

Figure 3: Gauge Factor plots against $(1/1+\varepsilon)^2$

Combining equations (1) to (4), ignoring the transverse contraction during the deformation, the gauge factor can be represented as the following equation:

Eq. 5 $$\frac{\partial Rt}{\partial \varepsilon} = \frac{(Np_o - 1)\,a}{Ne_o} + \frac{R_f\,[-Np_o]}{Ne_o\,(1+\varepsilon)^2} = C_1 - \frac{C_2}{(1+\varepsilon)^2}$$

RESULT AND DISCUSSION

The gauge factor expressed by Eq.5 suggests that it is adversely proportional to $(1+\varepsilon)^2$, their relationship is shown in figure 3. The linear correlation coefficient r = 0.62. It is noted that the negative sign of the $-C_2/(1+\varepsilon)^2$ indicates that gauge factor can switch from positive to negative depending on the extension level applied. This result coincides with the previous finding [Rossi 1999] that the strain gauge factor changes from + ve sign for a Ppy film to negative for Ppy-coated Lycra fabric. The obvious scattering of data may be due to the non-uniform contraction of the fabric and variations in the yarn properties, which are under our current investigation.

REFERENCE:

1. Collins, G.E. and Buckley, L.J., Synthetic Metals, 1996, 78, 93-101.
2. Heisey, C.L. and Wightman, J.P., Pittman, E.H. and Kuhn, H.H., TRJ, 1993, 63(5), 247-256.
3. Kuhn, H.H. and Kimbell, W.C., Worrell, G., and Chen, C.S., ANTEC, 1991, 760-764.
4. Rossi, D.D., Santa, A.D., Mazzoldi, A., Materials Science and Engineering, 1999, C1, 31-35.

Biography of Presenting Author:

Presenter: Dr. M.Y. Leung

Dr. M.Y. Leung is a Lecturer of the Institute of Textiles of Clothing, the Hong Kong Polytechnic University. Dr. Leung gained her PhD in Fabric Objective Measurement from the Hong Kong Polytechnic University in 2000. Her research interests cover: fabric objective measurement techniques for textiles and clothing. fibre and fabric physics. Currently she participates in the investigation of conducting polymers for smart textile application. Her current teaching specialisms includes product quality and evaluation, non-apparel textiles, textile product development.

Heat Resistance and Flammability of High Performance Fibers for Protective Clothing (Virgin Fibers and Blends of High Performance and Natural Fibers)

Xavier Flambard [1], Serge Bourbigot, Manuela Ferreira and Bernard Vermeulen
Laboratoire de Génie et Matériaux Textiles (GEMTEX), UPRES EA2461, Ecole Nationale Supérieure des Arts et Industries Textiles (ENSAIT), BP 30329, 59056 Roubaix Cedex 01, France

The demands of the market for high performance fibers are "faster, stronger, lighter, safer". Fortunately, high performance and high temperature resistant fibers have been developed to aid in allowing products to meet these challenges. High-performance fibers are driven by special technical functions that require specific physical properties unique to these fibers. They usually have very high levels of at least one of the following properties: tensile strength, operating temperature, heat resistance, flame retardancy and chemical resistance. One might define the fibers under consideration as those with very high performance characteristics. Those fibers can be used alone or blended with other fibers (natural fibers for instance) in order to obtain synergistic effects.

In a first part, heat and flame resistance of main virgin high performance fibers are reviewed according to literature data. Some selected high performance fibers are then evaluated using the cone calorimeter as fire model to provide realistic data on fire behaviour of the fibers. They are also examined in terms of heat resistance using TGA. The results are discussed and compared with literature data. Heterocyclic rigid-rod polymers (poly(p-phenylene-2,6-benzobisoxazole or PBO (Zylon®) and poly(2,6-diimidazo (4,5-b:4',5'-e) pyridinylene-1,4 (2,5-dihydroxy) phenylene or PIPD (M5)) exhibit the best performance (no contribution to fire, low smoke and good heat resistance) and offer good combination between heat and flame resistance and mechanical properties .

In a second part, textile blended structures with natural and high performance fibers have been studied. High performances fibers as para-aramides, polyphenylenebenzobisoxazole, polyimide, polyether-etherketone…, have been developed to provide properties such as high operating temperature, heat resistance, flame retardancy. But these fibers are the low UV resistance and a bad handle in fabric. In opposite, natural fibers such as cotton or wool have a good handle but a poor fire resistance. Recently, we have shown combining p-aramides with wool a synergistic effect in terms of heat release. Combinations Wool-PPTA (Poly-p-phenylenediamine-terephtalamide fibers or Kevlar®) were blended fibers by fibers using spinning process. Synergistic effect are observed at low amount of PPTA (30 wt.-%) (Figure 1). This combination has an other advantage : decreasing the cost.

A new spinning process, Dref technology, as been performed to produce new blended yarns of PPTA fibers, covered by wool. This process allows to obtain a better protection against UV but decreases synergistic FR performances.

[1] *To whom all correspondence should be addressed*

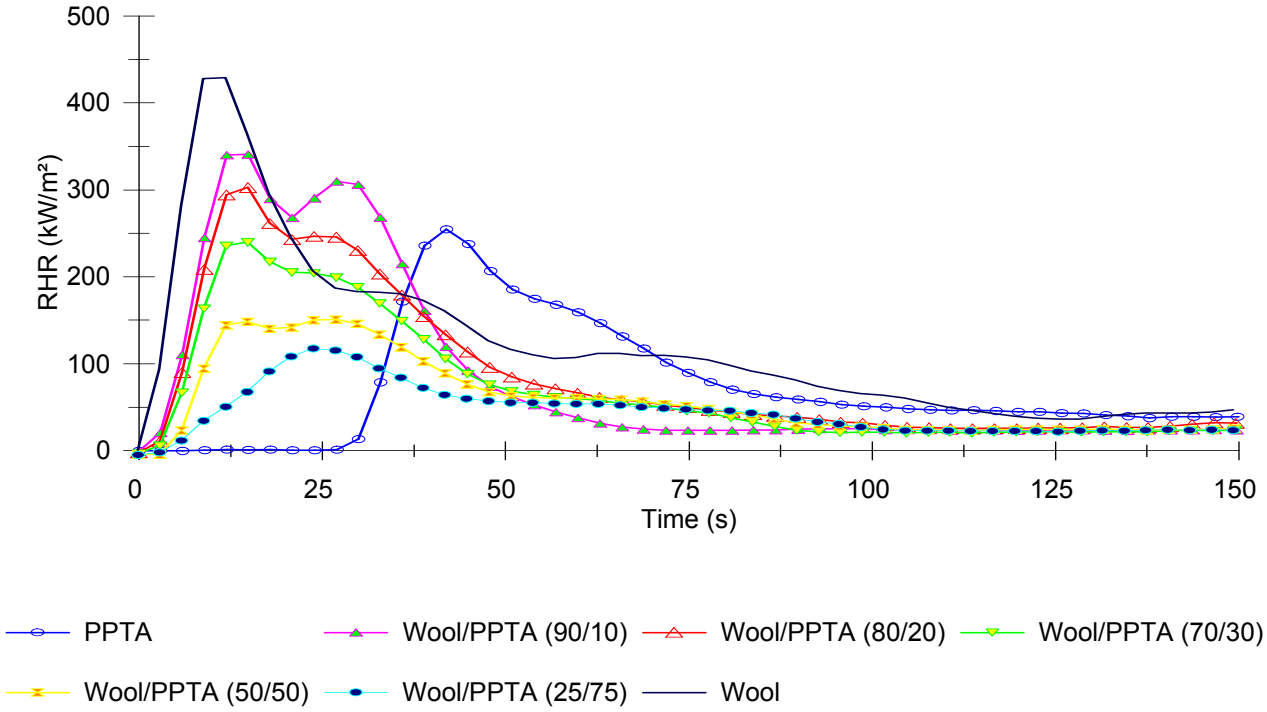

Figure 1 : *Rate of Heat Release (RHR) curves of blends Wool/PPTA (Poly-p-phenylenediamine-terephtalamide fibers or Kevlar®) (external heat flux = 75 kW/m²).*

The combination of wool with high performance yields fabric with the properties of interest (flame retardancy) and a good-hand. In the pursuit of our efforts to make high performance fabrics at acceptable cost, this work investigates combination of wool with high performance fibers (phenolic fibers (Kynol®) and oxidized polyacrylonitrile (PANox)) in order to detect possible synergistic effects. Recycled fibers (PPTA, PANox) are also considered because of their low cost. The reaction to fire of the fabrics are evaluated using the cone calorimeter as fire model. The heat resistance of the fabrics is measured using thermal analyses. Finally, the mechanisms of degradation of the fabrics are discussed.

Curriculum vitae

Dr. Xavier Flambard

Date of birth : 16 th january 1968 (34 years old)
French nationality

Assistant Professor at ENSAIT
Head of the Knitting department of ENSAIT
Knitting Teacher – researcher in thermal, fire and mechanical protective textiles

ENSAIT (Ecole Nationale Supérieure des Arts et Industries Textiles)
9, rue de l'Ermitage (B.P. 30329), 59070 Roubaix Cedex 1
Phone : +33 (0)3.20.25.64.78 Fax : 03.20.27.25.97
E-Mail : mailto:xavier.flambard@ensait.fr

Education

1992 :	Equivalent to a Master of Science in Textile Engineering
in french	Diplôme d'Ingénieur ENSAIT
1993 :	Equivalent to a Master of Science in Polymer Chemistry
in french	Diplôme d'Etudes Approfondies (D.E.A.)
2000	PhD in mechanical at Lille I
	Title : Technical knitted textiles for thermal, fire and mechanical protection

Fields of competence

Knitting technology
Flame retardant behavior of protective fabrics
Cutting resistance of protective fabrics
Stab resistance of protective fabrics

Antibacterial Activity of Polyamide Fabrics

D. Saihi [1,*], A. El-Achari [1], A. Ghenaim [2], C. Caze [1]
[1] GEMTEX Research Laboratory, Ecole Nationale Supérieure des Arts et Industries Textiles, F-59056 Roubaix Cedex 1, France, [2] Ecole Nationale Supérieure des Arts et Industries de Strasbourg, F-67084 Strasbourg Cedex, France
* Corresponding author. Fax: +33 (0) 3 20 27 25 97, E-mail address: **dhouha.saihi@ensait.fr** (D. Saihi)

Graft copolymerisation of methacryloyloxyethyl trimethyl ammonium chloride monomer (METAC) on polyamide fabrics using benzoyl peroxide as initiator was carried out. The content of METAC on polyamide fabrics is an important factor to affect their antibacterial activity. The graft yield was studied as a function of the different variable conditions such as monomer concentration, initiator concentration, temperature, and reaction time.

Antibacterial activities of grafted polyamide fabrics were evaluated by a viable cell counting method. Treated textile is put in contact with a bacteria medium. The numbers of viable cells were calculated by counting the numbers of the colonies.

The impact of the grafting is evaluated by several techniques: crystallinity (Thermal Analysis), surface topography (Atomic Force Microscope and profilometer) and wettability (Digidrop instrument).

DSC allowed us to measure crystallinity of polyamide crystallites before and after grafting, thus, to localize grafted monomer chains. By using AFM / lateral force microscopy, a comparative study of the topography as well as the tribological properties was done. From the surface topography, the surface roughness corresponding to variations in the height of the surface

relative to a reference plane was measured. AFM imaging was achieved in air under atmospheric conditions with a commercial scanning probe, Nanoscope III, from Digital Inc. Profilometer allows characterizing and studying the surfaces and roughness as well as the chemical elements. This device is used to measure the vertical profile of samples such as substrates. It records the step-heights of the sample and traces them onto a grid (macroscopic scale). By characterising surface free energy, the degree of water repellency can be evaluated. The DigiDrop from GBX is an instrument for precisely measuring contact angle. This method is used to determinate the surface fabric wettability by probe liquids (water, mineral oil).

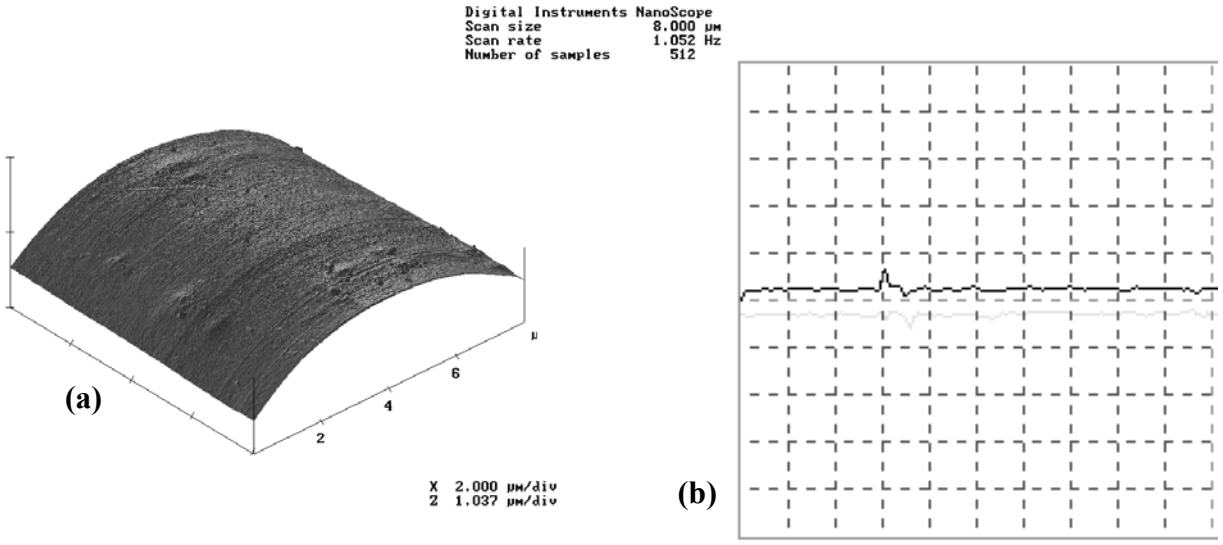

Figure : Polyamide fiber (a) topographic image ;

(b) scope-mode forward and backward scanned AFM and LFM signals.

Innovative Assembly- Future Clothing Fabrication Processes

Steve Szczesuil, Steven Paquette, Brian Corner, and Peng Li
U.S. Army Soldier Systems Center, Natick, Massachusetts

Compared to other technologies, the history of apparel manufacturing has changed little since the invention of the sewing machine by Elias Howe in 1854.

Other technologies such as aircraft, medical, construction, plastic, automobile, electronic and computer that essentially started during early to mid 1900's, have all accelerated at light speed compared to the sewn apparel trade thanks largely through continuing R&D efforts.

The sewn trade has borrowed from the computer industry the capability to computerize the sewing machine with automatic stitch length control, counters, embroidered design pattern control and automatic backtacking. Also, there has been developed specific automatic function controls for attaching collars, cuffs, front plackets, buttons, zippers and hemming equipment for shirts and waistbands, pockets, automatic leg seaming, etc. operations for trousers.

However, the majority of mass production equipment still remains to be the basic sewing machine. The American apparel trade stands at the crossroads of competition from workers within the US, NAFTA, foreign and strict internal regulations. The answer for the sewn trade is a higher level of R&D effort, to achieve greater automation and possibly develop an alternative apparel fabrication process, including Three-Dimensional (3-D) body scanning to create the patterns for the end-item.

Since 1989, the military has taken the lead in attempting to develop 'Stitchless' technology as a viable alternate fabrication process. During this time frame Clemson University developed a two-step 'Stitchless' process, for use on a Chemical Protective uniform. They proved the concept, but could not automated, due to multiple steps in the process.

The latest development comes from Clemson again with the promise of a single step process patented under the name of 'Dura-Seal'. Upon completion of some baseline equipment, the seam shall offer a hermetically sealed seam with 100 percent seam-efficiency with baseline CP and rainwear types of fabric. The process even works with Butyl rubber coated fabric. For environmental resistant end-items, the 'Dura-Seal' provides a significant hydrostatic resistance to maintain waterproofness.

In an attempt to develop a link between this novel manufacturing process and a made-to-measure process of clothing design and fabrication for applications such as chemical protection, it was decided to use the Extended Cold Weather Clothing System (ECWCS) parker and trouser as the initial test case. U.S. Army Natick anthropologists utilized a 3D whole body scanning system to provide body size information for a sample of three individuals. These individuals ranged in body size from small to xxx-large for both the upper and lower body garments. The anthropometric data used to create custom ECWCS garments were generated from laser scans using a specialized data extraction software (Natick-measure) which automatically measures the human body and outputs this information for use. Each individual's anthropometric data were then sent electronically to Clemson for pattern generation and manufacture. The coats and trousers were then fabricated in a matter of days and then shipped back to Natick for fit evaluation on the original test subjects. Results of the subject fit tests indicate that the ECWCS garments generally provided an acceptable level of fit, especially for the size medium test subject. Jacket and trouser length for the other two subjects tended to be somewhat long, but overall the items fit well. Follow-on efforts will attempt to improve the translation of the body size data to pattern dimensions. Overall, the results of this study indicate that the concept of integrating fully automated measuring with custom fabrication of a stitchless garment is viable for military applications such as chemical protection and it holds promise for other uses where a quick turnaround is required.

Studies on the internal structure of Nanofibers

R. Dersch, Taiqi Liu, A. K. Schaper, A. Greiner, J.H. Wendorff
Department of Chemistry and Material Science Center,
Philipps University, Marburg, Hans-Meerwein-Strasse, D-35032 Marburg, Germany

The production of very thin fibers in the range below one micrometer gives opportunities for many applications such as special filters or nanoreinforcement among many others. It is desirable to understand and control the internal structure of these fibers to allow a controlled modification of their mechanical and other properties. In our studies we were interested in the crystal modifications and orientations that could be obtained via electrospinning. The structure formation takes place very fast, so that the resulting structure in the fiber should be far from equilibrium. We found for polyamide 6, that the electrospun fibers consisted of the rather disordered γ-phase. This has also been reported for fibers with diameters well above the micrometer range obtained by extrusion.

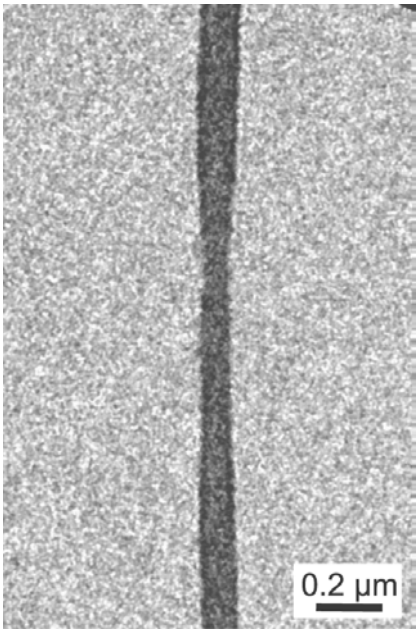

PA 6 fiber

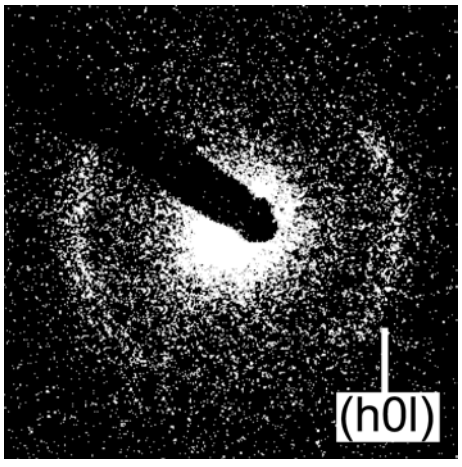

(a)

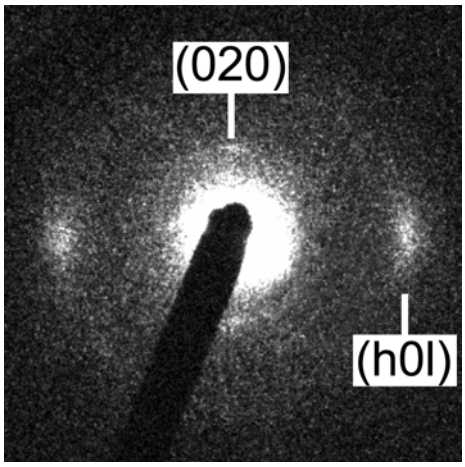

(b)

Electron diffraction patterns of different regions along a PA 6 fiber:

a) low orientation showing only (h0l) equatorial reflections
b) high orientation displaying even the meridional (020) reflection

Nucleating agents like polyamide-66, Al_2O_3 and $Ca(C_{17}H_{35}COO)_2$ did not affect the structure formation. X-ray diffraction studies showed that the azimuthal intensity distribution measured on sets of parallel fibers was approximately homogenous. So despite the strong elongation and the rapid structure formation during the spinning process no significant average crystal orientation could be observed. Electron diffraction studies on single fibers showed that the orientation of the crystals along the fiber axis is very inhomogeneous. Both areas of high and low orientation could be found along individual fibers. For polylactide we found that the electrospinning process also had little influence on the average degree of crystallinity. With electron diffraction studies no inhomogenities could be detected. Additional studies have been made for other partly crystalline polymers like PVDF.

Biography:
R.Dersch was born in 1974. He studied Chemistry in Marburg and Edinburgh and received his Diploma in Marburg 2001. His thesis was about complex structured electrospun fibers made by phase separation processes or by incorporation of different additives. He is currently working on his Ph.D.thesis in the group of Prof. J.H. Wendorff at the Philipps-University in Marburg. His areas of interest include structure formation in electrospun fibers and the investigation of single fiber properties.

Resistance of Staple Yarns to Dynamic Loading

Maria Cybulska
Department of Textile Architecture, Faculty of Textile Engineering and Marketing,
Technical University of Lodz, Poland

Most publications on mechanics of staple yarns are primarily concerned with the tensile behavior of yarns under a static load. However, when processed, yarn is subjected to many different loads, most of them of dynamic character. It has been shown [1] that qualitative evaluation of yarns based on static characteristics, like breaking load and elongation determined on the Instron tester, is not reflected in yarn behavior in industrial conditions, for instance, during weaving process. For this reason new testing methods have been applied in the study, among others CTT-BU Lawson-Hemphill tester and micropulsator developed at the Department of Textile Architecture, TU Lodz, to simulate loads, yarn is subjected to during processing, in order to analyze the yarn resistance to real loads taking place in industrial processes.

Material and methods

The following kinds of staple yarn have been chosen for study: air jet yarn, cotton/ polyester 50/50, 30 tex; vortex yarn, cotton 100, 22 tex, 685 twist/m; open end yarn cotton/polyester 50/50: 20 tex, 850 twists/m; 30 tex, 870 twists/m; 35 tex, 870 twists/m; 50 tex, 632 twists/m; ring-spun yarn, cotton/polyester 50/50: 15 tex, 860 twist/m; 20 tex, 825 twists/m, 25 tex, 803 twist/m; 30 tex; 554 twists/m; 40 tex, 580 twists/m.

Yarns were subjected to uniaxial loading on Instron tensile tester for sample length 300 mm and the cross-head speed 200 mm/min.; on CTT-BU Lawson-Hemphill tester for the yarn transport speeds 30, 50, 200, 350 m/min.; on the micropulsator for the load $F=F_0 \sin \omega t$, $F_0=70$ cN, $\omega=10/s$. Structural parameters of yarns were determined using image analysis methods [2].

For each yarn mean values of static breaking load F_S and elongation at break E_S, dynamic breaking load F_D and elongation at break E_D, mean value of the number of pulses till the yarn breakage N_P and values of yarn diameter, hairiness and twist parameter were determined.

Results of data analysis

Table 1: Correlation between mechanical properties and structural parameters of staple yarns

	Mechanical properties of yarn				Structural parameters of yarn			
	F_D	E_D	F_S	E_S	Diameter	Twist parameter	hairiness	Linear density
F_D					**0,8209 p=,001**	**0,707 p=,010**	-0,1687 p=,600	**0,8928 p=,000**
E_D	**0,819 p=,001**				**0,8371 p=,001**	**0,6892 p=,013**	-0,1621 p=,615	**0,85 p=,000**
F_S	**0,8395 p=,001**	**0,7181 p=,009**			**0,8797 p=,000**	0,5142 p=,095	-0,1106 p=,732	**0,8923 p=,000**
E_S	-0,1749 p=,587	-0,3193 p=,312	-0,0277 p=,932		-0,1915 p=,551	-0,1368 p=,672	0,058 p=,858	-0,2032 p=,527
N_P	**0,602 p=,038**	**0,607 p=,036**	0,2865 p=,366	-0,0321 0,921	0,466 p=,126	**0,8461 p=,000**	-0,5237 p=,081	0,5319 p=,075

All parameters characterizing yarn resistance to static and dynamic loading and structural parameters of yarn were analyzed using methods of correlation and regression. Table 1 presents coefficients of correlation, and corresponding significance levels, between all parameters on consideration. Results of data analysis show strong relationship between yarn structural parameters and

mechanical properties of yarn. Static breaking load depends mainly on yarn linear density. Elongation at break doesn't show any relation to the yarn structure.

Parameters characterizing the yarn resistance to dynamic loading - F_D, E_D and N_P, strongly depend on the twist parameter. Higher the twist parameter, higher the yarn resistance to dynamic loads. Dynamic breaking load and elongation depend also on the linear density of yarn.

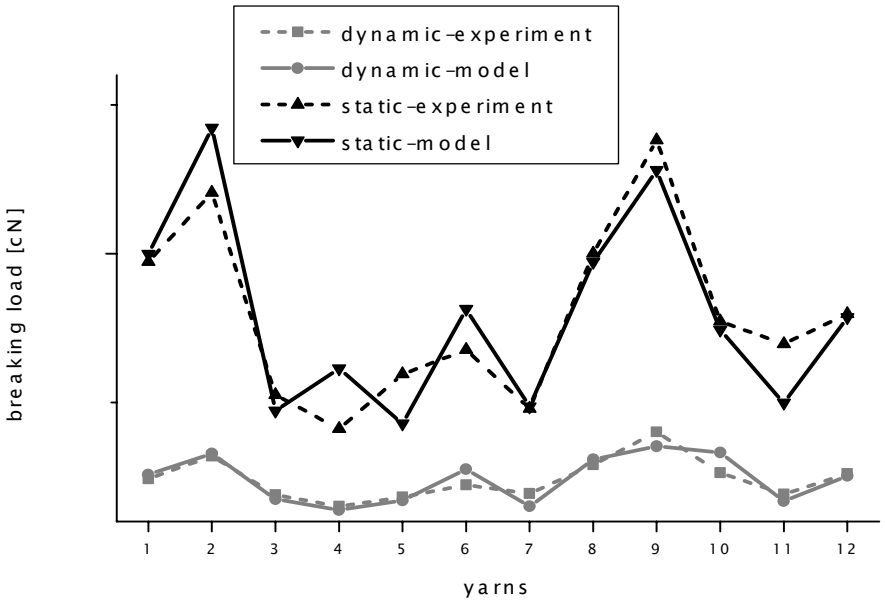

Figure 1: Static and dynamic breaking load - mean values obtained form experimental data and results of modelling on the basis of structural parameters of yarn

Figure 1 presents mean values of dynamic and static breaking load and results of modeling these parameters on the basis of linear density and twist parameter. It can be seen that dynamic and static breaking load, although correlated, are significantly different.

Elongation at break (Figure 2) under dynamic and static loads are even not correlated. In the same time parameters characterizing yarn behavior under dynamic load are mutually dependent. Yarn resistance to pulsatory loading doesn't depend on static yarn characteristics while it depends on dynamic breaking load and elongation.

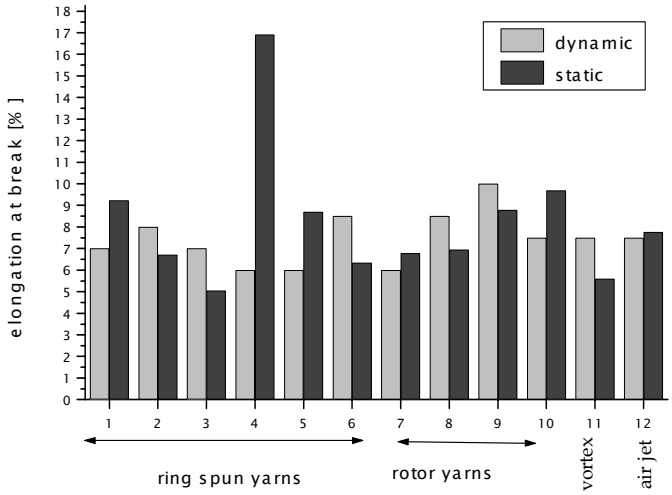

Figure 2: Static and dynamic elongation at break

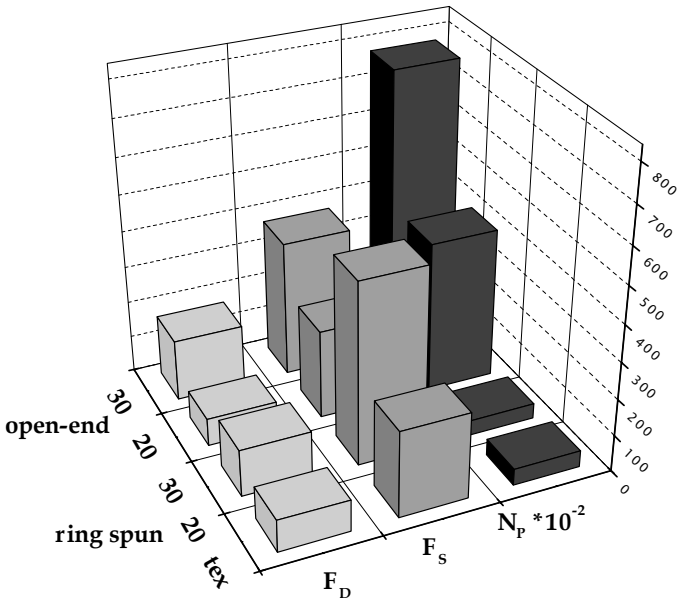

Figure 3: Static and dynamic characteristics of exemplary ring spun and open-end yarns

Although using structural parameters one can predict some tendencies in the number of pulses till break, it depends mainly on the yarn internal structure resulting from different yarn technology. It can be shown that despite yarn structural parameters, open-end yarns and air-jet yarns can be characterized with higher resistance to pulsatory loading than ring spun yarns. In Figure 3 one can see the diagram of static and dynamic breaking load and the number of pulses till break for 2 ring spun and 2 open-end yarns of the same linear densities. Resistance to the pulsatory loading of open-end yarn is about 10 times higher than that of ring spun yarn, while their static and dynamic breaking loads are similar.

Conclusions

Both dynamic and static characteristics of the yarn tensile behavior significantly depend on the yarn structure.

Static breaking load and elongation, although correlated with some dynamic characteristics of yarn, do not allow for a good prediction of the yarn behavior under dynamic loading, especially for prediction of the yarn behavior under pulsatory loading.

Yarn resistance to dynamic loading depends mainly on twist parameter which can determined in a way the compactness and "closure" of the yarn structure.

The results obtained show that yarn resistance to dynamic loading differs for different types of yarn. Open-end and air jet yarns due to their structure, among others the presence of wrapper fibbers, form more "compact and closed" structure, and are generally more resistant to the dynamic loading than more “open” ring spun yarns.

Acknowledgement: The research was financially supported by the Polish Committee for Scientific Research, project 7T08E 043 20

References

[1] Szosland, J.; Słodowy, J.; Snycerski, M..: Qualiwave- Quality Aspects in Weaving, University of Gent, ISBN 83-911159-0-9, Gent, (1998)

[2] Cybulska, M.: Assessing Yarn Structure with Image Analysis Methods , *Textile Res. J.*, **Vol.** 69 (1999) No.5, pp. 369-373

Author: Maria Cybulska, Ph.D., Department of Textile Architecture, Faculty of Textile Engineering and Marketing, Technical University of Lodz, Ul. Zeromskiego 116, 90-543 Lodz, Poland, Phone: +(48) (42) 631-33-37, fax: +(48) (42) 636-32-74, e-mail: cybulska@wipos.p.lodz.pl

Biography: M.Sc. in Applied Mathematics, Ph.D. at the Textile Faculty, TU Lodz, 1996, 1998-99 post-doc at Clemson University, from 2000 assistant professor - Department of Textile Architecture, TU Lodz, Poland.

Hot Compaction of PET Fibers: Influence of Processing on Crystallinity and Mechanical Properties

P. Rojanapitayakorn, P. T. Mather, R. A. Weiss, A. J. Goldberg†
Polymer Science Program and Dept. of Chemical Engineering,
University of Connecticut, Storrs CT 06269, USA
†UCONN Health Center, University of Connecticut, Farmington, CT 06034, USA

It has been demonstrated during the past decade that strongly anisotropic polymeric articles may be processed from semicrystalline polymers by compressing a weave of fibers at high pressure and at a temperature near, but below, the melting temperature – a process termed hot compaction. While being attractive in its simplicity, fundamental understanding of this process is lacking, leading to trial-and-error approaches when applying the process to a new polymer. In the present study, hot compaction was used to prepare thick films from commercial polyethylene terephthalate (PET) fibers. For each compaction run, a bundle of fibers was wound around a metal frame with a custom winder and subsequently compressed at a prescribed pressure and temperature followed by controlled cooling. Wide-angle x-ray diffraction (WAXD) was used to measure the degree of crystallization and molecular orientation of the resulting plaques. While the starting fibers had a degree of crystallinity of about 40 %, the compacted films were optically transparent but had a higher degree of crystallinity (55%). The molecular orientation of the PET increased by 38 %(from a Hermans orientation parameter of about 0.54 to 0.75) during the compaction process, which may be the result of constrained contraction of the fibers when compacted close to the melting temperature. The compacted films were anisotropic, with higher strength and modulus (180 MPa and 7 GPa) in the fiber alignment direction than that (30 MPa and 2 GPa) of unoriented PET. Scanning electron microscopy was used to investigate the adhesion between fibers in the compacted samples, revealing significant interfiber welding with some proportions of the fibers being melted during the process. Details of this microstructure are thought to control the mechanical properties, especially the transverse strength.

The presenter is Dr. Pichet Rojanapitayakorn

Dr. Pichet received his Bachelor degree in chemical engineering with the second honor from Chulalongkorn university, Bangkok, Thailand in 1994. He received a scholarship to pursue his Master/PhD study on polymer blend at the same university, during which he spent one year doing a research at Imperial College, university of London. After his PhD, he moved to university of Connecticut to continue doing a research in the polymer field as a postdoctorate fellow.

Characterization of conducting polymer nanofibers prepared via electrospinning

N.J. Pinto[1,*], Y.X. Zhou[2], M. Freitag[2], A.T. Johnson[2] and A.G. MacDiarmid[1]
[1]Department of Chemistry, University of Pennsylvania, Philadelphia, PA 19104
[2]Department of Physics and Astronomy, University of Pennsylvania, Philadelphia, PA 19104

Abstract

The conducting polymer, polyaniline, blended with poly(ethylene oxide) has been electrospun in air to give fibers with diameters in the range 4 nm – 20 nm. These fibers were captured on a wafer of degenerately doped silicon by placing the wafer in the path of the fiber jet formed during the electropinning process for a few seconds. Individual fibers were studied using Scanning Conductance Microscopy. Preliminary results from the scanned conductance images showed uniform conductivity along most of the length of the nanofiber. Efforts are underway to prepare fibers of similar diameters of pure polyaniline and to investigate the effects of gating on the conductivity of individual fibers. Scanning probe techniques will also be used to study the effect of "local" properties along the length of the fiber.

Introduction

Although the conducting polymer, polyaniline, (PANi) has been the focus of intense research during the past 20 years relatively little has been reported on ultrathin fibers of polyaniline either in the doped or undoped form[1,2]. In this work we report our recent studies on ultrafine fibers of doped polyaniline blended with poly(ethylene oxide) (PEO). Our goal is to be able to electrically characterize single fibers and to study the effect of a gate bias on their conductivity. We also plan to study if the fibers formed via electrospinning have better chain alignment along the fiber axis when compared to the bulk film and if annealing the fiber leads to improved conductivity due to increased crystallinity.

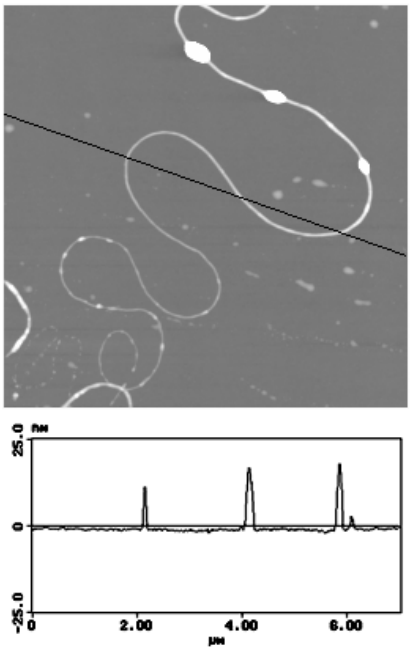

Figure 1: Section analysis of the fibers

Experimental

100 mg of PANi was doped with 129 mg of camphorsulfonic acid and dissolved in $CHCl_3$ for a period of 6-8 hours. The resulting deep green solution was filtered and 10 mg of PEO was added to the solution and stirred for an additional 2 hours. The solution was left in a capped bottle for a period of 72 hours after which time a small precipitate was observed. Prior to electrospinning, this solution was filtered using a 0.45 µm PTFE filter to give a homogenous solution. About 1 ml of the solution was placed in a B-D® 1ml $26^{3/8}$ hypodermic syringe that was mounted a few degrees below horizontal and the metal tip of the needle connected to 8 kV. The fibers were collected on a degenerately doped Si wafer at a distance of 30 cm from the tip of the hypodermic needle.

Results and Discussion

Figure 1 shows the topographic AFM image of a selected portion of the wafer with the corresponding height analysis of a section of the scanned image. It is clear from this image that all of the fibers have diameters less than 20 nm with the smallest diameter recorded being ~ 4 nm. Images taken on subsequent samples of fibers prepared using the above method all had fibers with average diameters in the range of a few tens of nanometers. Figure 2 shows the topographic and scanned conductance image of the fibers. The scanning conductance image shows a dark halo along the length of the fibers. This dark feature is an indication of the fiber being conducting as inferred from scanning conductance images of conducting single walled carbon nanotubes[3]. Such an image has not been reported before for nanofibers of conducting polymers and shows that the conductivity is uniform along the length of the fiber. Parts of the fiber whose diameter was < 6 nm do not show this halo. While cast films of the polymer do not appear to have any phase segregation it may be possible that at such small diameters there could be phase segregation of the polyaniline and the PEO. Efforts are underway to prepare fibers of pure polyaniline and to measure the current voltage characteristics of individual fibers under the influence of a gate bias. Local electrical properties along the length of the fiber will also be studied using scanning probe techniques. Results of these measurements will be presented.

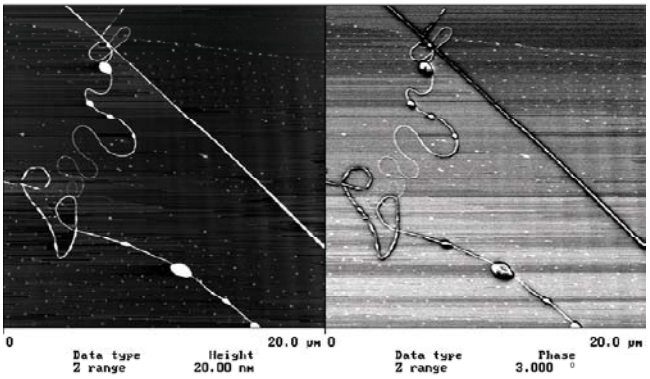

Figure 2. Topography (left), Scanning Conducrtance Image (Right)

Conclusions

Using the electrospinning technique we were able to produce ultrafine diameter fibers of conducting polymer blends in the range 4nm – 20nm. Scanning conductance microscopy images show uniform conductivity along the length of the fibers. However, at very small diameters the fibers do not show conducting characteristics which suggest a possible phase segregation of the doped polyaniline and PEO. Scanning conductance images on conducting polymers have not been reported to date and represent a new method in analyzing ultrafine diameter fibers of conducting polymers.

Acknowledgements: This study was funded partly by the by the US Office of Naval Research under contract number N0014-92-J-1369 and the University of Pennsylvania Materials Science Laboratory (NSF Grants: DMR9872689 and DMR0098603).

References:

*On sabbatical leave from the University of Puerto Rico – Humacao
[1]I.D. Norris, M.M. Shaker, F.K. Ko and A.G. MacDiarmid, Synth. Metals **114**, 109 (2000).
[2]A.G. MacDiarmid, W.E. Jones, I.D. Norris, J. Gao, A.T. Johnson, N.J. Pinto, J. Hone, B. Han, F.K. Ko, H. Okuzaki and M. Llaguno, Synth. Metals. **119**, 27 (2001).
[3]M. Bockrath, N. Markovic, A. Shepard, M. Tinkham, L. Gurevich, L.P. Kouwenhoven, M.W. Wu, L.L. Sohn, Nanoletters **2**, 187 (2002).

Biography:

Presenting author's name: Nicholas J. Pinto
Address: Department of Physics and Electronics
University of Puerto Rico
Humacao, PR 00791-4300

Email: nj_pinto@cuhac.cuhac.upr.clu.edu

Telephone: (787) 850-9381
Fax: (787) 850-9308

Ph.D. (Physics), December 1992 - Montana State University, Bozeman, Montana.
MS. (Physics), May 1987 - Bowling Green State University, Bowling Green, Ohio.
B.Sc. (Physics), June 1985 - University of Bombay, India.

1993 -1994: Research Associate and Lecturer, Department of Physics, Wichita State University, Wichita, Kansas.

1995 - 1998: Assistant Professor, Department of Physics and Electronics, University of Puerto Rico – Humacao.

1998 - present: Associate Professor, Department of Physics and Electronics, University of Puerto Rico – Humacao.

2001-2002: Sabbatical (visiting postdoc) – University of Pennsylvania.

Determination of Orientation Parameters and the Raman Tensor of the 998 cm^{-1} Band of Poly(ethylene Terephthalate)

Shuying Yang and Stephen Michielsen
School of Textile and Fiber Engineering, Georgia Institute of Technology, Atlanta, Georgia 30332-0295, USA.

The physical properties of the polymers depend strongly on the detailed morphology of the material where morphology refers to the degree of orientation of the polymer molecules and the level of crystallinity. Many techniques such as polarized Raman spectroscopy, polarized fluorescence, NMR, interference microscopy and X-ray diffraction have been used to measure the orientation of the polymer chains. Among them, polarized Raman microscopy is unique in that it can provide both the second- and fourth- order Legendre polynomials, P_2 and P_4, which describe the orientation, for particular *vibrations* within the samples. The results of the present study show that polarized Raman microscopy can provide qualitative and quantitative information about the crystalline and overall orientation of PET fibers.

Following the theory developed by Bower for polarized Raman spectroscopy, five spectra are required to determine the five parameters, the three Raman tensor components, P_2 and P_4. We used both backscattering mode and right-angle scattering mode to obtain the five spectra needed, and two additional spectra to normalize the spectra.

We studied PET samples that were made at different spinning speed (pure spin series) and post draw ratios. The full quantitative analysis was performed on the 998 cm^{-1} band of the PET spectra. From normal mode analysis, this band has been assigned to the symmetric stretching of the O-CH_2 bond and the stretching of the C-C bond in ethylene glycol units in *all-trans* configuration in crystalline PET. During the curve fitting process, we observed that this band is a pure Lorentz band. This implies that the vibration contributing to this band is from a single environment---crystalline region. We observed that the I_{33} spectra intensity of the samples has a linear relationship with Lorentz density of the samples. This is also evidence that the 998 cm^{-1} is related to the crystals of the samples. As such, we proposed that the 998 cm^{-1} band should provide information about the crystal orientation of the samples.

Our full analysis showed that the second order and fourth order orientation parameter P_2 and P_4 of the 998 cm^{-1} band are larger than those of 1616 cm^{-1} (It has been shown that the 1616 cm^{-1} band can provide information about the overall orientation of the PET fibers). This makes sense since the crystals are believed to align better and closer with fiber axis than the average of crystalline and noncrystalline parts. We also found that the orientation parameters P_2 and P_4 both increase with spinning speed at low speeds, but they remain constant (about 0.94) when the spinning speed exceeds 3000 m/min, which is the onset of stress oriented crystallization of PET observed by the X-ray study of Desai et al. This observation is consistent with Heuvel et al.'s observation that the orientation of the crystalline region of PET saturates rapidly (with f_c approximately equal to 0.97) while the orientation of amorphous region is gradual. This shows that what we are observing from Raman microscopy is exactly what is seen by X-ray. The result shows that after the onset of stress oriented crystallization, the increase of the orientation of the crystals is small.

Additionally, our result shows that the Raman tensor ratios of the 998 cm^{-1} line a_1 and a_2 ($a_1 = \alpha_1/\alpha_3$, $a_2 = \alpha_2/\alpha_3$, where α_1, α_2 and α_3 are the three principal components of the Raman tensor of band 998 cm^{-1}) appear to be of opposite signs. Although there is considerable scatter, it appears that one of the Raman tensor ratios, a_1, which is positive, increases along with crystal orientation; while the other one, a_2, is negative and decreases as the crystal orientation P_2 increases. Finally, our analysis indicates that the quantity of α_3^2 for the 998 cm^{-1} band is also dependent on orientation. This is the first time that the orientation parameters of the crystals of PET as determined by polarized Raman spectroscopy have been reported.

Shuying Yang

Currently pursuing her PHD degree in polymers under the guidance of Dr. Stephen Michielsen at School of Textile and Fiber Engineering, Georgia Institute of Technology. Her thesis project is about orientation characterization of PET fibers using polarized Raman microscopy and interference microscopy. She also worked on the antimicrobial polymer project where she surface modified polypropylene using ammonia plasma treatment. She got her Master degree in Plastic Engineering from Chengdu University of Science & Technology. Her master thesis is about surface modification of carbon black to improve its distribution and dispersion in polymer matrix. She once worked on the project of polyethylene as insulating material (to replace PVC) for communication cables in a plastic company.

Physics of Electrostatic Production of Nanofibers (Electrospinning)

S. V. Fridrikh[a,*], J. H. Yu[a], M. P. Brenner[b], G. C. Rutledge[a]
[a] Department of Chemical Engineering, Massachusetts Institute of Technology, 77 Massachusetts Avenue, Cambridge 01239, MA
[b] Division of Engineering and Applied Sciences, Harvard University, 29 Oxford Road, Cambridge 02138, MA [*] Presenting & corresponding author: fridrikh@mit.edu, tel: (617)253 6483, fax: (617)253 0546.

Electrospinning is a method of producing submicron (nano-) fibers by the stretching of a polymer solution jet in an external electric field. Due combined action of surface tension, charge relaxation, and the repulsion of the surface charges, the jet undergoes a set of electrohydrodynamic instabilities. The varicose instability causes the jet to break into the drops, while the whipping instability is responsible for the strong stretching of the jet and for the formation of nanofibers.

The potential applications of nanofibers are numerous. Their high surface area makes them an attractive candidate for filtering and absorbing applications. Due to their small diameter nanofibers may be used as a component in various composite materials. Non-wovens electrospun from biocompatible materials may be used for wound dressing and artificial tissue scaffolding. The first experimental accounts of successful applications of nanofibers as tissue scaffolds have emerged in the literature[1].

Though many groups have been successful in production of various non-woven fabrics by means of electrospinning[1-6], the issue of predicting of the whipping amplitude and the final diameter of the fibers as a function of the material and process parameters is still not resolved. In this talk we present the model of the whipping jets based on the approaches presented in our previous publications[7-8]. The jet is treated as a slender viscous rod and the parallels with behavior of thin elastic rods are used.

The model quantitatively predicts the final diameter of the whipping jet, and gives criteria for the "saturation" of the whipping instability – the regime when the jet does not stretch any more. The final diameter of the jet (fiber) is set by the balance of surface tension and electrostatic repulsion

of the surface charges. The simple analytical expression for the final diameter as a function of the *surface tension, flow rate and electric current* only is derived. For the most of fluids studied experimentally, it gives an estimated fiber diameter of about 1μm in agreement with published experimental data. Our experimental data on diameters of PCL fibers electrospun from methanol + chloroform solution show good agreement with theoretical predictions over a rather broad range of fiber diameters.

We also present numerical simulations and analytic formulae demonstrating both the whipping of the centerline of the jet, coupled to the thinning of the fiber diameter as it advects downstream. Predictions for the envelope of the whipping jet and the diameter of the jet as it changes along the jet's contour are presented. The experiments for testing these predictions are currently on the way.

Accurate prediction of the fiber diameters and identification of how this diameter depends on experimental properties opens the door for inventing novel ways of controlling the fiber diameter.

References:

[1] W.J. Li, C.T. Laurencin, E.J. Caterson, et al., *J. Biomed. Mater. Res*., 60, 613 (2002).
[2] D.H. Reneker, I. Chun, *Nanotechnology,* 7, 216 (1996).
[3] J. Doshi, D.H. Reneker, *J. Electrostatics*, 35, 151 (1995).
[4] H. Fong, I. Chun, D.H. Reneker, *Polymer*, 40, 4585 (1999).
[5] A. Buer, S.C. Ugbolue, S.B. Warner, *Text. Res. J*., 71, 323 (2001).
[6] S. Erel, S.B. Warner, *Text. Res. J*., 71, 22 (2001).
[7] M.M. Hohman, Y.M. Shin, G. Rutledge and M.P. Brenner, *Phys. Fluids***,** 13, 2201 (2001).
[8] M.M. Hohman, Y.M. Shin, G. Rutledge and M.P. Brenner, *Phys. Fluids***,** 13, 2221 (2001).

Presenting author: Dr. Sergey Fridrikh

Sergey Fridrikh, a Research Associate at the Department of Chemical Engineering at M.I.T. earned a Ph.D. in polymer physics at the Institute of Macromolecular Compounds, St.Petersburg, Russia. He also holds a M.S. degree in statistical physics from St.Petersburg State University. Sergey did postdoctoral research at Universite du Maine (France), Cambridge University (England) and at Dartmouth College. His research interests include rheology and statistical properties of polymer solutions and various liquid crystalline systems.

Lewis Acid Complexation of Nylon 66 and the Effect of Hydrogen Bonding on Film Drawability

Richard Kotek, DongWook Jung, Alan E. Tonelli, Nad Vasanthan*
College of Textiles, North Carolina State University, Box 8301, Raleigh, NC 27695, *TRI/Princeton, 601 Prospect Ave., P.O. Box 625, Princeton, NJ

Introduction

It is generally believed that hydrogen bonding makes polyamides important engineering plastics, because of the high strength it imparts. It was thought that studies with hydrogen-bonded nylons would extend the art of crystalline-state draw into polymers with melting points higher than the polyolefin's. Nevertheless, nylon 6 has been among the most difficult to draw to high ratio and tensile modulus. Generally, drawing processes result in a maximum draw of about 5. The inability to ultradraw nylon 6 is largely due to the presence of intermolecular hydrogen bonding between adjacent amide groups that do not allow the chains to slip through crystals. Their presence and extent are responsible for many nylon characteristics, including that only low molecular weights give good properties. During drawing, the hydrogen bonds in crystals act as quasi-crosslinks, inhibiting the sliding of chains along the hydrogen bond plane. Drawing thus occurs exclusively in the softer amorphous phase with strain-induced crystallization, restricting draw even further. The highest reported modulus of drawn nylon 6 is 13 GPa [1]. This is only a small fraction of its calculated theoretical modulus of 250 GPa.

To facilitate nylon deformation, an idea was proposed to relieve hydrogen bonding during processing. This is the reversible plasticization idea, i.e., a plasticizer is imbedded in the nylon that will subsequently be removed after deformation [2,3]. Anhydrous liquid ammonia has been used for the extrusion draw of nylon 6 [3]. This plasticizer temporarily disrupted hydrogen bonds in the amorphous phase and made the draw easier. It was found that ammonia incorporation in preformed ribbons of nylon 6 prior to extrusion significantly alleviated the processing difficulty encountered with untreated nylons and aided the rapid extrusion of a highly oriented ribbon. The extent of orientation was documented by the high birefringence, by the significant increase in crystallinity, and by the enhanced tensile moduli (13 Gpa). Plasticization with liquid ammonia occurs only in the amorphous phase of nylon 6, with its crystals still inaccessible on drawing. For the reversible plasticizer, iodine that can enter in both the amorphous and crystalline phases has been used [4]. This is based on the ability of the α-crystals to transform to the γ-crystals by treatment with an aqueous KI solution (only for even-odd, odd-even, and some α-amino acid type of nylons). Solid state extrusion has been performed on the nylon 6-I_2 complex, with iodine subsequently removed with sodium thiosulfate to generate back a transparent, drawn nylon 6. At 55°C, a DR of 7.9 has been obtained, considerably higher than previously reported for nylon 6, but the modulus was only 6 GPa [4]. Chain slip likely occurs within the complex.

In our research, Lewis acid was used for the reversible plasticizer to make nylon 66/$GaCl_3$ complexation. The nylon 66/$GaCl_3$ complex, in which the hydrogen bonds have been severed, has been prepared and found to be optically transparent and amorphous. The pure nylon 66 was recovered from its nylon66/$GaCl_3$ complex by extraction of $GaCl_3$ with water.

Experimental

Polyamide chips were obtained from North Carolina State University Spinning Lab. The molecular weight of nylon 66 chips was determined from the Mark-Houwink equation: $[\eta] = 0.74$ in 90% formic acid, MW = 16,772 g/mole. The theoretical draw ratio is 11. The Lewis acid complexation of polyamide was accomplished by dissolving $GaCl_3$ and nylon 66 chips in nitromethane under nitrogen atmosphere.

$GaCl_3$ complexes of the nylon 66 were prepared by adding a 1:1 ($GaCl_3$: amide group) stoichiometric amount of polymer to a solution of $GaCl_3$ in nitromethane. The mixtures were stirred when feasible and heated at 40 – 50°C until complete polymer dissolution. Films of nylon 66/$GaCl_3$ complexes for measuring tensile properties were prepared by casting the solution onto a Petri dish followed by evaporation of the solvent in vacuum at around 60°C for 24 hours. The films dimensions were 1 by 3cm. The film thickness was 0.004 inches. In addition regenerated films were prepared by leaving to soak in water to remove the Lewis acid with under tension for 24 hours. Tensile properties of those films were measured after drying the regenerated nylon 66 samples.

Results and Discussion

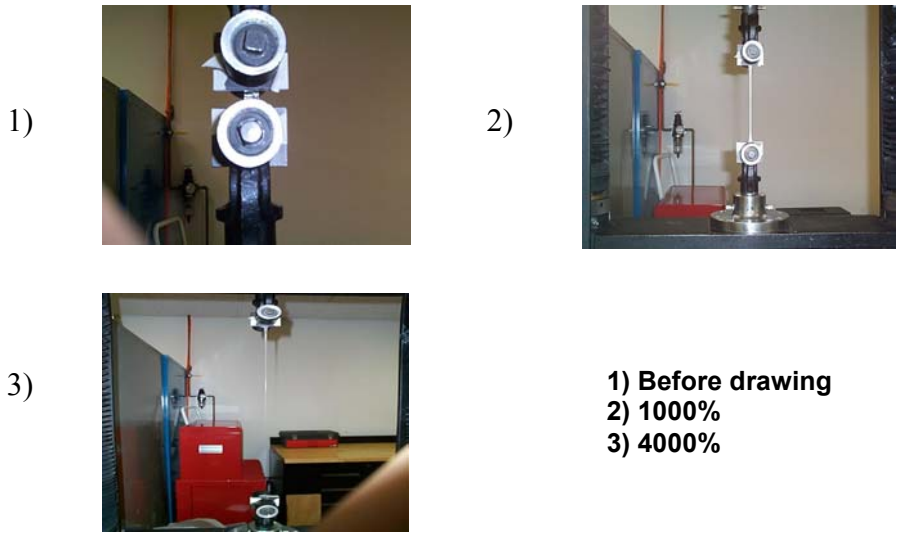

Figure 1. Drawing of N66/$GaCl_3$ films with different draw ratios.

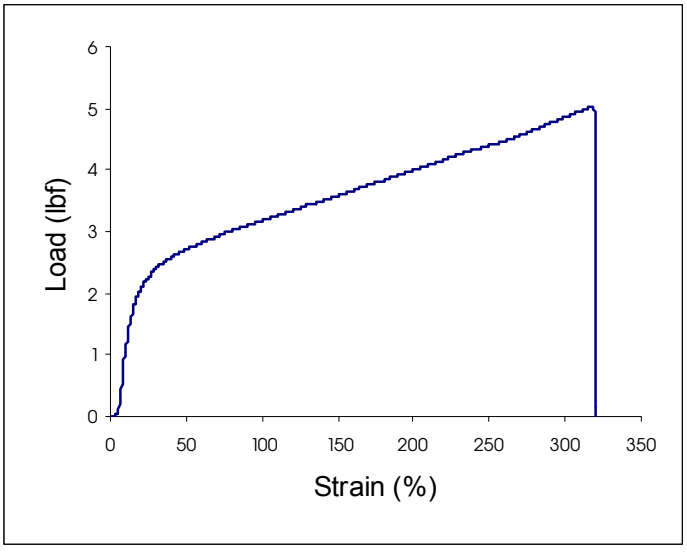

Figure 2.Tensile test of recovered Nylon 66 film N66/$GaCl_3$ complex film

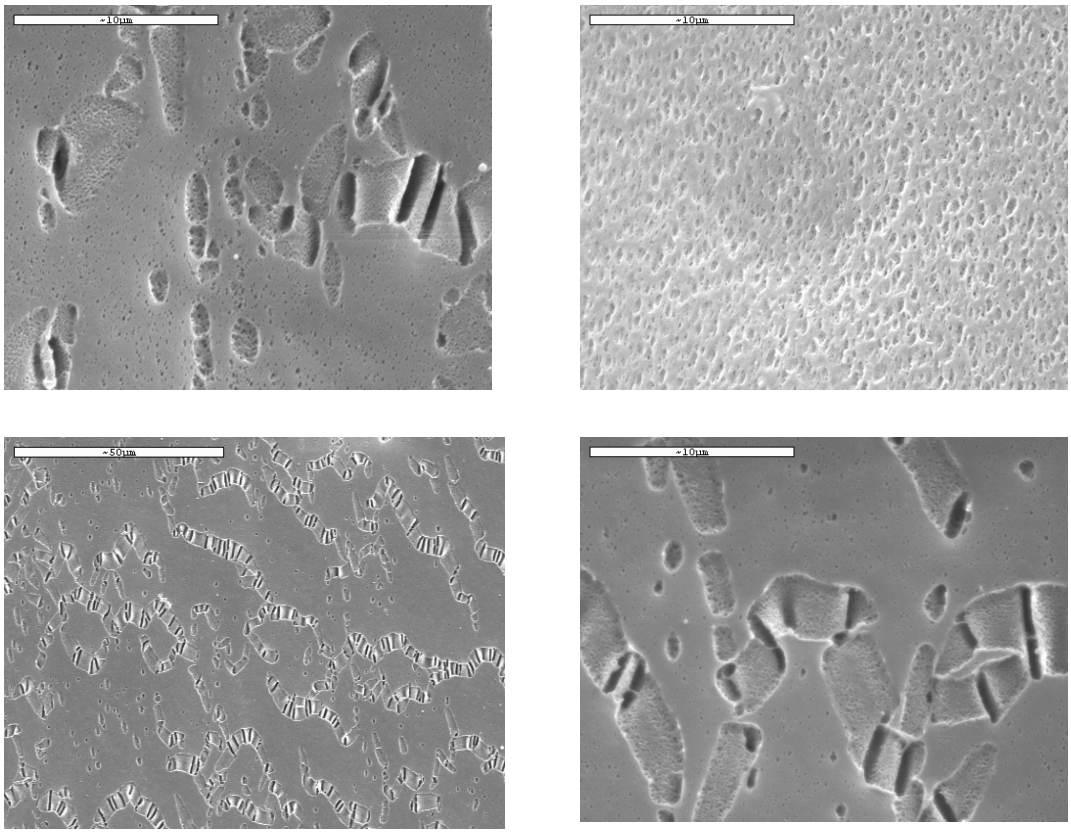

Figure 3. SEM of regenerated N66 film after stretching. Draw ratio of 14

Table 1. Density of Regenerated Nylon 66 Film by Using Sink-Float Method

Toluene	CCl_4 (ml)	CCl_4 (g)	Density of Mixture Solvent (g/ cm^3)	Position of Sample			
				Nylon66 chips	DR = 5	DR = 10	DR = 14
	6.0	9.540	1.1400	Bottom	Bottom	Bottom	Bottom
10ml	6.1	9.699	1.1428	Bottom	Bottom	Bottom	Bottom
(8.7 g)	6.2	9.858	1.1456	Middle	Bottom	Bottom	Bottom
	6.3	10.017	1.1483	Surface	Bottom	Bottom	Bottom
	6.4	10.176	1.1510	Surface	Bottom	Bottom	Bottom
	6.5	10.335	1.1536	Surface	Bottom	Bottom	Bottom
	6.6	10.494	1.1563	Surface	Bottom	Bottom	Bottom
	6.7	10.653	1.1589	Surface	Bottom	Bottom	Bottom
	6.8	10.812	1.1614	Surface	Bottom	Bottom	Bottom
	6.9	10.971	1.1640	Surface	Middle	Middle	Middle
	7.0	11.130	1.1665	Surface	Surface	Surface	Surface

Anhydrous N66/$GaCl_3$ solutions are stable. When exposed to moisture the viscosity of these solutions, however, may dramatically increase. Figure 1 shows that the superb drawability of up to 4000% for N66/$GaCl_3$ complex films has been demonstrated for N66 with the molecular weight of 16,773 g/mol. This means the hydrogen bonding in adjacent amide groups was broken. Figure 2 shows the drawability

of regular nylon 66 film. The draw ratio is about 300%. After evaporating solvent from a N66/$GaCl_3$ solution, the film is transparent and amorphous (no polymer melting point by DSC was seen). This indicates that there are no more hydrogen bonding in the N66/$GaCl_3$ films. The moduli of these N66/$GaCl_3$ complex films were very low. The average peak stress was 2.36 g/d. Fiber modulus of drawn nylon fibers was relatively low. This modulus can be expected for a low M. W. polymer. We may improve the modulus by using a high molecular weight of nylon 66.

The pure nylon 66 was recovered from its N66/$GaCl_3$ complex by extraction with water. Figure 3 shows the morphology of regenerated nylon by SEM. The irregular surface on the film was due to the solvent evaporation. In addition we could see the ribbon type shape morphology. One of them (upper right photo) shows also the porous morphology.

The density of N66 chips and regenerated nylon having different draw ratio (DR = 5, 10, and 14) was calculated by a sink-float method using toluene-carbon tetrachloride mixtures. Drawn nylon showed higher density than that of its original nylon chips. And the degree of crystallinity was calculated by a standard method using a crystal density of 1.230 and an amorphous region density of 1.084 g/cm^3 [5]. The crystallinities of nylon 66 chips and drawn nylon films are each 42.19% and 54.79% respectively. The crystallinity of drawn nylon 66 film increased about 30%.

Conclusions

The superb drawability of nylon film was obtained by making nylon66/$GaCl_3$ complex solution, and then recovering nylon 66 film by extracting $GaCl_3$. The crystallinity increased in the ultradrawn nylon film about 30% than that of the original nylon polymer chips. The hope is that films and fibers produced from high molecular weight N66 will have high tenacity and modulus.

References

[1] D. Acierno, F. P. LaMania, G. Polizotti, G.C. Alfonso, and A. Ciferri, *J. Polym. Sci.,Polym. Lett. Ed.,***15**, 323 (1977).
[2] A. E. Zachariades and R. S. Porter, *J. Polym. Sci.,Polym. Lett. Ed.,***17**, 277 (1979).
[3] A. E. Zachariades and R. S. Porter, *J. Polym. Sci.,Polym. Phys. Ed.,***20**, 1485 (1982).
[4] H. H. Chuah and R. S. Porter, *Polymer,* **27**, 241 (1986).
[5] T. Kunugi, T. Ikuta, M. Hashimoto, *Polymer,* **23**, 1983 (1982).

Biography

Richard Kotek
College of Textiles, North Carolina State University
Box 8301, Raleigh, NC 27695-8301
E-mail: rkotek@unity.ncsu.edu
919-515-6585 (office),
919-515-6532 (fax)

Professor Kotek graduated from the Man-Made Fibers Institute at Lodz Polytechnic in Poland where he specialized in man-made fiber technology and polymer chemistry. He developed flame-retardant polyester fibers and completed his Ph D. thesis under the direction of Professor B. Laszkiewicz. Following completion of his Ph. D., he worked at the Man-Made Fibers Institute and then came to the United States to work as a postdoctoral research associate for Professor W. R. Krigbaum at Duke University. While with Professor Krigbaum, Dr. Kotek carried out a liquid crystalline polymer research program. His work involved a new monomer and polymer synthesis. Soon after completing his postdoctoral assignment, he joined the R&D department at BASF Corporation (where he gained valuable industrial experience). He was involved in expanding fundamental understanding of spinning processes and also carried out studies on fiber morphology and molecular orientation. He developed and patented a new semi-continuous process for the depolymerization of nylon 6 polymer. Dr. Kotek also holds patents for making hollow fibers. He has extensive experience in fiber extrusion, particularly nylon and polyester fibers. Dr. Kotek joined the College of Textiles at North Carolina State University in August 1999. Dr. Kotek is a polymer chemist with an interest in fundamental research on the structure/property, processing, and manufacturing (or synthesis) of fiber forming polymers.

Nanoclay Modified Dyeable Polypropylene

Qinguo Fan*, Samuel C. Ugbolue, Alton R. Wilson, Yassir S. Dar, Yiqi Yang[1]
Dept. of Textile Sciences, University of Massachusetts Dartmouth, North Dartmouth, MA 02747-2300, [1]Dept. of Textiles, Clothing & Design and Dept. of Biological Systems Engineering, University of Nebraska-Lincoln, Lincoln, NE 68583-0802 *: corresponding and presenting author

Polypropylene is one of the major textile fibers like nylon and polyester. However its poor dyeability limits its acceptability in clothing and upholstery industries. Using approaches like polyblends, copolymers, plasma treatment, and specially designed dyes to provide dyeability increase the cost of the fiber manufacturing or the dyeing operation considerably. Such a cost increase certainly affects the price advantage of polypropylene over nylon and polyester. Moreover, some of the technologies are not capable of producing the fine fibers used for clothing materials. So far none of the researches mentioned above has had success for commercial production of dyeable polypropylene for fine textile fibers used in clothing and upholstery, mainly because these efforts lead to: (1) the significant increase of the price of polypropylene; (2) the decrease of the mechanical properties of the material; and (3) the uneven and weak treatment resulting in poor dyeability.

This preliminary research proves that dyeable polypropylene can be produced via nanotechnology. The dyesites in the nanocomposite polypropylene (nanoPP) are the prospective areas where nanoclay is located. One of the commonly available nanoparticles is nanoclay, which is montmorillonite, $(OH)_4\ Si_8\ Al_4\ O_{20}\ nH_2O$, modified with quaternary ammonium salt .

Since the clay is normally purified and properly surface modified after mining and before being used, it is possible in the modification process to introduce some chemical groups onto the surface of the nanoclay. This would provide the desired dye affinity in the polymer system in which the nanoclay is distributed within the polypropylene matrix depending on the dye classes to be used. In practice, cationic surfactants are used to modify the nanoclay. Such cationic surfactants act effectively to attach acid dyes due to the electric charge attraction. Another possibility to create the dyesites needed in the polypropylene arises from the free volumes created by oriented nanoparticles in the polymer system. This is advantageous for dyeing with disperse dyes and is achievable because the heat resistance of the nanocomposite polypropylene will be improved. The dyeability of the nanoclay modified polypropylene can also be contributed to hydrogen bonding and van der Waals force between nanoclay and dyes.

Nanoclay was introduced to the polypropylene matrix in a melting/dissolving process with the help of heat and organic solvent plus mechanical blending including the use of ultrasonication. This nanoPP was then molded into a film by using a laboratory hot press. C.I. Acid Red 266 and C.I. Disperse Red 65 were used to dye the resultant nanoPP according to normal acid dyeing (acidic pH) and disperse dyeing (high temperature) procedures.

The effects of add-on of nanoclay and the homogenization conditions like ultrasonication time, pulse and amplitude on dyeing were studied. SEM, optical microscopy and spectroscopy were used to determine the structure of the nanoPP and the dyeing results. AATCC standards were followed for colorfastness test.

The nanoPP prepared is dyeable using acid leveling and azo disperse dyes as shown in the scanned photographs of the control and nanocomposite dyed samples.

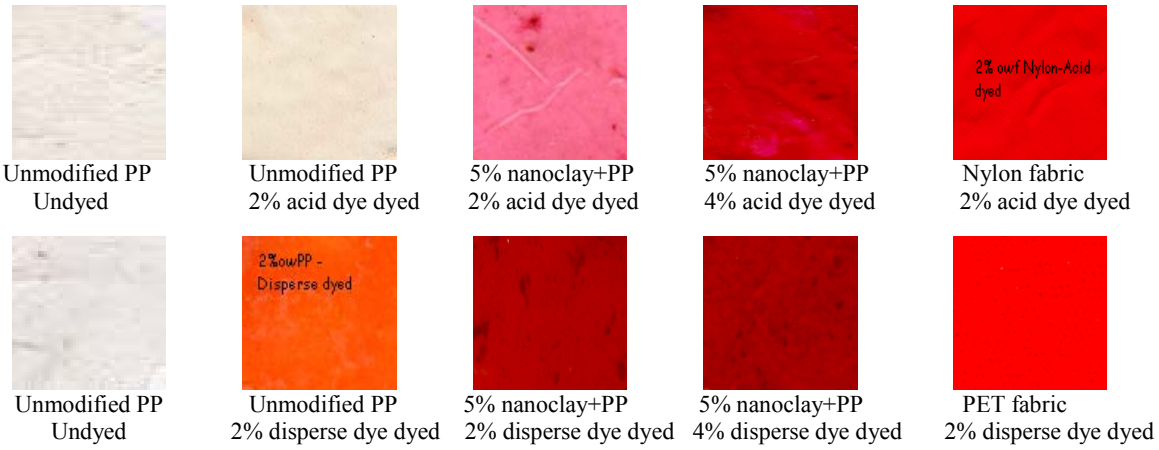

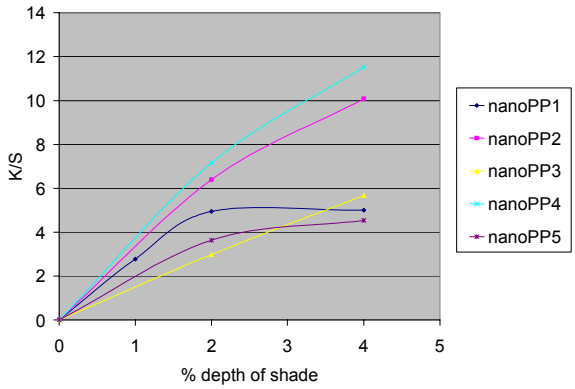

Fig. 1 Dye build-up curves of PP nanocomposites dyed with acid dye

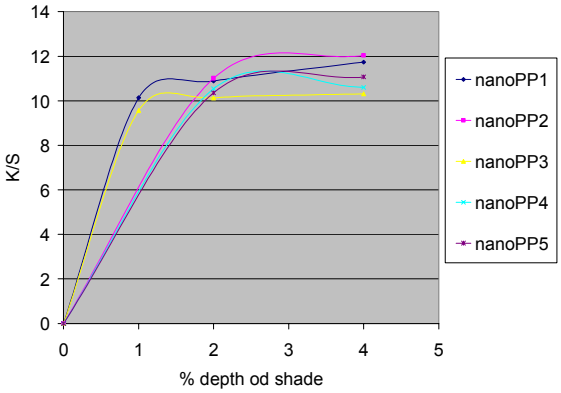

Fig. 2 Dye build-up curves of PP nanocomposites dyed with disperse dye

The dye build-up curves of PP nanocomposites are shown in Figs.1 and 2.

From our experiments, the following conclusions were made:

1. The color yield of the nanoPP is influenced by the add-on of nanoclay in the nanocomposite polypropylene.
2. The levelness of dyeing is dependent on the uniformity of the nanoparticles distribution in the polypropylene matrix.
3. A longer homogenizing time generally produced a comparatively level dyeing.

Qinguo Fan, an Assistant Professor of Textile Chemistry at the University of Massachusetts Dartmouth, earned his Ph. D in Color Chemistry from Leeds University, UK in 1995. He received an MS and a BS in Textile Chemistry from China Textile University in 1988 and 1982 respectively. Before joining the faculty at UMD in 1998, he was a Textile Chemist in charge of R&D, dyeing and finishing, wastewater treatment and customer service in Novel Textile Ltd. in Mauritius. His research interests include textile chemistry, color science, polymer and environmental compliance of textile wet processing.

Polycarbonate Fibers by Electrospinning and Ceramic Coating on Nano-Fibers for Photovoltaic Cells

Jamila Shawon[1*], Christopher Drew[2], Changmo Sung[1]
1 Department of Chemical Engineering and Center for Advanced Materials, University of Massachusetts Lowell2 Department of Chemistry and Center for Advanced Materials, University of Massachusetts Lowell
*Corresponding Author

Electrospinning is a superior process compared to other conventional spinning methods for the production of fibers in the sub-micron to nanometer scales. Such fiber membranes have exceptionally large surface areas and small pore sizes. The process requires an electrostatic force at the surface of a polymer solution or melt which overcomes the surface tension and viscoelastic forces to create an electrically charged jet (1). When the jet dries or solidifies, an electrically charged fiber remains, which can be directed or accelerated by the electrical forces and then collected in non-woven fiber membrane or other useful shapes. The electrospinning process in our lab consists of an electrode connected to a high voltage power supply (range 10-30kV) inserted into the polymer (polycarbonate) solution with solvent mixtures of THF and DMF contained within a capillary tube. Spun fibers are collected on a grounded target.

The electrospun fibers on the desired collector were then characterized by SEM (FIG.1) and TEM. The spun fibers have the characteristics of strong bonding with each other. The feature of the fibers is like the spider web. It is observed that with low concentration of solvent mixture (low THF and high DMF ratio) and low electric potential, the fibers did not produce a good network. As the concentration of THF as well as the electric potential was increased, the net structure like spider web formed (FIG.2).

The goal of this research is to characterize the polycarbonate fibers by electrospinning and to form nanofibers (diameters <10nm) at suitable conditions. The solvent mixture has a significant role on the morphology of the fibers. The spun fibers showed the characteristics of strong networking as a result of splaying and splitting during solvent evaporation. The spinning voltage, viscosity and surface tension also play major roles to change the fiber morphology. The bead shape also showed different features under these conditions. With lower solvent mixture ratios, the bead shape is like globule mushroom, but with higher ratios, the beads formed the shape of spindle. The ultimate goal of the research is to produce ceramic tubes coated on an electrospun fiber template. The current research demonstrates the first successfully ceramic-coated electrospun nanofibers. Polycarbonate nanofibers were electrospun and subsequently coated with titanium dioxide by aqueous liquid phase deposition. It was found that coating method coated the electrospun fibers well without binding the fibers together (FIG 3). The high surface area and porous nature of the electrospun membrane remained largely unaffected by the coating process. The coating thickness depends on duration of coating time. The higher coating time is preferable for more complete coating (FIG.4). The future aim of the research is to extract the polymer from the coating and thus make nanotube for advanced photovoltaic cells (2).

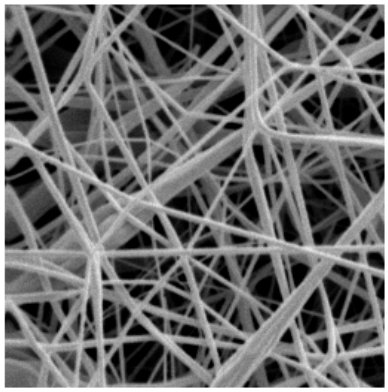

FIG. 1

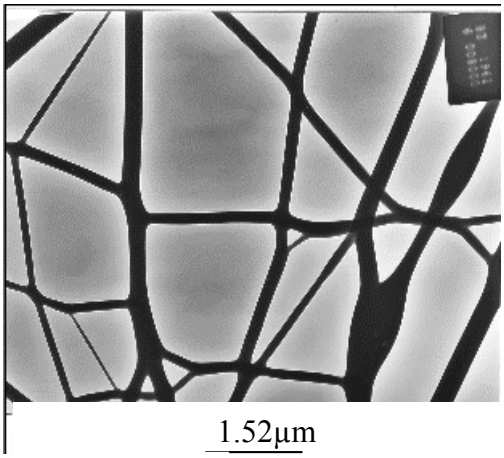

FIG. 2

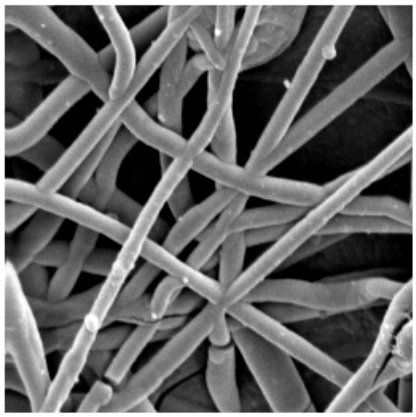

FIG 3

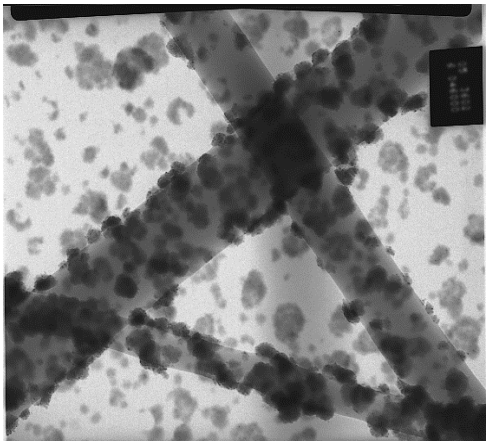

FIG 4

FIG. 1: SEM image of electrospun14% concentrated polycarbonate fiber with solvent ratio THF: DMF (60:40) at 30 kV before coated with TiO_2.
FIG.2: TEM image of electrospun14% concentrated polycarbonate fiber with solvent ratio THF: DMF (70:30) at 25 kV before coated with TiO_2.
FIG.3: SEM image of same fibers of FIG.1 after coated with TiO_2 for 14hrs.
FIG 4: TEM image of same fiber of FIG. 2 after coated with TiO_2 for 7 hrs.
References:
1.Y.M.Shin et al., Journal of Polymer 42 (2001) 9955-9967.
2. B. O'Regan et al., Journal of Nature 1991*, 353* (October 24), 737-9.

Biography of Presenter Author:

Jamila Shawon, originally from Bangladesh, has pursued her bachelor's degree in Chemical Engineering from her homeland. Currently she is doing her master's degree in Chemical Engineering at University of Massachusetts Lowell. Her major concentration is Materials Science. She is the research assistant at the Center for Advanced Materials (UMASS Lowell) and is engaged with research related to nanofibers by electrospinning and nanotube. She won "best student poster award" at graduate student poster competition 2002 from Chemical Engineering department of UMASS Lowell and "Best student poster award" at NESM spring meeting, 2002. Recently she has been selected as a speaker for MSA meeting (Quebec). She is also involved with polymer projects with Madison CMP and NSF.

Corresponding Author:

Jamila Shawon

Graduate Student of Chemical Engineering

University of Massachusetts Lowell, MA 01854

Telephone# 978-934-3540; Fax# 978-970-2435

E-mail: Jamila_Shawon@student.uml.edu or jamila_shawon@hotmail.com

Unique Micro and Nanostructured Morphologies on Electrospun Materials

JS Stephens[1], CL, Casper[1], JF Rabolt[1] , NG Tassi[2], DB Chase[2]
[1]Department of Materials Science and Engineering, Delaware Biotechnology Institute, University of Delaware, Newark, DE 19716, [2]Central Research and Development, Dupont, Wilmington, DE 19880

The scope of this research is to build a stronger fundamental understanding of the electrospinning process by studying its structure/property/process relationships. A variety of polymer/solvent systems have been studied by varying the processing parameters to produce nanoporous surface morphologies on the fibers (Fig.1A) (1). This addition of pores results in fibers with ultra high surface area (up to 1200 m2/g). Since the pores are only present on the surface of the fibers the structural and mechanical integrity of the fibers is maintained. The size, shape, and distribution of pores can be controlled by changing the processing protocols, and therefore the desired surface texture for a specific application can be obtained. Also through the use of a judicious choice of the electrospinning processing parameters we have been able to create webs of nanofibers (5 – 25 nm) from collagen, spider silk, nylon, and denatured collagen (Fig. 1B). The porous structure on the surface of the fibers and the nanoweb morphology greatly increase the surface area of the fibers making them excellent candidates for filtration devices, membranes, and scaffolds for tissue engineering applications. These structures have been characterized using FESEM, TEM, and AFM, and solvent evaporation profiles are being generated using “real time” Raman spectroscopy (2).

The aim of this research is the use the structure/property relationships developed to tailor these materials for applications that require high surface areas. An application that requires a high surface to volume ratio is the nanofibers used for tissue engineering platforms. Tailoring fiber size, shape, and surface morphology of electrospun fibers to optimize the interaction with cells will provide mechanisms for promoting bone repair, wound healing, and tissue regeneration. The combination of the above properties and the ability to control the structure/property relationships of electrospun fibers makes them an excellent candidate for tissue engineering platforms.

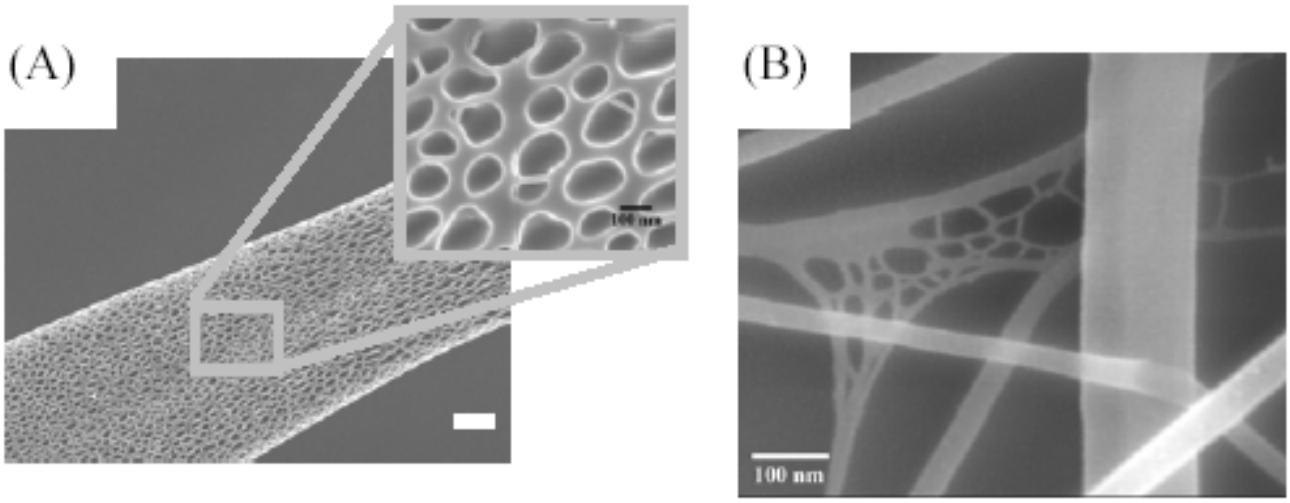

Figure 1. Nanostructural Morphologies
(A) nanoporous fiber, PS from THF, (B) nanoweb, collagen from formic acid.

References:

1. S Megelski et al, Macromolecules, accepted for publication.
2. JS Stephens et al, Applied Spectroscopy, (55) 1287, 2001.

Presenting Author Biography: Jean S Stephens (Jeannie)

jsteph@udel.edu , (302) 831-0791 (office), (302) 831-4545 (fax)

Jeannie graduated from Auburn University in 1999 with a Bachelors of Textile Engineering. She interned for BP Amoco Fabrics and Fibers Business Unit while attending Auburn and before entering graduate school at the University of Delaware in the Department of Materials Science and Engineering. Her research is on building a stronger fundamental understanding of the electrospinning process by studying the structure/property/process relationships of the system and exploring tissue engineering applications of the materials that are produced. Her research is advised by Professor John F Rabolt and collaborations with Dupont and the Delaware Biotechnology Institute. She has also published several papers and written a patent on the research to date.

Morphological and Orientation Effects on the Optical and Electronic Properties of Conjugated Electroactive Organic Polymeric Fibers

Richard V. Gregory
School of Materials Science and Engineering and NSF/ERC Center for Advanced Fibers and Films, Clemson University, Clemson, South Carolina 29637, USA. 864-656-5961 (OF) 864-656-5973 (FAX) Richar6@Clemson.edu

General Introduction:

The electronic and optical properties of conjugated polymeric fibers and films have been shown to be highly dependent on the orientation, microstructure, and morphology of the film/fiber-forming polymer. We have previously reported these effects for electrical conductivity.[1,2] These effects need to be quantified and fully characterized prior to use in composite structures, or as coatings on fiber or other materials to impart a desired electronic or optical effect for use as sensors, memory storage devices, or all organic optical processors. Changes in the electronic, optical and/or photonic properties, due to morphological changes induced by orientation of the polymeric films and electroactive fibers prepared from these materials, are related in this study to the polymer morphology. The developed microstructure is discussed and related to the optical and molecular chain axis, the electronic and photonic properties, and finally to the formed film or fiber morphological structure. The potential for tuning the morphological structure to specific end uses by selectively changing the polymer microstructure during processing will also be discussed. In addition we will briefly discuss the study and characterization of the visco-elastic properties of wet-spun polyaniline fibers and highly oriented films and the subsequent effect on optical and electrical properties. This work has shed light on the interaction of the polymer chains in this important conductive polymer, which lead to a more complete understanding of the observed electronic/photonic and electrical properties. This can be seen in Figure. 1 that clearly shows the effective change in refractive index (at 1550nm) of a polyaniline film that has been drawn.

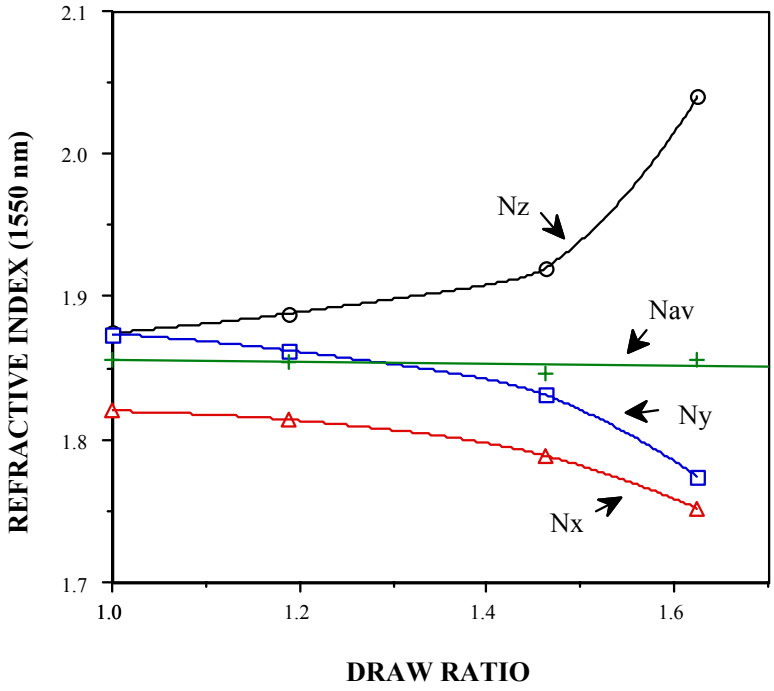

Fig.1 Refractive index change in spin coated and drawn polyaniline emeraldene film base film measured at 1550nm.

The resultant change in the refractive index, measured in all three principle directions, is highly anisotropic although the average refractive index remains unchanged indicating no phase change in the material. Although a fiber attachment is presently being developed, a film was used in this case, as the current configuration of the prism wave-guide coupler used in the measurement is better suited to this geometry. We have modeled the effect and will report the experimental verification of the model for several different organic conductive fiber systems. [3]

We will also present a brief summary of recent unique emissive polymers synthesized for application to fiber micro-ring lasers. [4,5] These micro-rings are being developed for application as fiber based optical logic circuit devices. We have demonstrated that the microrings will act as luminescent devices until a critical energy level is reached where lasing action occurs based on the development of whispering gallery modes in the all-organic laser cavity. This type of lasing action has been shown to be highly efficient and not subject to the inherent problems demonstrated in all organic wave-guided lasing action of thin flat film lasers. The "circular" fiber geometry is necessary for the formation of these types of whispering gallery mode systems.

A laser burst from an all-organic microring of di-octyloxy-paraphenylene vinylene (DOO-PPV) can be seen in Figure 2.

Fig. 2 Laser "Burst" from an excited DOO-PPV micro-ring on an optical fiber. Emission scatter due to water vapor used to enhance the image

We will demonstrate the potential use of these micro-rings on fibers as optical logic circuit devices as well as their potential, when reversed biased, as photo driven micro-current generation devices for powering fiber based electronics. We will also briefly discuss the use of micro-sphere lasers and luminescent devices embedded in fiber forming polymers for use in a wide variety of smart fiber applications raging from sensors and power generation devices in conductive fibers to optical amplifiers.

References:

Gregory, R. V. "Solution Processing of Conductive Polymers: Fibers and Films from Emeraldine Base Polyaniline." In T. Skotheim, R. Elsenbaumer, and J. Reynolds, eds., *Handbook of Conductive Polymers*, 2nd Edition, Chapter 18. New York: Marcel Dekker, 1997.

Gregory R.V. "Fibers from Electrically Conductive Polymers" Chapter 10; *Structure formation in Polymeric Fibers*, Hanser Garner Publishers - Munich, David R. Salem editor. 2001

Makradi, A.; Ahzi, S.; Gregory, R. V. ; "Modeling of the Mechanical Response and Evolution of Optical Anisotrophy in Deformed Polyaniline" *Polymer Eng. and Science*, **40**, 7, 2000 pp. 1716 - 1722

Ou. R, Samuels, R. J., Wang, X., Gregory, R. V. ; "Characterization of Anisotropic Structure in poly(Phenylene vinylene) Films" *Polymer Engineering and Science*, **Vol. 41**, 10, 1705-1713, 2001

Frolov SV, Fujii A, Chin D, Yoshino K, Vardeny V, and Gregory RV. "Cylindrical Microlasers and Light Emitting Devices from Conductive Polymers." *Applied Physics Letters*, 77: 2811-2814 (1998).

Short Bio - Richard Gregory - Director School of Materials Science and Engineering

Richard (Dick) Gregory is a Professor of Polymer and Materials Science and currently serves as the Director of the School of Materials Science and Engineering at Clemson University. Professor Gregory received his BS degree in chemistry from Old Dominion University and a PhD in physical chemistry from Clemson University in 1984. After a one-year post-doctoral fellowship he joined Milliken Research Corporation where he helped develop one of the earliest industrially feasible applications of electrically conductive polymers to textile fibers. In 1990 he returned to Clemson University as a faculty member. His current research focuses on the application and development of all organic conductive and optical polymers for fiber applications. He has published over one hundred papers in the area of conductive and optical polymers for smart fiber applications. Professor Gregory also holds several patents in the area of smart materials, textiles, and organic conductive polymers. In conjunction with colleagues at the University of Utah he helped develop the first all organic fiber based micro-ring lasers. Professor Gregory served as the Fiber Society Lecturer during the 1999 -2000 academic year and in 2001 he was awarded then SEAM Award for scientific excellence by the Hermann Mark Polymer Institute at Brooklyn Polytechnic for his early pioneering work in polyaniline fibers and optical devices. In addition to his duties as School Director he serves as a Thrust Leader in Clemson University's National Science Foundation Center for Advanced fibers and Films.

Molecular simulation of polymer crystallization: growth kinetics

Numan Waheed, Min Jae Ko, and Gregory C. Rutledge
Department of Chemical Engineering, Massachusetts Institute of Technology, Cambridge, MA 02139

Crystallization during processing of polymeric fibers has been a phenomenon of long-standing interest, since the melt-spinning work of Ziabicki. However, even for the relatively simple case of quiescent crystallization of polyethylene (PE), the physical steps involved during melt crystallization are still unclear. Experiments on polyethylene reveal a complex morphology, for which the temperature dependence of the spherulitic growth rate is consistent with crystal growth controlled by secondary nucleation, an activated process by which a new layer of chains is added to an existing crystal structure. Prevailing theories of polymer crystallization are based on secondary nucleation, although most invoke other assumptions that are obtained by analogy to single crystal formation in dilute solution and would benefit from a molecular description of the process.

Previously, we have employed molecular dynamics for short alkanes in the presence of a surface potential to study physical mechanisms underlying secondary nucleation. We have shown that secondary crystallization rates for n-eicosane ($C_{20}H_{42}$) are directly observable over a range of quench temperatures. Techniques for the measurement of linear growth rates have been developed, by quantifying the increase in local chain order and local density that accompany the phase change, and fitting the growth front to a functional form. In addition, the growth process has been decomposed into elementary ordering and melting processes, which may serve as inputs to a more course-grained kinetic Monte-Carlo algorithm, that could model long range growth.

Now we apply the same analysis to $C_{100}H_{202}$ chains, for which length scales and time scales are significantly longer. The simulations consist of 40 $C_{100}H_{202}$ chains of united-atom beads between two pre-existing surfaces and are initially equilibrated to 500 K, and then quenched to various temperatures. They were conducted at constant temperature, constant stress of 1 atm in the z-dimension, and fixed x and y dimensions to match the periodic boundary conditions of the x- and y-corrugated potential, modeling a [110] surface. In contrast to the n-eicosane simulations, which yielded a large amount of orientational order data at each time point as a function of distance from the initial surface, the $C_{100}H_{202}$ simulations yield a large amount data as a function time, over a short distance from the initial surface. While the overall growth is limited due to time and length scales, the fluctuations in the order parameter within the first few growing layers allow us to determine elementary ordering and melting rates, by the same methodology. Results of this research will be discussed, in light of implications for predictive, multi-scale modeling of the fiber spinning process.

Corresponding Author
Gregory C. Rutledge
Department of Chemical Engineering
66-368
77 Massachusetts Ave.
Massachusetts Institute of Technology
Cambridge, MA 02139
Phone: (617) 253-0171
Fax: (617) 258-0546
Email: rutledge@mit.edu

Presenting Author
Numan Waheed
Department of Chemical Engineering
66-453
77 Massachusetts Ave.
Massachusetts Institute of Technology
Cambridge, MA 02139
Phone: (617) 253-6484
Fax: (617) 258-0546
Email: nwaheed@mit.edu

Presenter's Biography: Numan Waheed received his bachelor's degree from Cornell University, and is currently is a Ph.D. candidate at the Massachusetts Institute of Technology. He works with Professor Greg Rutledge, in the area of polymer molecular simulation. His research in polymer crystallization kinetics is a part of the NSF Center for the Advancement of Engineering Fibers and Film.

Control of Deposition & Orientation of Electrospun Nano-Fibers

Navin Bunyan, Inan Chen, Julie Chen, Samira Farboodmanesh, Kari White
Advanced Composite Materials and Textile Research Laboratory, Department of Mechanical Engineering, University of Massachusetts Lowell, Lowell, MA 01854

Electrospinning is a nano-fiber manufacturing process that uses a voltage potential to initiate the spinning of a charged polymer solution. A jet of polymer solution is ejected from the conical formation at the tip of the orifice, towards the grounded target. As the solution travels through the air, electrostatic forces acting on different sections of the jet make it unstable, which leads to a complex behavior known as whipping. This whipping action elongates the fiber and decreases the diameter, enabling the formation of nano-fibers. The fibers are typically collected on the grounded target as a randomly oriented fiber mat. The primary objective of this research is to understand the effect of electrodynamics on the fiber formation, orientation, and deposition process and ultimately redesign the existing process to control the resulting fiber deposition. Controlled fiber orientation can yield products such as braided, woven and patterned nano- and micro- structures, tissue scaffolds, conductive nano wire grids and filters. Desired orientation of the fibers can be achieved by potentially addressing three aspects: the jet path control, the target design and the solution properties. The fibers can be directed towards the target by introducing a transverse electric field that causes an electric potential concentration. Fiber deposition with direction orientation on the target can be obtained by using either mechanical forces or potential variation on the target by design modification. Adding conductive nano-particles to the solution can enhance the response of the polymer to electrostatic forces.

The critical parameters influencing the fiber deposition were isolated and their effect on the process studied. The effect of flow rate, voltage and source to target distance with respect to the fiber deposition current was analyzed. To study the effect of target geometry, wire meshes with different patterns were used. Figure 1a shows an optical microscope image of fibers deposited on 3.8mm wire mesh. It shows regions of higher fiber concentration due to the electric fields generated by the wire mesh, but an SEM image of the pattern (Figure 1b) indicates no specific orientation of the fiber direction. Thus the target geometry affects the fiber deposition on a macroscopic scale but to achieve fiber orientation on a micro- (or nano-) scopic scale we need to understand the path of the jet and the forces acting.

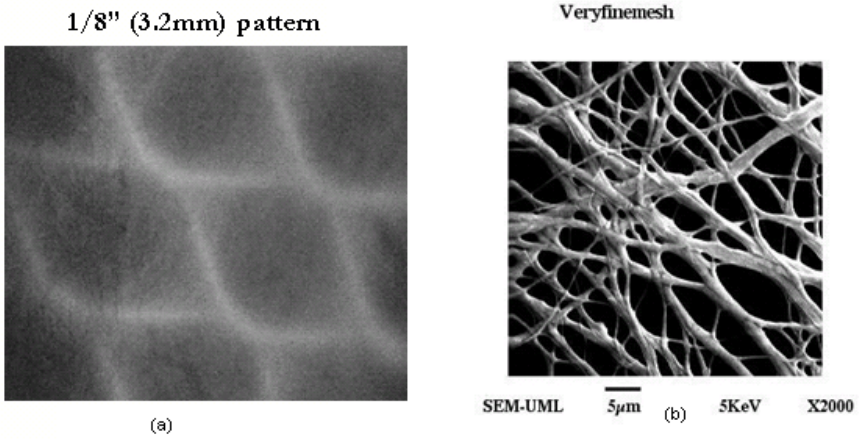

Figure 1 Fiber deposition on wire mesh target

The fiber deposition current gives an idea of the amount of charge being deposited on the target, through which the forces acting on them can be derived. Since electrostatic forces dominate the electrospinning process to a large extent, it is possible to control the jet by manipulating the field acting on the system. As the solvent evaporates and the charge/mass increases, the electrodynamic behavior of the jet becomes critical for understanding the fiber deposition. The ion-jet charge transport in electrospinning can be modeled using the steady state charge distribution with the two electrodes. The modeling for the distribution between two parallel plates was modified for a point and a plate electrode namely the voltage source and the grounded target respectively. The conservation law for current continuity under steady state conditions can be written in the form

$$\frac{\partial q(r,z)}{\partial t} + \nabla J(r,z) = 0$$

where q represents the charge density and J the current density. The units of q and J are C/m^3 and A/m^2, respectively. The change in the total charge in a section is equal to the total current going out through its ends. The electrode at the source is called the disc electrode with radius Rd (Figure 2). Disc electrode radius can be varied from Rd = Rs (source radius, i.e., no disc electrode) to as large as the target.

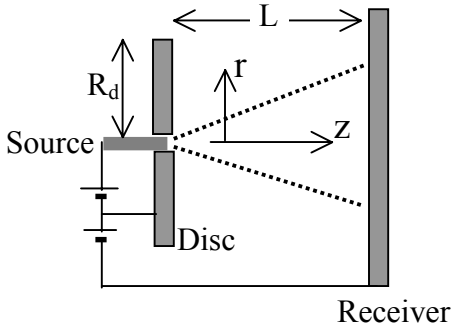

Injection go= $\frac{\varepsilon \mu Vo}{L^2} >> 10^{-14} (S/cm)$

ε = *permittivity*

Where μ = *mobility*

Vo = *appliedvoltage*

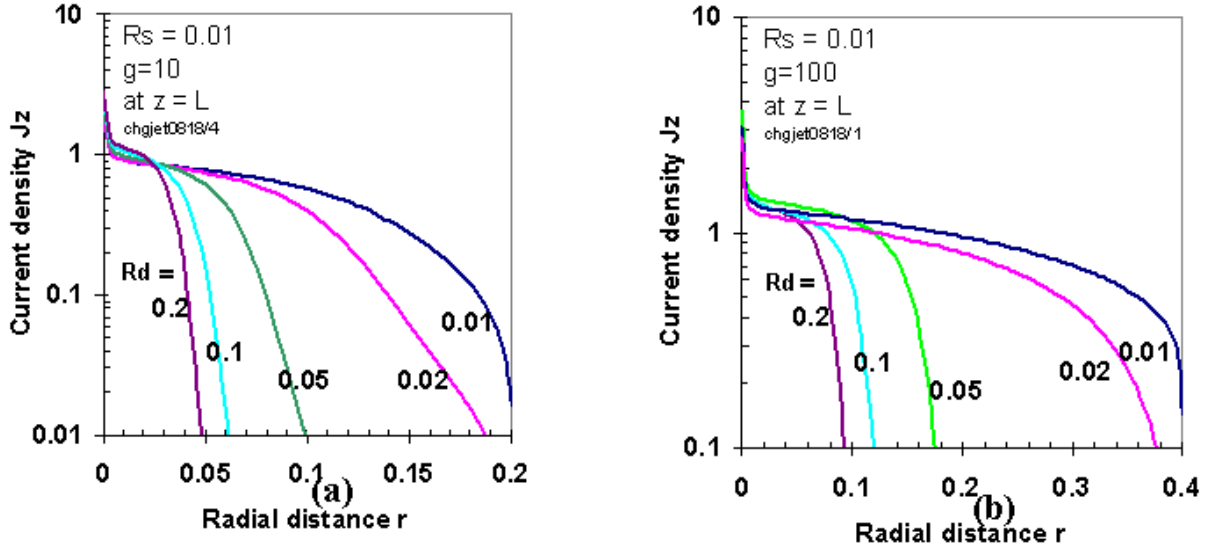

Figure 2 Prediction of decrease in the deposition spread at the target with an increase in the source radius

The voltage Vw applied to the disc electrode can be the same as or lower than that applied to the source electrode Vs. For modeling purpose, the source radius was fixed at 0.01L, where L is the distance between the source and the target. The radius of the disc electrode is varied from 0.01L (equal to Rs) to 0.2L. The same voltage is applied to both the source and disc, Vs = Vw.

On applying the boundary conditions the equations were solved by numerical iteration. Figure 2a shows the plot of current density verses the radial spread of the fibers on the target (i.e., at z = L). It is seen that when the radius of the source electrode is increased from 0.01L to 0.2L, there is a several order decrease in the spread of the fibers at the target. From the figure, the radius of fiber deposition decreases from ~0.2L for a point electrode to ~0.05L. The flat region from the shape of the curves indicates that there should not be any significant difference in the amount of fiber mass collected (related to current density) at each radius. Note that increasing the injection parameter g, which is related to the flow rate and applied voltage, by an order of magnitude increases the spread by a factor of 2 (Figure 2b).

The modeling results were verified using the setup shown in figure 3. An aluminum disc was used as a disc electrode and was placed just behind the syringe tip. The voltage potential from the power source was applied to the polymer solution taken in the syringe and the disc electrode. The distance of the target from the source was 16cm. The spread of the fibers on the target was measured for different disc electrode diameters and flow parameters.

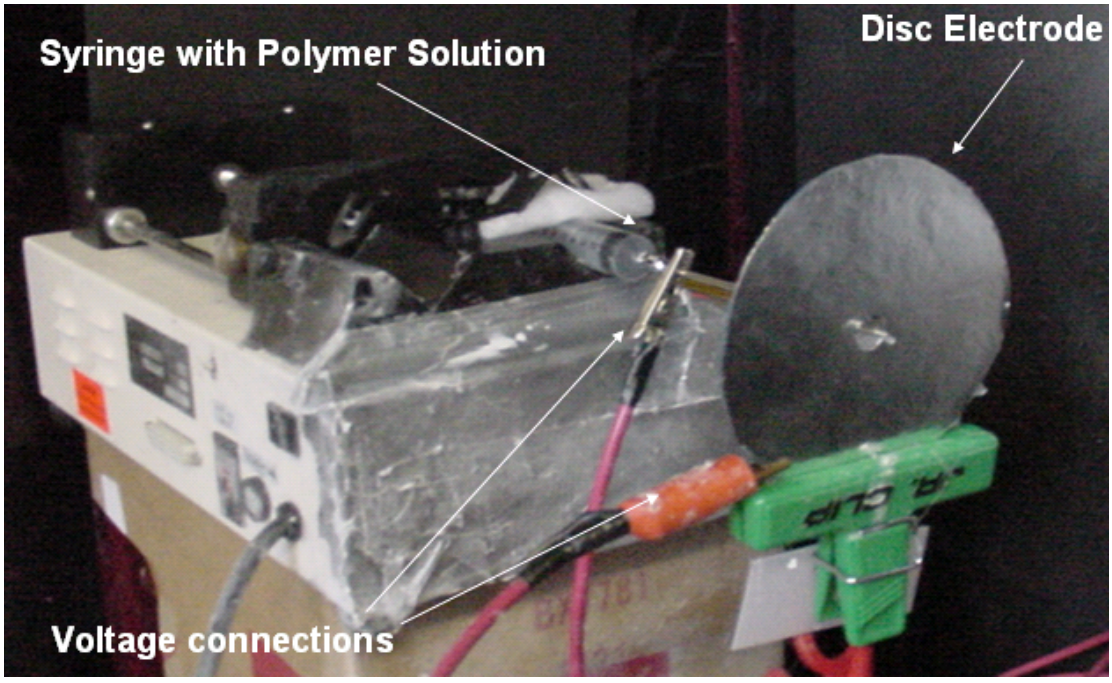

Figure 3 Experimental set-up with disc electrode

Figure 4 shows the effect of the disc radius and flow rate, for a disc diameter of 5cm and flow rate of 0.06ml/min, the spread decreased from 20cm (without disc) to 10.5cm. On further increasing the disc diameter to 10cm, the fiber spread decreased to 6.5cm. Next it is seen that the increase in the flow rate to 0.09ml/min increased the spread of fibers on the target.

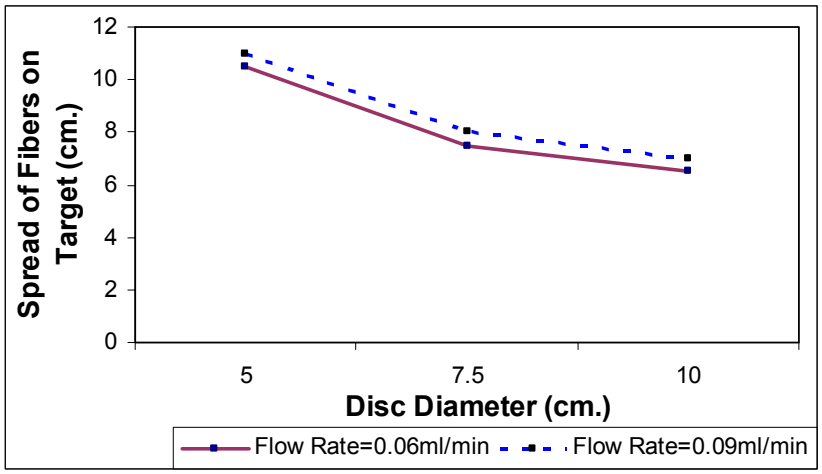

Figure 4 Plot of spread of fibers on target to the disc diameter

These results matched well with the modeling results and is can be concluded that by having an optimum disc electrode, the spread can be controlled and secondary fields could be designed for steering the jet onto the target. Additional studies are underway to model and experimentally measure the effect of transverse electric fields on the fiber deposition and orientation.

The presenter's Biography:

Navin Bunyan is a graduate student at the University of Massachusetts Lowell in the Mechanical Engineering Department. He joined the Advanced Composite Materials and Textile Research Laboratory (ACMTRL) in September 2001. Originally from Bangalore, India, Navin obtained his BS in Mechanical Engineering from Karnatak University, India in 1998. Shortly thereafter, he became a Senior Design Engineer in the R&D Dept. of Wipro Peripherals. For approximately 3 years at Wipro Peripherals, he worked on the design of printers.

Currently he is working on his thesis topic titled *Electrospinning – Fiber Deposition and Control*; this project is funded by the National Science Foundation (NSF). The present work forms a part of the research which concentrates on controlling the electrospinning jet from the source to form controlled fiber deposition and orientation on the target.

False Twist Induced Loss of Yarn Tenacity

Urs Meyer
ETH Zurich

Changes in the twist in spun yarns have an impact on tenacity. Local introduction of false twist is changing the twist of the yarn on both sides of the point of introduction. On one side, the false twist adds to the original twist of the yarn, on the other side, it reduces the original twist. This effect, leading to possible yarn breakages in yarn processing, is investigated in two aspects.

First, what are the basic principles for unwanted false twist induction on the yarn in processing, and how much false twist is to be expected? This theoretical assessment points to measures for reducing or eliminating false twist by adequate feeding and guiding of yarn.

Introduction of false twist into a moving yarn is caused by any kind of surface friction force in a direction perpendicular to the yarn axis. This is e.g. given if the yarn is pulled in a cork srew path around a stationary pin, or pulled off a rotating godet in a direction out of the plane perpendicular to the godet axis. However, the most common place where false twist is introduced by surface friction is the common overhead pull-off of the yarn from a bobbin.

In each of these cases, the tension imposed on the yarn increases along its path of motion. As a practical consequence, the yarn path should be arranged in a way that the false twist introduced locally tends to increase the original twist of the yarn in the part following the point of introduction, and tends to reduce the original twist in the part preceding the point of introduction.

In yarn processing, lateral movement of a yarn can be predominant, e.g. in the case of the pigtail of the ring spinning position, or in the shed of the warp on a weaving loom. This case is especially investigated in its consequences on yarn untwisting.

In the second, experimental part, the loss of breaking strength due to untwisting is measured on a wide range of different yarns. It was found that yarns with perfectly regular twist, as ring yarns, are more susceptible to loss of tenacity due to untwisting, than yarns with a more irregular fiber configuration, as open end yarns. By a number of examples, the sensitivity of a yarn to untwisting is related to a qualitative assessment of the yarn structure, taken by a deep focus microscope, providing an image of the fiber arrangement in all three dimensions, by a revolving sample carrier.

Omnidirectional Measurement of the Compliance of Woven Fabrics

Claudio Caccia
Politecnico di Milano

A new measurement method for fabric compliance in the low-stress area, is presented, with the target to provide useful information for the development of new fabrics, and for quality control during production.

In the past few years, elastic woven fabrics have become increasingly important for many kind of apparel. This calls for more research on the elastic properties of fibers, yarns, and fabrics. The goal is to find the correlation between the basic characteristics of the fabrics (such as properties of fibers and yarns and the structure of the fabric) and the total elasticity of the fabric itself.

Theoretical models and calculations of fabric compliance made in the past have mostly treated the elastic properties in a single direction, either warp or weft. As a basis for new, enlarged investigations on the effect of fabric compliance, a new measuring machine, has been developed which allows measures of compliance in all directsions, including warp and weft.

The fabric sample to be analyzed is put on the measuring machine by means of a carrier, equipped with pins to fix the sample with a definite pretension. In order mount the sample with this pretension, a pre-tensioning frame is used.

The measures are made by a measuring head with a force sensor. The force is imposed to the sample by a clamp. The machine has three linear axes, each one driven by a motor: one motor moves the measuring head up and down, in order to clamp the sample; another motor rotates the table with the sample in order to put it in the desired direction; finally a servomotor moves horizontally a sledge holding the sample, providing the displacement to generate a force on the measuring head corresponding to the compliance of the fabric. By this, a force-displacement diagram is taken, in any direction respective to the warp of the fabric.

The experiments have been made on six different samples of fabrics, all made of polyester yarn, with different types of weft, different fabric construction, and different finishing. These tests were at different levels of force, and in warp and weft direction. They demonstrate that the force-displacement curves in weft and in warp direction are quite different, giving reason to continue the tests in all directions.

Further tests have been made measuring the compliance at every direction between warp and weft. They provide a directional plot of the compliance in function of the angle from the warp direction. The measures show, in general, a good repeatability.

In a second part, the force-displacement behavior of fabrics has been evaluated relating to the linearity of the compliance, its symmetry when changing direction, and the hysteresis work during one complete cycle of load. Indications have been found that point to a strong influence of the internal stresses of the yarn, and of the inter-fiber frictional properties.

Size Reduction of Clay Particles For Nanocomposite Polypropylene

Gopinath Mani*, Qinguo Fan, Samuel C. Ugbolue and Isabelle M. Eiff
Department of Textile Sciences, University of Massachusetts Dartmouth, MA 02747-2300

This research work is about combining both ball milling and ultrasonication to produce nano-size clay particles. Not only is the particle size a crucial parameter for polymer nanocomposites but also it plays a vital role in paints, pigments, inks, toners, chemicals, talc, drugs, pharmaceuticals, cosmetics, confectionary, chocolate liquor, etc. Our work emphasizes on increasing the specific surface area of montmorillonite clay by reducing the particle size to nanometer dimensions.

Cloisite-15A was used in our study. It has 2:1 layered structure (two silica tetrahedral sheets linked to one aluminum octahedral sheet). The thickness of the particle is in nanometer dimensions, length and breadth in micrometers. These particles have been surface modified with onium ion substitution reaction to convert the surface from hydrophilic and hydrophobic. The Particle Size Distribution (PSD), Specific Surface Area (SSA), Surface Weighted Mean (SWM), and Volume Weighted Mean (VWM) of the as-received clay particles are 0.5μm to 35μm, 1.22m^2/g, 4.9μm, and 8.451μm respectively. The characterization of the nanoparticles was done by Particle Size Analyzer based on laser diffraction and by morphological studies.

In ball milling, a number of glass balls, 3mm and 5mm in diameter and hardened stainless steel balls, 5mm and 8mm in diameter were used. The Thumblers tumbler is a steel hexagon barrel with removable rubber lining and it is 9cm in diameter and 8cm wide. A glass bottle with 5.5cm in height and 2.5cm in diameter is used inside the tumbler for the ball mill of clay. The speed of the tumbler is 20rpm; slower the speed, greater the chance for the balls to have contact with many particles, hence the impact energy is even and also the centrifugal forces wouldn't overcome gravity. The ratio of balls-to-clay particles in the tumbler media was 100:2.5 grams and it was allowed to run for 24 hours. The total kinetic energy is the same for all the four types of balls, However in the case of 3 mm glass balls which has higher surface area, more contact with the particles occurs and when the glass bottle is rotating inside the tumbler, because of its lower mass (0.0363 gm), more number of balls hits the top surface of the bottle and fell down, which leads to higher potential energy for 3mm glass balls than the other types of balls. It should also be noted that the number of balls makes the difference. Overall, there are more impacts and higher impact energy in the case of 3 mm glass balls. So does the rotational energy ($I*\omega^2$) is also high in case of 3 mm glass balls, because the velocity of these balls is faster than the other types of balls during the tumbler rotation. For a rolling ball, its total energy is the sum of its kinetic and rotational energy. The Grinding energy was

calculated under two different stages; the first stage is when the particle was between two different balls and the other stage is when the particle was between the ball and tumblers wall. These shear and tensile stresses which are produced during the milling operation acting at weak points (internal pores, surface fissure, surface pores and micro cracks) of the clay particles that ultimately paves the way for particle size reduction. The PSD, SSA, SWM, and VWM of the 3mm glass balls milled samples are 0.5μm to 15μm, 2.92m^2/g, 2.052μm, and 3.172μm respectively. Although the particle size is reduced by ball milling, dry powders usually consist of aggregates and agglomerates, which was dispersed in xylene to produce individual units. When the particles are dispersed in xylene, there was a drastic change in the particle size and particle size distribution. In xylene, the PSD, SSA, SWM, and VWM of the clay particles are 0.5μm to 33.570μm, 36.8m^2/g, 0.163μm, and 1.022μm respectively.

Ultrasonication was done on milled samples in xylene. One of the main mechanical effects caused by the ultrasonication is the disaggregation and deagglomeration of particle assembly. Cavitation is the important phenomenon in ultrasonication. The particles in xylene are considered the nuclei for the cavitation of bubbles. The high energy produced due to the collapse of bubbles at very high temperature responsible for breaking the particles. The so-generated shock waves can cause the particles to collide into one another with great force, since these are similar charged particles, problem of agglomeration is reduced and particle size reduction is achieved. An investigation on the amplitude, pulsation rate and time of the ultrasonication process was done with respect to particle size distribution. The optimized conditions in our lab were determined: 90% amplitude, 8 sec. on and 4 sec. off pulsation rate and 4 hours. When the amplitude is increased from 80% to 90%, with pulse rate 5 sec. on and 5 sec. off, the SSA increases from 40.38m^2/g to 45.48m^2/g in 1 hour and from 35.38m^2/g to 46.98m^2/g in 4 hours. Amplitude is directly proportional to the intensity, which is a measure of the amount of energy available per unit volume of liquid. Hence when the amplitude increases, higher energy will be imparted to the cavitation bubble and greater the intensity of the energy released in the implosion of that bubble and obviously the energy is used for deaggregation and deagglomeration. Time is a vital factor. Greater the time allowed for ultrasonication, better the results. When the ultrasonication time is changed from 15mins to 1 hour and to 4 hour, the SSA increases from 38m^2/g to 45.4m^2/g and to 46.9 m^2/g respectively. The PSD of the treated samples also decreased accordingly. When the pulsation rate is changed from 5sec. on and 5 sec. off to 8 sec. on and 4 sec. off, for 4 hours, the SSA increases from 35.5m^2/g to 49.5m^2/g. The PSD is also greatly reduced from 18 to 10, which indicates narrower particle size distribution. The treated clay particles were obtained in nanometer dimensions and the reduced particle size range is from 50 nm to 350 nm, specific surface area is dramatically increased to 48.2 m^2/g, surface weighted mean and volume weighted mean are drastically decreased to 128 nm and 650 nm respectively.

*** Corresponding and Presenting author:**

Gopinath Mani,
Department of Textile Sciences,
University of Massachusetts Dartmouth,
285 Old Westport Road,
North Dartmouth,
Massachusetts, MA 02747-2300.
E-Mail: mgopitex@hotmail.com
Phone: 508-999-8430
Fax: 508-999-9139

Biography:

Gopinath Mani, a Research Assistant in the Dept of Textile Sciences at UMass Dartmouth, earned a B.Tech in Textile Technology from Anna University (Chennai, India) in 2000. He is working on a National Textile Center funded Research Project "Dyeable Polypropylene via Nanotechnology". His research interest includes nanocomposite fibers, characterization of nanoparticle size, dispersion of nanoparticles in polymers, dyeing polyolefin fibers and color chemistry. He has participated in Northeast Student Chemistry Research Conference, Boston University and SigmaXi Research Conference, University of Massachusetts Dartmouth. He is a student member of American Association of Textile Chemists and Colorists (AATCC) and Texas Nanotechnology Initiative.

Ultrafine Fibers from Electrostatic Solution Spinning

Veli E. Kalayci [*], Prabir K. Patra, Samuel C. Ugbolue, Yong K. Kim and Steven B. Warner
Textile Sciences Department, College of Engineering, University of Massachusetts, Dartmouth

During the last ten years extensive research has been conducted and published on various aspects of electrospinning. These efforts include spinning of many different polymer and solvent pairs, fiber characterization and process modeling. In this work we explain some issues related to charging of the polymer solution in terms of charge quantification of electrospun fibers and different charge delivery designs. To know the charge, charge location and charge density in the jet at all distances from the Taylor cone is ideal, but not yet realized. A simple measure of the current that flows into the solution or the charge that flows in the electrospinning column of fiber and air may be inaccurate due largely to the presence of plasma entrained with the moving fiber mass. In addition, we address some important process-fiber relationships i.e. voltage, viscosity dependence of fiber diameter and morphology.

Our electrospinning apparatus consisted of a syringe pump, 0-50 kV DC power supply, an ammeter and various take up devices including metal screens, belts and other targets. Charge is measured using a Faraday cup coupled to a nanocoulomb meter.

We have used a solution of poly(acrylonitrile) in dimethyl formamide for charge measurements. Viscosity measurements were performed using a Brookfield DV-II+ programmable viscometer; electrical conductivity was measured with a Corning CD-55 conductivity meter; and surface tension was calculated using the results of contact angle and capillary rise measurements. The contact angle was measured using a Nrl-Ca Goniometer when a glass capillary is immersed into a polymer solution. Electrospun fibers were viewed using JEOL-JSM 5610 scanning electron microscope and fiber diameters were measured from the SEM photomicrographs. The results were then compiled into classes in order to obtain fiber diameter distribution profiles.

The charge of the fiber was measured with a nanocoulomb meter connected to a Faraday cup. The fibers were spun onto a polyethylene film (sampler) and transferred to the Faraday cup immediately after spinning. After measuring the amount of charge on the substrate, it was weighed using a Mettler Toledo AG135 analytical balance. We measured the charge per mass for electrospun PAN fibers as a function of collection time. The change in charge per mass was also investigated at various voltages and solution concentrations. In order to understand the effect of solvent evaporation to the current flow from the grounded electrode, we electrosprayed pure solvent and measured the current.

The highest current flow from the collector to ground was achieved in the absence of any solvent. This current was formed by discharge of the air caused by the high electric field strength. All sprayed media were measured in terms of their voltage-current characteristics, which have a typical parabolic shape. The magnitude of the current varied with the solvent conductivity. The

[*] Currently at Donaldson Company, Inc., Minneapolis, MN

charge density varied with the deposition time, applied voltage and solution properties. Generally, the range was found to be in between 40 – 60 nC/mg. Theoretical charge density calculations are found to be in agreement with the experimental measurements.

A momentum balance equation considering only the electrostatic forces acting upon a segment of stable jet is derived as follows:

$$\sum F = \rho \frac{2}{3}\frac{\pi h}{12}\left(D^2 + Dd + d^2\right)\frac{dx^2}{dt^2} = \left(yn_1 qE\right) - \left[n_1\, 6\pi\eta\mu E\left(r_{ni} - r_{pi} - yr_{ni}\right)\right]$$

where ρ is the solution density, h is the height of the jet column, D is the diameter of the upper jet column, d is the diameter of the lower jet column, dx^2/dt^2 is the acceleration of the jet in the given jet segment dx, y is the ratio of the difference between oppositely charged species and the initial number of unipolar species, q is elementary charge, E is the electric field strength, n_1 is initial number of unipolar species, η is the solution viscosity, μ is the ion mobility, and r is the hydrodynamic radius of charged species. The theoretical calculations show that at a 30 % relative difference in the number of oppositely charged species, the resulting column of solution acquires a charge density of 90 nC/mg. This approximation is in agreement with the measured charge density values of electrospun PAN fibers.

While contact charging using a negative potential is known in electrospinning, experimental studies are limited. We employed a negative charging unit that is ordinarily used for flocking. To make a good comparison between negative and positive contact charging systems we electrospun once with a positive voltage of 40 kV and once with a negative voltage of 40 kV. The negative charging device was an Ero-Flock hand-held flocking instrument, model VDE0875. The positive charging device was purchased from Gamma High Voltage Research, model E-50P. The fiber diameters created from both systems are practically in the same range. However the difference might be explained by different saturation currents of the high voltage supplied.

We studied the importance of free ions created by the electric field as a source of fiber charge. To understand the effect of free ions created by discharge in air, we adapted the ionized field charging technique. We disabled any direct contact of charges to the system and instead placed the syringe-needle system through an O-ring electrode, which was stressed with a high potential. This modified electrospinning system resulted in the formation of nanofibers, which can be characterized with larger average fiber diameters compared to their counterparts produced by contact charging systems. The process itself was also different in comparison to the contact charging systems; in this case the polymer solution was forming fibers in a pulse-mode rather than a continuous manner.

Our fiber characterization involved fiber size, morphology, surface roughness and crystallinity as a function of parameters such as solution concentration, viscosity, and applied voltage. Details of these studies will be published soon. In this presentation we will talk about fiber diameter and morphology study. The effect of solution viscosity was found to play a much greater role than the effect applied voltage on the fiber diameter. After extensive fiber sizing we have derived an empirical equation that governs the PAN fiber size as a function of solution viscosity. The following equation is valid for low concentration solutions (≤ 8 wt%) and we found that high

concentration (13 wt%) solutions do not follow the same regime. The regime between 8 and 13 wt% is not determined. And below 5 wt% solution concentration, the consistent spinnability became an issue due to very low viscosity.

$$d = 19.49\,\eta^{0.43}$$

where d is the fiber diameter (nm), η is the solution viscosity (cP). The fiber diameter calculation shows a standard deviation of ±15 nm. Fiber morphology study was carried out on poly(caprolactone) fibers spun from solutions in acetone. Our observations revealed that the fiber morphology depends on solution concentration and viscosity. The bead-like structures disappeared as the concentration increased, whereas the fibers produced therefrom broadened.

This work has been supported by the National Textile Center through collaboration with the Department of Chemical Engineering at Massachusetts Institute of Technology.

Biography:

Veli Kalayci joined Donaldson Company, Inc. in April 2002. He earned a BS degree in Textile Engineering from Ege University, Izmir, Turkey in June, 2000. He earned his MS degree in Textile Technology from University of Massachusetts, Dartmouth in July, 2002. His current responsibilities include process development and theoretical modeling.

Physical Properties and Morphology of Polypropylene/Nylon 6 Alloy Filaments

B. S. Gupta[(1)] , R. Kotek[(1)], M. Afshari[(2)]
[(1)] Textile Chemistry and Engineering Department., P. O. Box 8301
North Carolina State University, Raleigh, NC 27695-8301
[(2)] Textile Eng. Dept., Amir Kabir University of Technology,
P. O. Box 15875-4413

Introduction

The purpose of blending of polymers is obtaining materials suitable for specific needs by tailoring one or more properties with minimum sacrifice in other properties [1,2]. An immiscible blended polymer system has generally a microstructure of the phase separation. This system is, therefore, a new polymeric material with special features of each polymer. In immiscible polymer blends, the major component forms a continuous matrix while the disperse phase forms in different shapes (droplet, rod, fibril or lamellar) [3]. For improving interfacial interactions and stability of the morphological structure in immiscible polymer blends interphase modifiers are added [4].

It has been reported that fiber spinning of immiscible polymer blends from melts was an interesting and useful method for change in properties of fibers. Blending of polymers is promising method for improving properties of synthetic fibers and generating fibers with synergistic property [5].

Production of PP fibers has increased at accelerated rates in the world due to simplicity of production technology and excellent fiber properties i. e. very low density, chemical resistance, sufficient high physical characteristics, including high resistance to wear. Blends of PP and nylons have received much attention in recent years [6]. PP and N6 are immiscible that leads to materials with improved chemical and mechanical properties. PP-g-MAH can be a proper compatibilizer for PP/N6 blends [7]. The elongation force field in melt spinning process is effective for producing the fibrillar morphology [8].

In the present study, we have produced undrawn and drawn filaments from PP/N6 blends as specified in Table 1. The blends were also compatibilized with polypropylene grafted maleic anhydride (PP-g-MAH) at two take-up speeds of 300 and 800 m/min. Then the filaments were drawn with a draw ratio of 3.5 and 2 for 300 and 800 m/min take-up speed respectively. Morphology of filaments observed by LSCM and physical properties (tenacity, elongation at break, modulus, sonic modulus, birefringence, and wettability) and the structure of fibers (orientation factor of crystalline region and crystal size) by WXRD are studied. Different models for explaining experimental results for the tenacity and modulus data were applied. The unique dyeability of these fibers with disperse dyestuffs is also reported in this paper.

Table I. Polymer Compositions and Spinning Conditions

Sample Code	PP(%wt)	N6(%wt)	PP-g-MAH (%wt)	Take up speed(m/min)	Draw Ratio
A1	100	0	0	300	-
A2	90	10	0	300	-
A3	85	10	5	300	-
A4	75	20	5	300	-
A5	100	0	0	800	-
A6	90	10	0	800	-
A7	85	10	5	800	-
A8	75	20	5	800	-
A9	100	0	0	300	3.5
A10	90	10	0	300	3.5
A11	85	10	5	300	3.5
A12	75	20	5	300	3.5
A13	100	0	0	800	2
A14	90	10	0	800	2
A15	85	10	5	800	2
A16	75	20	5	800	2

EXPERIMENTAL

MATERIALS

Commercial a fiber grade isotactic polypropylene known as Escorene was supplied by ExxonMobil Chemical Company (MFI= 16.7 g/10 min, density = 0.97 g/cm ^{3}, T_m=170 °C). A fiber grade nylon 6 was supplied by Honeywell Co., (MFI= 27.6 g/ 10 min, density = 1.14 g/cm^3, T_m=220°C). PP-g-MAH (Polybond® 3150) from Uniroyal Chemical Co., melt flow index 50 g/10 min., MAH Index 1.5% and density of 0.9 g/cm^3 was used.

FIBER SPINNING & DRAWING

Before melt spinning, the polymer alloys were dried in a vacuum oven at 80°C for 24 hours. Melt spinning process was performed on a melt spinning machine provided by Alex James & Assoc. Inc. The spinneret had 20 orifices of 0.6 mm diameter and L/D= 2.3. The spinning temperature was controlled at 5 different zones of the extruder, i.e. the feeding, metering section and die zones. The temperature profile of the extruder was 235°C/245°C/250°C/265°C/270°C. The undrawn filaments were produced at two take-up speeds of 300 and 800 m/min. The undrawn yarns were drawn on a Dienes single position experimental drawing unit (Dienes Apparatebew GMBH, Mulheim, West Germany.

RESULTS

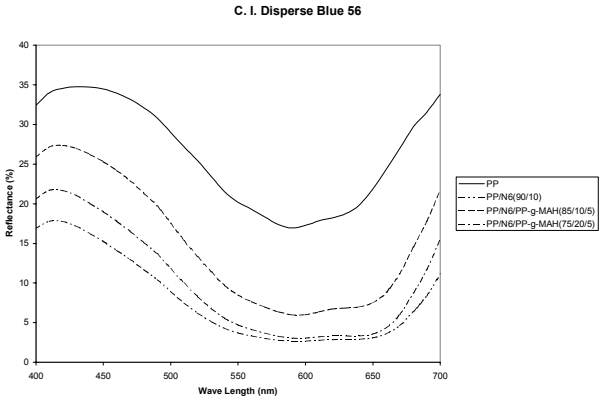

Figure 1. Reflectance Curves for PP and PP/N6 Fabric after Dying with C. I. Disperse Blue 56.

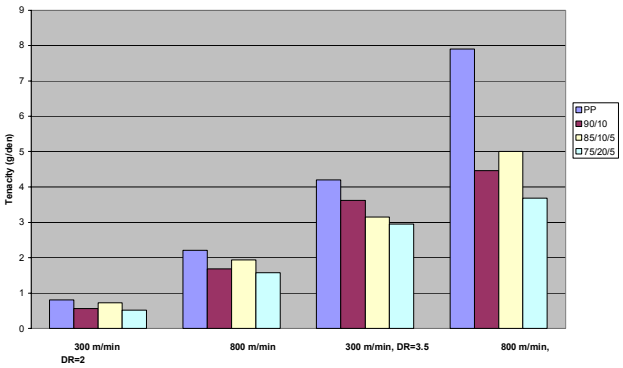

Figure 2. Tenacity of PP and N66/PP fibers

Table II. Contact Angle and Wettability Index of PP and N66/PP Allot Filaments (spun at 800 min)

Code	F_a (dyne)	F_r (dyne)	Θ_a (degree)	Θ_r (degree)	WI_a	WI_f
A5 (PP)	-2.2280	-1.9804	93.61	92.23	-4.58	-2.83
A6 (90/10)	-2.1599	-1.9280	93.23	91.94	-4.10	-2.46
A7 (85/10/5)	-2.1293	-1.8925	93.06	91.74	-3.88	-2.21
A9 (75/20/5)	-2.0917	-1.9243	92.85	91.36	-3.27	-1.73

CONCLUSIONS

1. We have demonstrated the feasibility of spinning of compatibilized N66/PP fibers. 2. These fibers have slightly improved wettability. 3. The compatibilized N66/PP fibers can be dyed with dispersed dyestuffs. 4. A technique for the determination of the amorphous and crystalline orientation fibers has been demonstrated for the bicomponent fibers.

REFERENCES:

1. Xanthos M. Polym. Eng. Sci. 1988;28:1392
2. Utracki L. A. Commercial Polymer Blends, London: Chapman & Hall, 1998.
3. Hersh S. P. J. Appl. Polym. Sci. Applied Polymer Symposium, 1977;31:37.
4. Heikens D, Barentsen W. Polymer 1977;18:69.
5. Tseberenko M. V. Yudin A. V. Polymer 1976;17:831.
6. Paul D. R. Newman S. editors, Polymer Blends Vol 2, New York, Academic Press 1978.
7. Park S. J., Kim B. K., Jeong H. M. Int. Polym. J. 1990;26:131.
8. Li X., Chen M., Huang Y., Polymer J. 1997;29:975

Biography

BHUPENDER S. GUPTA

Professor, Department of Textile Engineering, Chemistry, and Science
College of Textiles, North Carolina state University
Raleigh, NC 27695-8301, USA

Received his undergraduate education in Textile Technology from the Punjab University, India, and his doctoral degree in Textile Physics from the University of Manchester Institute of Science and Technology, Manchester, England. After having worked in industry for a short period, he joined the College of Textiles, North Carolina State University, Raleigh, North Carolina, USA, as a faculty and is currently a professor in the Department of Textile Engineering, Chemistry, and Science.

In 1985, he received a Fulbright grant to lecture in areas of fiber science at various institutions in India. His teaching and research interests have included physical and mechanical properties of fibers and fibrous assemblies, structural mechanics of assemblies, biomaterials, surface friction and energetics, and absorbent structures, the last being the area in which he has focused his research during the past 20 years.

Membership in professional societies includes the Technical Association of Pulp and Paper Industry (TAPPI), Fiber Society, and the Textile Institute of which he is a Fellow.

Micromorphology Characterization of Electrospun Nanofiber Webs Using Multi-fractals and Random Functions

Jooyong Kim*, Sung Weon Byun, Hyungsup Kim and Dae Young Lim
*Dept. of Textile Engineering, Soongsil University, Seoul, Korea
Korea Institute of Industrial Technology, ChonAn, Korea

Electrospun fibers have long been known as a promising candidate for filtration and membrane application mainly due to their large specific surface areas and micro-porous structure. The morphology of the nanofiber webs was found to depend on process parameters such as solution concentration, the electric field strength applied, flying distance, throughput, etc. While the process of electrospinning has been relatively well understood, knowledge on how the process conditions affect the structure of the resulting nanofiber webs is currently very limited. The study is aimed at investigating the effect of the process variables on the morphology of the resulting nanofiber webs. The fractals and random functions have been employed in order to find some systematic variations in the seemingly random nanofiber structures. Structural changes in nanofiber webs along with throughput have been detected and quantified by a set of fractal dimensions and random functions. The non-homogeneity and variability in spatial distribution of micropores has been also elucidated by the fractal theory, while random functions make natural connections between the fractal dimension and the irregularities. The results show that a proper combination of the fractal dimensions and the statistical parameters characterize the non-homogeneity and the microstructure of the nanofiber webs.

Analysis of scanning electron microscope(SEM) images

The images consisting of only surface fibers have been extracted in order to estimate the parameters for pore size distribution. The images have been thresholded and converted into the black and white binary formats for further processing. The pores have been automatically counted and ordered according to the size. Stable distributions for pore size have been obtained by counting at least 300 data points in SEM images with a magnification of 5,000. Figure 1 shows a original and thresholded SEM images of a Nylon 6 nanoweb

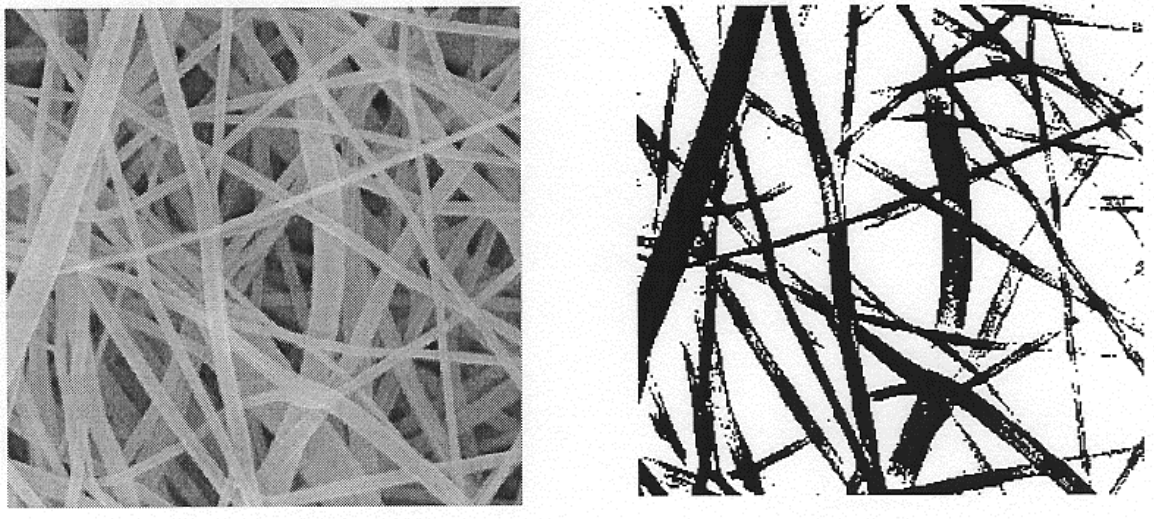

Figure 1. Comparison of two SEM images of a Nylon6 nanweb
(left: original and right: thresholded)

Effect of Throughput on pore size distribution

Figure 2 shows the effect of throughput on pore size distribution for Nylon 6 nanowebs. As the nozzle pressure increases from 2 to 6 by by 2kgf/cm^2, the throughput changes to 20, 21.5 and 22, respectively. As show in the figure, it is evident that average pore size increase with the throughput. This is the case for other polymers such as Nylon66.

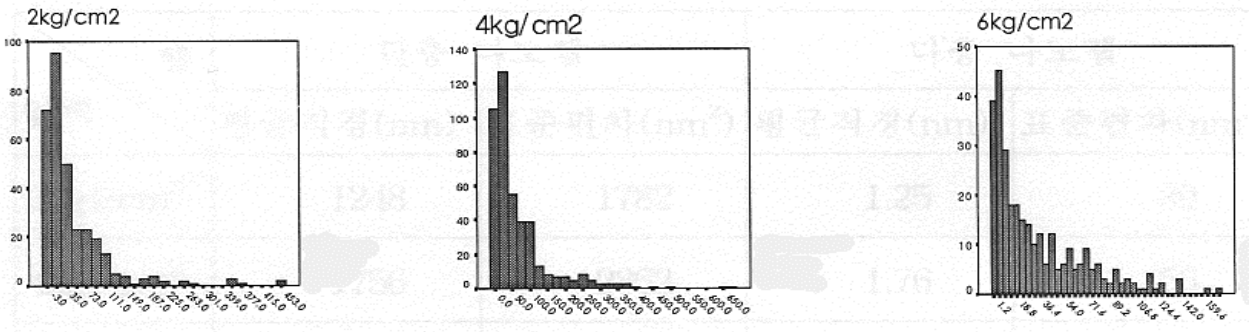

Figure 2. Pore size distribution (a: 2kgf/cm2, b:4kgf/cm2 and c:6kgf/cm2)

References

1. Helen H. Epps and Karen K. Leonas " Pore Size and Air Permeability of Four Nonwoven Fabrics", INJ Summer (2000).
2. E. Ghassemieh, H.K. Versteeg and M. Acar , " Microstructureal Analysis of Fiber Segments in Nonwoven Fabrics Using SEM and Image Processing", INJ Summer (2001).
3. J.M. Deitzel, J. Kleinmeyer, D. Harris, N.C. Beck Tan, " The Effect of Processing Variables on the Morphology of Electrospun Nanofibers and Textiles ", *Polymer*, **42**, PP261-272 (2001).

*Corresponding and Presenting Author

Name: Jooyong Kim
E-mail: jykim@ssu.ac.kr
Address: Department of Textile Engineering, Soongsil University,
Sando5, Dongjak, Seoul, Korea 156-743
Phone: 82-2-820-0631
Fax: 82-2-817-8340

Jooyong Kim, Associate Professor of Textile Engineering at Soongsil University, joined the faculty in 1999. He earned a Ph.D. in fiber and polymer science from North Carolina State University in 1998 and a M.S. and a B.S. in Textile Engineering from Seoul National University (Korea). He was a Fellow of integrated manufacturing laboratory at UCLA. His research interests include textile process control/optimization, stochastic signal/image processing and fuzzy/adaptive systems.

Viscosity Effect on Fiber Morphology in Highly Filled Fibers

Christopher Drew, Jamila Shawon[+], Xianyan Wang, Lynne Samuelson[°], Jayant Kumar*

Department of Chemistry and Center for Advanced Materials, University of Massachusetts, Lowell, [+]Department of Chemical Engineering and Center for Advanced Materials, University of Massachusetts, Lowell, ° Natick Soldier Center, U.S. Army Soldier, Biological, Chemical Command, Natick, Massachusetts, *Corresponding Authors

Introduction

Electrospinning has undergone a renascence in the last decade due to desire for interfaces of very large surface area. Applications like sensors[1], and biological scaffolds[2] have employed electrospun polymer membranes. Many other potential applications of electrospinning are made difficult because the desired materials do not electrospin well or even at all. For example, nanoscale particles of titanium dioxide are of great interest in dye sensitized photovoltaic applications[3]. The large surface area beneficial to such photovoltaic cells would seem to be a good application for electrospinning, however the particles alone will not forma fiber when electrospun. It is possible to blend the particles with a polymer that does electrospin well to form a composite fiber. Yet the polymer presence is undesirable in the final application as it interferes with the electrical connectivity of the particles and should, ideally be minimized.

It has been understood that the minimum polymer concentration for electrospinning was the crossover concentration at which polymer entanglements begin[4]. In practice, however, a successful electrospinning spin-dope must have a much higher concentration to provide the requisite viscosity to counter the surface tension of the liquid. We have investigated the feasibility of increasing the viscosity by the addition of a non-polymeric filler instead of a higher polymer concentration.

Experimental

A series of spin-dope solutions were made consisting of poly(ethylene oxide) (PEO) and titanium dioxide nanoparticles (TiO_2) in a water/ethanol solvent mixture. All chemicals were used as received. Titanium dioxide was acquired from Degussa and all other chemicals were from Aldrich. The resulting fibers were examined by a scanning electron microscope (SEM) (AMRAY 1400) and fiber diameter, bead diameter, and bead density were determined from the images. Viscosity was measured with a Brookfield viscometer.

Results and Discussion

Fibers were electrospun from three types of solutions: 1. Pure PEO in increasing concentration, 2. PEO and TiO_2 where the solid content was 10 weight percent, and 3. PEO fixed at 3 wt. % with increasing amounts of TiO2.

In all cases, adding TiO_2 increased the viscosity of the spin-dope solution. This increase in viscosity had similar effects on the fiber morphology for all three types of samples. As shown in Figure 1, the mean fiber diameter appears to increase logarithmically as the solution viscosity was increased. However, the added viscosity from TiO_2 did not increase the fiber size to the same size as a fiber from a pure PEO solution of the same viscosity. This may be due to aggregation of the particles in solution prior to electrospinning. This conclusion was also suggested by the relationship of bead diameter and beads per fiber with viscosity. The number

and size of the beads both increased with viscosity in solutions with TiO_2. No beads were present in the PEO only solutions except at very low concentrations.

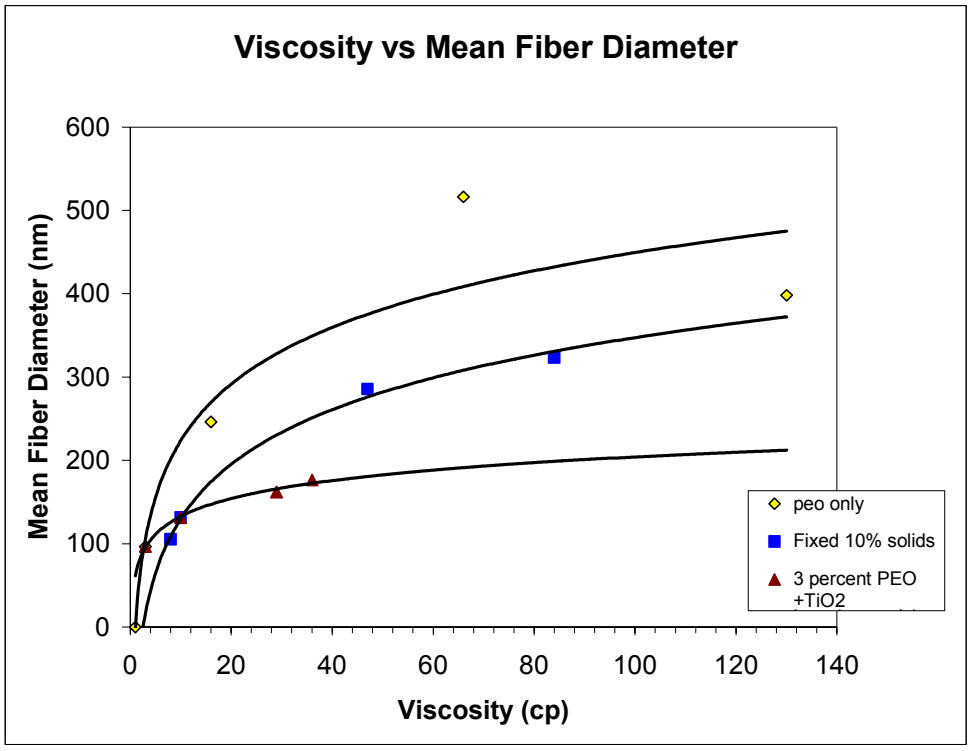

Figure 5: Fiber diameter as a function of spin-dope viscosity.

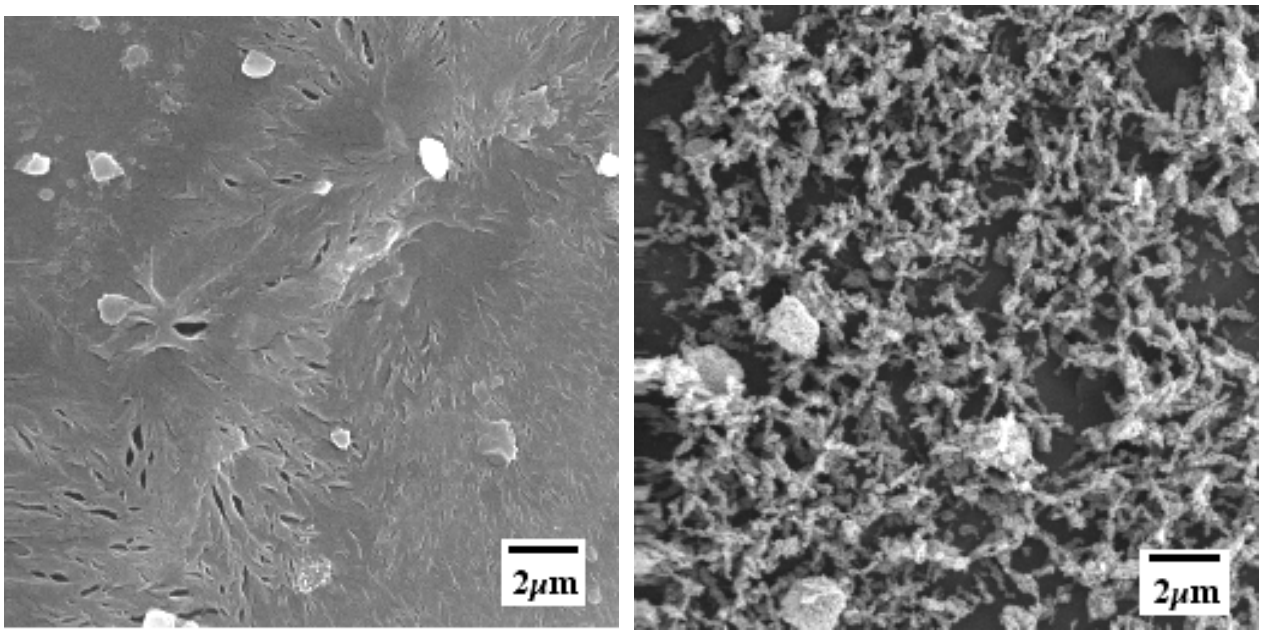

Figure 6: SEM images of electrospun PEO (2 wt. %) on top and the same solution with TiO_2 (8 wt. %) added on the bottom. Both images are 5000x with the scale bar representing 2 microns.

This effect of the filler material on viscosity can be of utility as shown in Figure 6. A solution of PEO at a concentration of 2 weight percent does not form a fibrous membrane. Upon addition of 8 weight percent TiO_2, fine fibers were readily electrospun under the same conditions. Light scattering data indicate the entanglement concentration of the PEO used in the water/ethanol solvent used to be about 2 weight percent.

Conclusion

Fiber diameter was observed to increase with increasing viscosity of the spin dope solution, regardless of the component causing the increase. The occurrence of beads may also increase with viscosity from non-polymeric components, particularly if they tend to aggregate in solution. Thus, it is possible to electrospin fibers consisting largely of non-polymeric components that would not electrospin alone. We have demonstrated the formation of fibers in a composite system of PEO (2 wt.%) and TiO_2 (8 wt. %) where the pure PEO solution of the same concentration (2 wt.%) did not form fibers. The resulting fiber should only consist of about 20% polymer. This technique of highly filled polymer systems should greatly expand the utility of electrospinning, as small molecules, poorly solvated polymers and other materials could conceivably be incorporated into an electrospun fiber just as readily as TiO_2 was in this case.

Acknowledgements

Financial support from the US Army is gratefully recognized. The authors would also like to thank Ms. B. Kang, Mr. D. Ziegler, and Professor C. Sung for assistance with SEM imaging. This work is dedicated to Dr. Sukant Tripathy.

References

1.Wang, Xianyan; Drew, Christopher; Lee, Soo-Hyoung; Senecal, Kris J.; Kumar, Jayant; Samuelson, Lynne A. “Electrospining Technology: A Novel Approach To Sensor Application”. *Journal of Macromolecular Science* **2002** *In Press*.
2. How, T.V. US Patent 4,552,707, **1985**.
3. O’Regan, B.; Grätzel, M. “A Low-Cost, High-Efficiency Solar Cell Based On Dye-Sensitized Colloidal TiO_2 Films”. *Nature* **1991***, 353* (October 24) 737-9.
4. Doshi, J. *The Electrospinning Process and Applications of Electrospun Fibers.* Ph.D. Dissertation, University of Akron, Akron, OH **1994**.

*Corresponding Authors:
Lynne_Samuelson@uml.edu
Jayant_Kumar@uml.edu
Fax: 978-458-9571

Christopher Drew is a Ph.D. student in Polymer Science at University of Massachusetts Lowell. He received his B.S. in Industrial Engineering from University of Massachusetts Amherst and his M.S. in Plastics Engineering from University of Massachusetts Lowell. His research interests include nanotechnology, optical sensors, and organic photovoltaics.

Evaluating Single –Use Operating Room Gowns: The Influence of the Sterilisation Using Different Doses of Ionising Irradiation

L. Schacher[1], D.C. Adolphe[1], M.J. Abreu[2], M.E. Cabeço-Silva[2]

[1] Ecole Nationale Supérieure des Industries Textiles de Mulhouse, 11 rue Alfred Werner 68093 Mulhouse Cedex – France. - Tel. 33 (0)3 89 33 63 20 - Fax: 33 (0)3 89 33 63 39, e-mail: l.schacher@uha.fr, d.adolphe@uha.fr, [2]Universidade do Minho, Department of Textile Engineering, Campus de Azurem - 4810-058 Guimarães, Portugal - Tel: 351 53 510283 – Fax: 351 53 510293, e-mail: josi@det.uminho.pt; elisabete@eng.uminho.pt

Various single-use products and reusable materials have been proposed for operating room gowns and drapes with the aim of reducing micro-bacterial contamination and protecting the operating room staff from infection.

In Europe, the conversion from reusable to single-use has, so far, amounted to about 30% of this market, and non-woven medical single-use have great potentials to avoid bacterial infections, acquired in hospital, killing too numerous patients each year. However, industry has also to consider the environmentally conscious population when deciding between recycling potentially contaminated products or disposing the products in landfills.

The Directive 93/42/EEC on medical devices is the basis for evaluating surgical materials. A proposed mandatory European standard prEn 13795 "*Surgical drapes, gowns and clear air suits used as medical devices, for patients, clinical staff and equipment*", is being developed by the Committee of European Normalisation CEN TC 205 WG 14 and specifies the basic performance requirements and test methods for single-use and reusable materials.

In accordance to studied standards, the single-use non-woven based materials, which are not only textile materials but can also be laminates, polymer films and complexes, the evaluation have to be done after the sterilisation process.

However, until now, the performances of the used materials are mainly known from the manufacturers of surgical products before sterilisation, and for each component of the whole product, not knowing subsequently the changes that can appear after the ionising radiation over the combined material.

As sterilisation is performed through ionising irradiation processes (electron beam or gamma radiation's). These techniques are equivalent to ageing treatments and the changes that can appear after sterilisation are so unknown.

In the present paper the tested products are issued of surgical gowns and drapes composed of multi-layers. Multi layer components and composition are displayed in table 1 and 2.

Gown	Material	
	Outer Layer	Inner Layer
Type 1	Nonwoven	*Nonwoven*
Type 2	PE	Nonwoven
Type 3	Nonwoven	Laminate

Material	Nature
Nonwoven	45% PET – 55% Cellulose Spunlace
Laminated	*LDPE - 20 g/m² + Nonwoven 70% viscose – 30% PET*

Table 1 and 2

The common types of sterilisation methods are being exposed and the irradiation process used and conditions applied for our study are shown in table 3.

Radiation	Dose
β Radiation	25, 80 and 150 kGy
γ Radiation	25, 80 and 150 kGy
Electron beam	25, 80 and 150 kGy

Table 3

The impact of the sterilisation process – ionising radiation – over the most important properties of single or combined (multilayer) raw materials will be presented and results of the evaluation of the properties after irradiated at several doses will be detailed in order to optimise the process.

Short biography

Dominique C. Adolphe is 41 years old, he has defended his PhD theses in « Engineers Sciences » in 1990 on the studies of the physical properties vs. hydraulic behaviour of Nonwoven.

In 1991 he has been an Assistant Professor at the University of Mulhouse - School of Textile Engineering - France - in the area of textile testing, nonwoven and garments industries.

In 1999 he became Full Professor at the University of Mulhouse - School of Textile Engineering - France - and took the head of the Garment Industry Department.

He is Member of the standard working group AFNOR “Tactile Sensory Evaluation”

His Research interests are:

Nonwoven - Relation between Structure and Properties

Garment Comfort and comfort evaluation

Sensory evaluation of textile products

Modeling the Impact Behavior of High-Strength Fabric Structure

Yiping Duan[1], Michael Keefe[2], Travis Bogetti[3], Bryan Cheesman[3]
[1]Center for Composite Materials, University of Delaware; [2]Department of Mechanical Engineering, University of Delaware; [3]Composite and Lightweight Structures Branch, Army Research Laboratory

Fabrics made from high-strength aramid fibers possess good impact resistance ability and are often used in flexible body armor systems. It had been established that the impact energy during ballistic impact event is absorbed by fabric through the modes of kinetic energy of the deforming fabric, internal energy stored by the stretched yarns, and the interface sliding energy dissipated by friction between yarns at crossover points, between fabric layers, and between projectile and fabric surfaces. However, there are two issues need to be resolved. The first is what the contribution to impact energy absorption is by each mode, and the second is how strong the friction influences the impact behavior of fabric structures. In this paper, we use a commercial available dynamic explicit nonlinear finite element analysis code LS-DYNA to simulate the impact behavior of a plain-woven 600-denier Kevlar fabric. The yarns were modeled explicitly and considered as continuum with orthotropic material property. A three-dimensional finite element analysis (FEA) model was created for the fabric structure, as shown in Figure 1. Three types of boundary conditions were applied for the FEA model: all sides clamped, two opposite sides clamped and the other two sides free, and all sides free. For each boundary condition, the friction between yarns at crossover points and the friction between projectile and fabric surface during ballistic impact event were included and varied. The contribution to impact energy absorption by each of the energy modes were obtained from simulations for each boundary condition. The effect of friction on the impact energy absorption and the effect of friction on the projectile velocity-displacement curves were explored.

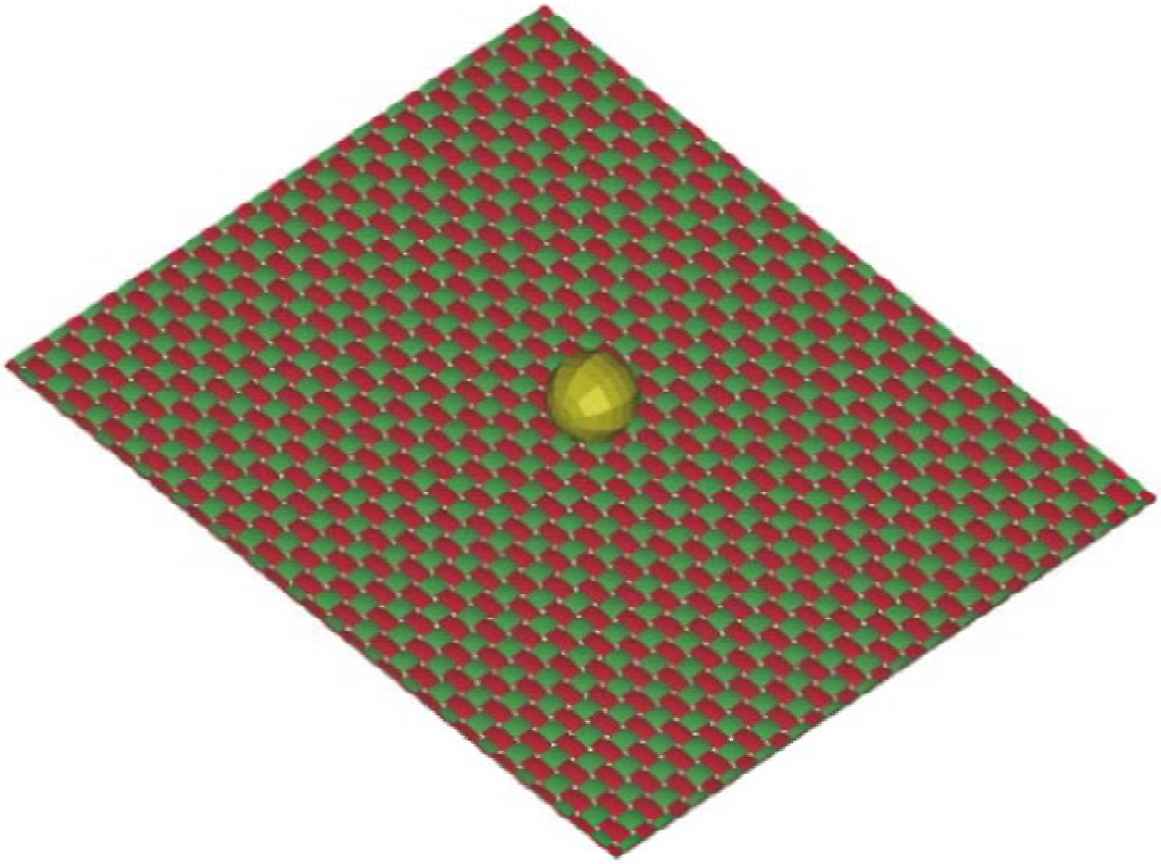

Figure 1 - A finite element analysis model for the Kevlar fabric structure

Brief Biography of Yiping Duan
(Presenting Author)

Yiping Duan is currently a Postdoctoral Fellow at the Center for Composite Materials, University of Delaware. He received his bachelor degree from North China Institute of Technology in 1993, his master's degree from Beijing Institute of Technology in 1997, and his Ph.D. degree in mechanical engineering from Tufts University in 2001. His current research interest is modeling the impact behavior of fabric structures and investigating the friction effects in ballistic impact events.

Novel Bonding Process for CBW Protective Electrospun Fabric Laminates

John D. Lennhoff[1], Poonam Narula[1], Karen Jayne[1], Heidi Schreuder-Gibson[2], Phillip Gibson[2]
[1]Physical Sciences Inc., 20 New England Business Center, Andover, MA 01810, [2]U.S. Army Soldier Systems Center, Natick, Massachusetts

Physical Sciences Inc. (PSI) has developed a method to adhesively bond conventional soldier uniform fabric with a Chem-Bio Warfare (CBW) barrier layer while retaining excellent fabric laminate breathability and drape. This work was performed under a Phase I SBIR program funded by the Army Natick Soldier Center. The Army Natick Soldier Center has developed a polyurethane (PU) based membrane with CBW barrier properties. These membranes hold promise as barrier materials for biological warfare agents and chemical aerosols, and as high surface area carriers for chemical warfare agent deactivating chemistries. In this effort, a laminate construction of woven fabric with the PU barrier layer and a non-woven liner was studied for different adhesive bonding scenarios. When this layered structure is laminated with conventional film adhesive methods, the fabric looses breathability and drape. PSI demonstrated the electrospun deposition of a nanofiberized adhesive with tunable bond strength that enables the construction of a CBW laminate fabric. The data and methods for this project will be discussed.

PSI formulated a moisture cured polyurethane adhesive that could be electrospun in either beaded (varicose), stable or whipping mode. Stable mode was used to achieve deposition in specific patterns, while whipping mode was used to deposit adhesive uniformly over large areas. PSI demonstrated the formation of a nanofibrous adhesive bond of tunable bond strength that did not affect fabric breathability and drape. Figure 1 shows the change in Relative Humidity across a fabric laminate constructed with electrospun adhesive, film adhesive, and fabric without any adhesive. The legend lists the adhesive areal density in grams of adhesive/meter^2 of fabric and the solids content of the spinning solution. The slope of these lines at early times in the exposure is a measure of water vapor transport rates across the membrane. The data shows no measurable decrease in the transport rate when the electrospun fiberized adhesive is used.

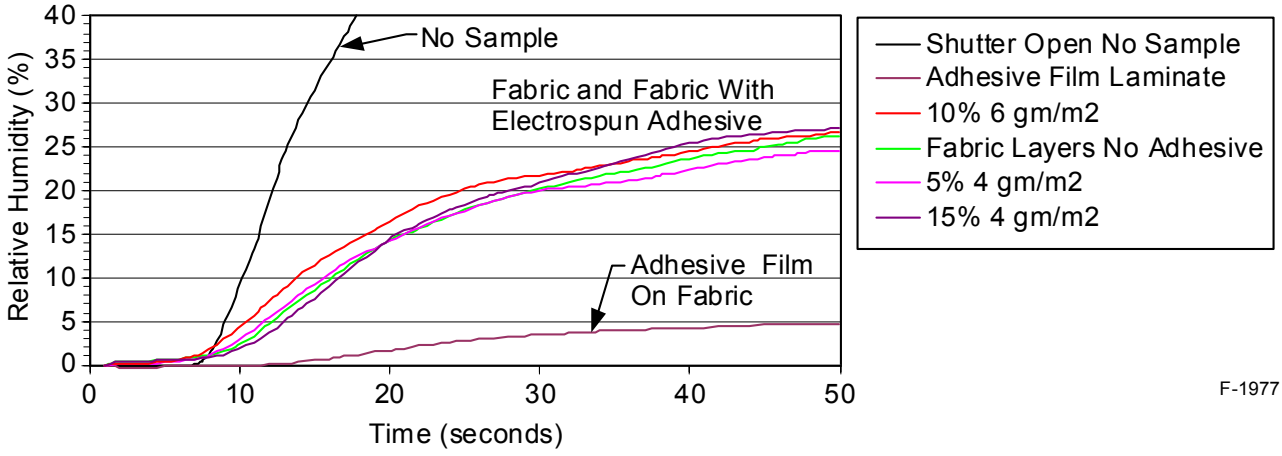

Figure 7. Moisture permeability of fabric laminates.

PSI has developed a variation of the electrospinning technique termed Patterned Electrospinning, which was used to produce adhesive features on the soldier fabric. Patterned Electrospinning utilizes a grounded template, in a user specified pattern, that promotes selective electrospinning deposition and, under proper conditions, sharp reproduction of the template, as shown in Figure 2. When a deposition film substrate (such as the soldier uniform fabric) is placed between the template and the electrospinning nozzle, deposition occurs on its surface. Templates from complex grid patterns to simple spots have been demonstrated in our labs. This presentation will show the adaptation of Patterned Electrospinning to the adhesive laminate, along with conventional electrospun adhesive deposition.

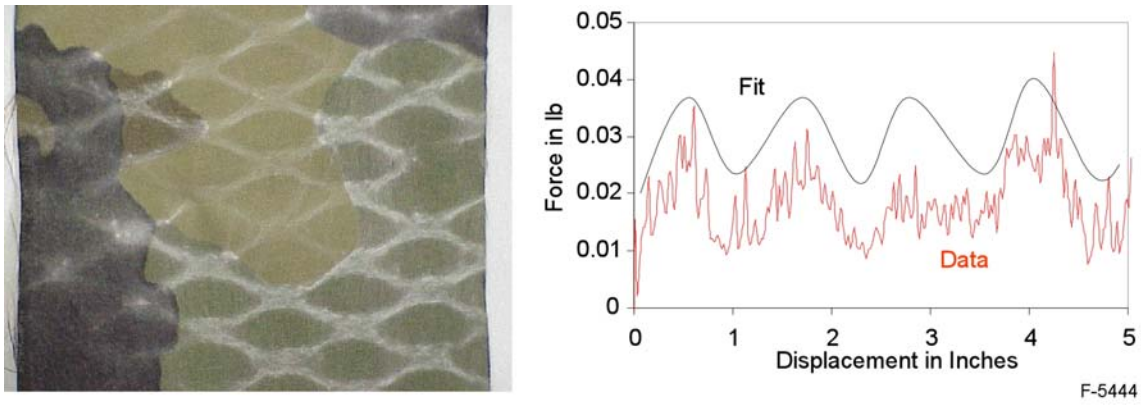

Figure 8. Optical image of patterned adhesive (left) and delamination force (right) of patterned electrospun adhesive laminate.

An optical image of the patterned electrospun adhesive on camouflage fabric is shown in Figure 2. The diamond electrospun adhesive (white) pattern in the left image is 1.2 in. by 2 in. The adhesive was used to laminate various layers to the camouflage, including non-woven polyester and polyurethane CBW type layers. The plot in Figure 2 shows the force required to delaminate the multilayer construction across the adhesive pattern. The periodicity of the force pattern matched the adhesive pattern period of 1.2 in. The patterned and continuous electrospun adhesive process development will be discussed and the characterization data presented.

Presenting Author:

John D. Lennhoff
Physical Sciences Inc.
20 New England Business Center
Andover, MA 01810
Tel.: (978) 689-0003
Fax: (978) 689-3232
e-mail: lennhoff@psicorp.com
http://www.psicorp.com

Dr. Lennhoff received his Ph.D. (1987) in Chemical Engineering from Worcester Polytechnic Institute in Catalytic and Materials Science. He spent a decade studying a wide range of materials, materials processes and materials characterization methods. Dr. Lennhoff joined PSI in the fall of 1999 where he manages the Materials Technologies Group. The group is developing advanced materials and processes for chemical sensors, electrochemical peroxide generation, electrochromic devices operating in the visible, infrared, and microwave, hybrid metal organic materials and small satellite based inflatable optics. Lennhoff is leading the development of electrospinning processes at PSI with a focus on applications including; thin polymer film rip-stop reinforcement, melt spinning of solar sails on-orbit, electrospun nanoscale ceramic cathodes for Li ion batteries, electrospinning processes for CBW laminates, and carbon nanofibers derived from electrospinning. He is a member of the American Chemical Society.

Characterization of the Mendability of Carpet Backing Fabrics

Mary Lynn Realff, Anneil Basnandan, Lindsay Evens,
Elizabeth McCartin, Matthew Realff
Georgia Institute of Technology

Our research examines the influence of yarn geometry and fabric density on the behavior of primary carpet backings. Backing fabric samples that varied in yarn geometry and number of filling yarns per inch were compared. A simulated tufting process was used to study the deformation of the fabric during tufting and the response of the fabric to the removal of yarns. This healing process is of great interest to the carpet tufting industry because it influences the amount of off quality goods that are made. A fabric with good healing properties can be mended to first quality, if a tufting process error occurs. One such error would be high tension in one of the ends, which causes the yarn to be pulled out of the backing.

Holding the pile yarn and maintaining strength are described as mendability. No tests have been developed to quantify "good" mendability, therefore, a method was developed. Primary carpet backing was placed on a frame and a single needle with pile yarn was used to puncture the backing. Figure 1a shows a snapshot of pile yarn embedded in the primary backing. Holes created when the fabric is deformed by the needle are identified using an image processing system. The yarn was then pulled out to determine the total area of damage as seen in Figure 1b.

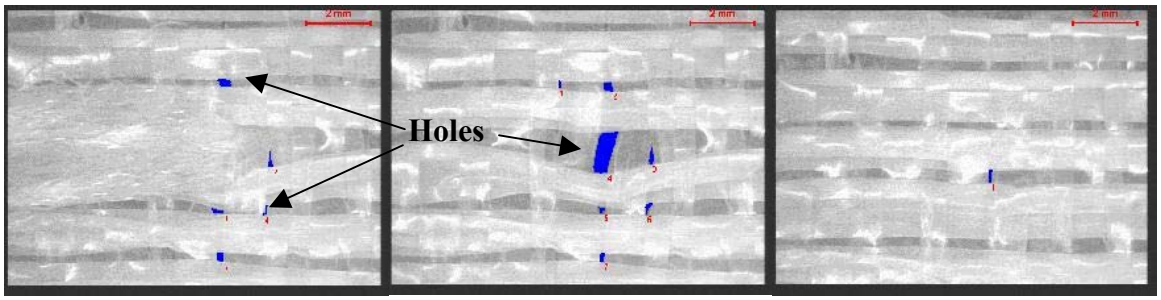

Figure 1: Carpet backing with (a) yarn in backing (b) yarn pulled out of backing and (c) healed backing

In the tufting process, there are times when tufting errors cause the yarn to be removed from the backing and a hole is left as seen in Figure 1b, but as the backing moves through a series of pulleys, the backing undergoes a healing process. Figure 1c gives an example of a backing where this healing process was simulated in the laboratory. This fabric showed a significant decrease in the damaged area after the healing process.

The total area of the holes was observed for 8 different fabrics which vary in yarn size and geometry as well as the fabric pick and end density. The results are shown in Figure 2. This graph shows that backings behaved differently. The fabrics with higher end density had less space in the fabric for the yarns to move back into the undeformed state. As the yarn density decreased, the ability of the fabric to heal increased. Yarn geometry also influenced the ability of the fabric to heal.

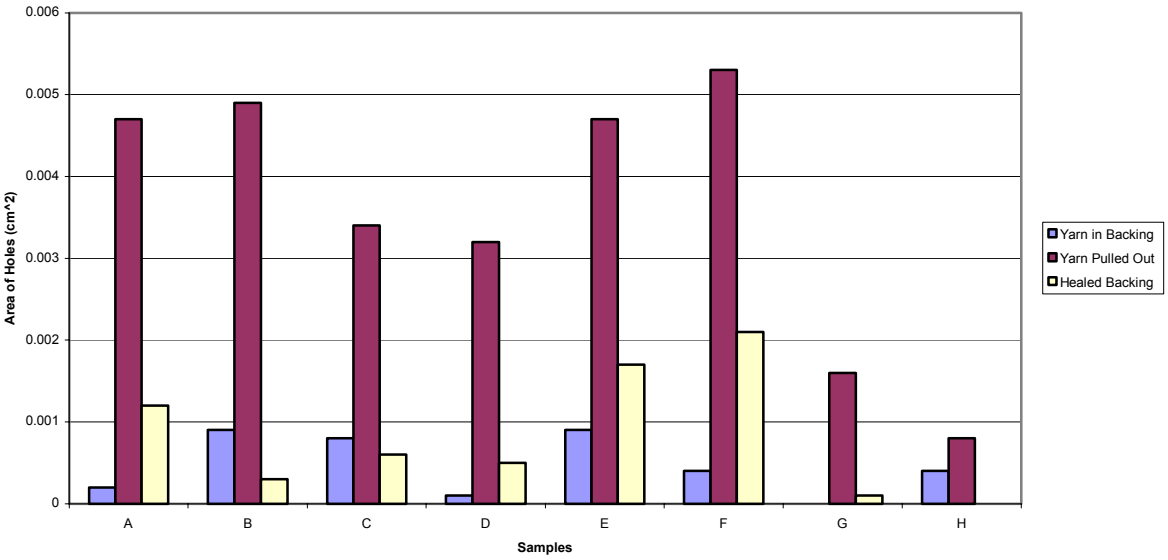

Figure 2: Comparison of Backings (for samples G and H, no holes were detected for the yarn in backing samples and the healed backing samples respectively).

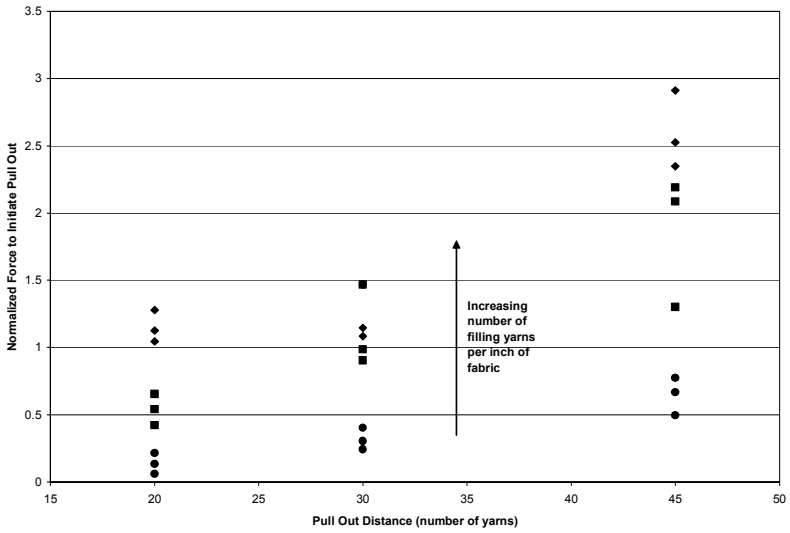

Figure 3: Results of warp yarn pull out tests for fabrics with varying number of filling yarns per inch of fabric

The fabrics also differed in the type of lubricant used on the yarns. To understand the influence of yarn geometry and lubricant, a series of yarn pull out tests were performed. In the test, one yarn was pulled out of the fabric after it was cut a given distance from the edge of the sample. Figure 3 shows the results for the pull out tests. As shown, the force to initiate the yarn pull out increased with fabric pick density. The pull out response also varied with the type of lubricant used.

The ultimate objective is to use this data to develop a mathematical model of the fabric response and therefore enable improvements in the design of new primary carpet backings.

Electrospinning of Poly(Vinyl Alcohol), Copolymers, and Derivatives

E.-R. Kenawy,[1] L. Yao,[1] J. Layman,[1] E. Sanders,[1] R. Kloefkorn,[1,#] G. L. Bowlin,[2] D. G. Simpson[3] and G. E. Wnek[1,*]
Departments of Chemical Engineering[1], Biomedical Engineering[2] and Anatomy[3]
Virginia Commonwealth University, Richmond, Virginia 23284, #NSF REU student
*gewnek@vcu.edu

Introduction

Recent work in our laboratories has focused on applications of electrospinning in medicine, specifically tissue engineering and drug delivery (1-6). In addition to collagen and elastin (3), Figure 1 illustrates polymers that we have successfully electrospun, including the biodegradable polymers poly(glycolic acid) (PGA), poly(lactic acid) (PLA), poly(caprolactone) and copolymers as well as the non-biodegradable but biocompatible materials poly(ethylene-co-vinyl acetate) or EVA, poly(ethylene-co-vinyl alcohol) or EVOH, and poly(vinyl alcohol) or PVA. The latter three polymers will be emphasized here.

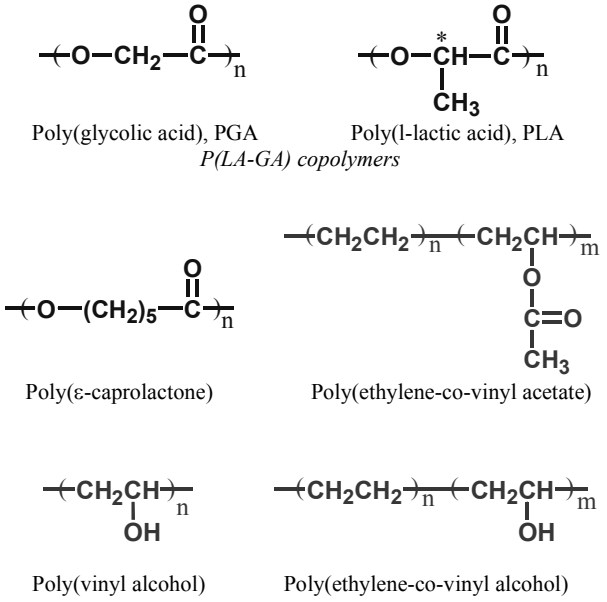

Figure 1. Structures of several polymers electrospun in our laboratories

Experimental

Our general approach involves preparing solutions of the polymer of interest in an appropriate solvent at concentrations suitable for electrospinning. Methylene chloride and chloroform are good solvents for EVA, while warm, 70/30 w/v 2-propanol/water is a good solvent for EVOH. We have found that 100% hydrolyzed PVA is difficult to electrospin from water and believe that this is due to the high surface tension of these solutions. Toward that end, we find that addition of small amount of Triton surfactant affords electrospinning of 100% hydrolyzed PVA from water. The positive output lead of a high voltage supply is attached to a blunt, 18 gauge needle on a syringe mounted on a syringe pump. A grounded target, usually rotating from 500-2,000 rpm, is used to take up the electrospun fibers. The electrospinning set-up is shown schematically in Figure 2.

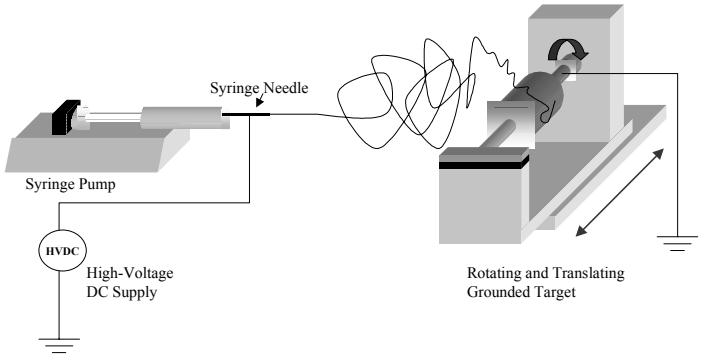

Figure 2. Electrospinning set-up

Results

All polymers studied produced electrospun mats with fiber diameters in the range of 0.1- 10 μm. Figure 3 shows SEMs of EVOH and PVA mats. Poly(ethylene-co-vinyl acetate) was electrospun in the presence of tetracycline hydrochloride, and the kinetics of release of the latter were studied (4). Each system will be discussed in detail in the presentation.

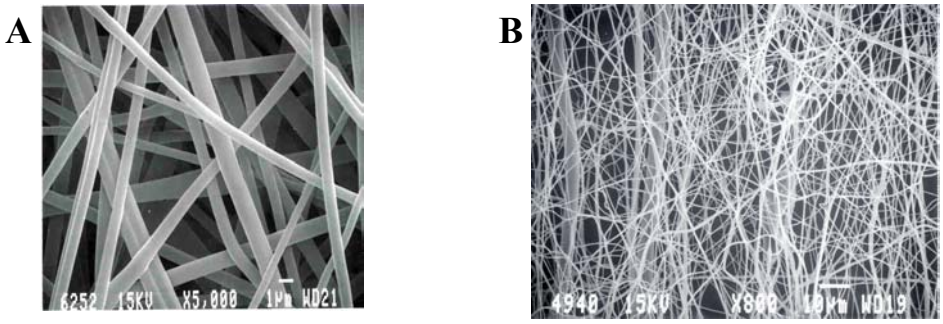

Figure 3. (A) EVOH fibers electrospun from 2-propanol water, 10% polymer by weight; (B) 100% hydrolyzed PVA fibers electrospun from water containing Triton X-100, 10% polymer by weight.

References

1. J. D. Stitzel, K. Pawlowski, G. E. Wnek, D. G. Simpson and G. L. Bowlin, "Arterial Smooth Muscle Cell Proliferation on a Novel Biomimicking, Biodegradable Vascular Graft Scaffold," *J. Biomaterials Applications*, **15**, 1 (2001).
2. E. D. Boland, G. E. Wnek, D. G. Simpson, K. J. Pawlowski and G. L Bowlin, "Tailoring Tissue Engineering Scaffolds by Employing Electrostatic Processing Techniques: A Study of Poly (Glycolic Acid)," *J. Macromol. Sci*., 38: 1231-43 (2001).
3. J. A. Matthews, G. E. Wnek, D. G. Simpson and G. L. Bowlin, "Electrospinning of Collagen Nanofibers," *Biomacromolecules*, **3**, 232-238 (2002).
4. E. R. Kenawy, G. L. Bowlin, K. Mansfield, J. Layman, D. G. Simpson, E. Sanders and G. E. Wnek, "Release of Tetracycline Hydrochloride from Electrospun Poly(Ethylene-co-Vinyl Acetate), Poly(l-Lactic Acid), and a Blend," *J. Contr. Release*, **81**(1,2), 57-64 (2002).
5. G. L. Bowlin, K. J. Pawlowski, J. D. Stitzel, E. Boland, D. G. Simpson, J. B. Fenn and G. E. Wnek, "Electrospinning of Polymer Scaffolds for Tissue Engineering," in Tissue Engineering and Biodegradable Equivalents: Scientific and Clinical Applications, K. Lewandrowsky, D. J. Trantolo, J. D. Gresser, M. J. Yaszemski, D. E. Altobelli and D. L. Wise, Editors, Marcel Dekker, Ch. 9, pp. 165-178 (2002).
6. E. R. Kenawy, J. Layman, G. L. Bowlin, J. Matthews, D. G. Simpson, and G. E. Wnek, "Electrospinning of Poly(Ethylene-co-Vinyl Alcohol) Fibers," *Biomaterials*, submitted.

Supported in part by the U.S. Army, the NSF Partnerships for Innovation Program (subcontract from Virginia Tech), and the NSF Research Experiences for Undergraduates Program

Combination of Electrospinning and Electrostatic Layer-by-Layer Self Assembly: A New Strategy for Sensor Fabrication

Xianyan Wang[1], Young-Gi Kim[1], Christopher Drew[1], Bon-Cheol Ku[1], Jayant Kumar[1*], Lynne A. Samuelson[2*]

[1]Center for Advanced Materials, Departments of Chemistry and Physics, University of Massachusetts Lowell, Lowell, MA 01854, [2]Natick Soldier Center, U.S. Army Soldier & Biological Chemical Command, Natick MA 01760

Introduction

In recent years, considerable attention has been drawn to the studies of fluorescent optical sensors. [1-3] Recently, we reported the use of electrospun membranes as highly responsive fluorescence optical sensors. [4] The sensors fabricated by the electrospinning technique had K_{sv} values 2-3 orders of magnitude higher than that from thin films of the same sensing material. We believe that this was due to the high surface area to volume ratio for electrospun membranes. The average diameter of an electrospun fiber is in the range of 10-1000 nm depending on the polymer and experimental conditions used. The diffusion of the quencher to the interior of the fiber is restricted due to steric hindrance and the polymer-quencher interactions. [1] To address this issue, here we report an extension and further improvement of the sensitivity of these electrospun membranes by combining electrospinning with electrostatic layer-by-layer self-assembly. The fluorescent tag, hydrolyzed poly[2-(3-thienyl)ethanol butoxy carbonyl-methyl urethane] (H-PURET), was electrostatically assembled onto the surface of a cellulose acetate (CA) electrospun nanofibrous membrane. This localization of the fluorescent tag, to the surface of an already high surface area nanofibrous membrane, resulted in significantly improved sensitivities in comparison to similar systems where the fluorescent polymer was distributed throughout the electrospun nanofibers. The fluorescence of these films can be quenched by extremely low concentrations of cationic electron acceptors in aqueous solutions due to the high surface area to volume ratio of the films and efficient interaction between the fluorescent polymer and the quencher. The fabrication and quenching behavior of this sensor to methyl viologen (MV^{2+}) is presented.

Experimental

All chemicals were purchased from Aldrich and used without further purification. Fluorescent conjugated polymer, hydrolyzed poly[2-(3-thienyl)ethanol butoxy carbonyl-methyl urethane] (H-PURET), was synthesized as described previously.[5]

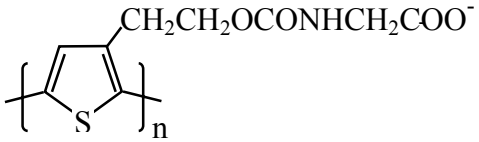

Scheme 1. Structure of H-PURET.

Electrospinning was used to fabricate the nanofibrous membrane as the substrate for electrostatic self-assembly of the sensing polymer. The spin-dope solution consisted of 4.5%, by weight, cellulose acetate (CA) dissolved in DMF. The applied electrospinning voltages used ranged from 15 - 20 kv. The distance between the tip and the glass slide was typically 15 to 20 cm. The collection time was about 90 seconds.

The ELBL self-assembly technique is a process which involves alternate adsorption of anionic and cationic polyelectrolytes on a charged substrate by sequential dipping of the substrate into aqueous polyelectrolyte solutions. The electrospun cellulose acetate (CA) membrane is insoluble in water but carries some negative charge from partial hydrolysis of surface ester groups. Poly(allylamine hydrochloride) (PAH) was used as a polycation and the fluorescent conjugated polymer, H-PURET, was used as a polyanion. The sensors thus made have 5 bilayers of PAH/H-PURET.

UV-visible absorption spectra were recorded using a GBC UV/VIS 916 spectrophotometer. The morphology of the membranes was determined using a scanning electron microscope (Amray 1400). The sensing capabilities of the membranes were determined by measuring the fluorescence quenching with a fluorescence spectrofluorometer

(SLM-AMINCO Model 8100). The electrospun membrane coated glass slide was fixed in a 1 cm quartz cuvette which was filled with the analyte solution. The emission spectra were measured from 560 nm to 600 nm.

Results and Discussion

A scanning electron microscope (SEM) image of an electrospun fiber of Cellulose Acetate with self-assembled layers is shown in Figure 1. The diameters of the fibers were approximately 800 to 1200 nm.

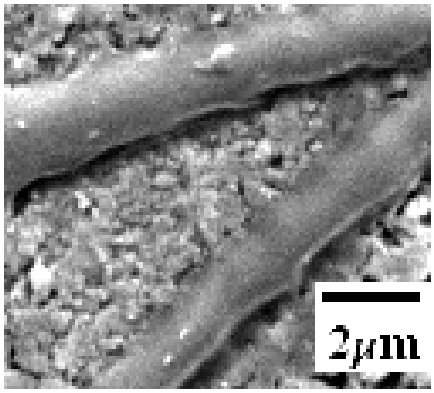

Figure 1. SEM image of the electrospun fiber

The quenching behavior of the sensor to electron deficient analyte MV^{2+} was studied by the measurement of the fluorescence spectra of the sensing film as a function of different concentrations of the quencher. Figure 2 shows the fluorescence spectra of the sensor varying with the concentrations of MV^{2+}. It was found that the fluorescence could be quenched by an extremely low concentration of analyte. As proposed by Swager's group,[6] the fluorescence emission of conjugated polymers can be made to responde to very minute quantities of analytes due to their efficient energy migration. Thus, a single quencher can quench hundreds of repeat units on the conjugated chain. The localization of the fluorescent polymer, to the surface of an already high surface area nanofibrous membrane, resulted in the high efficient fluorescence quenching.

The data obtained by performing a Stern- Volmer analysis in the sensor is shown in Figure 3. A linear plot between quencher concentration and I_0/I is obtained showing a Stern-Volmer relationship. The Stern-Volmer constant of the electrospun films, calculated from the slope of the plot was found to be 3.06×10^7 (M^{-1}). The sensor demonstrated a sensitivity of a few parts per billion and further optimization is expected in future studies.

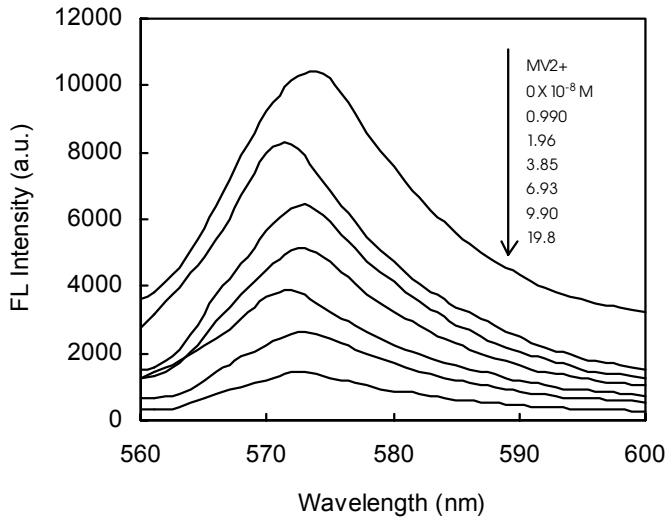

Figure 2. Fluorescence emission spectra of the sensing film with varying MV^{2+} concentration.

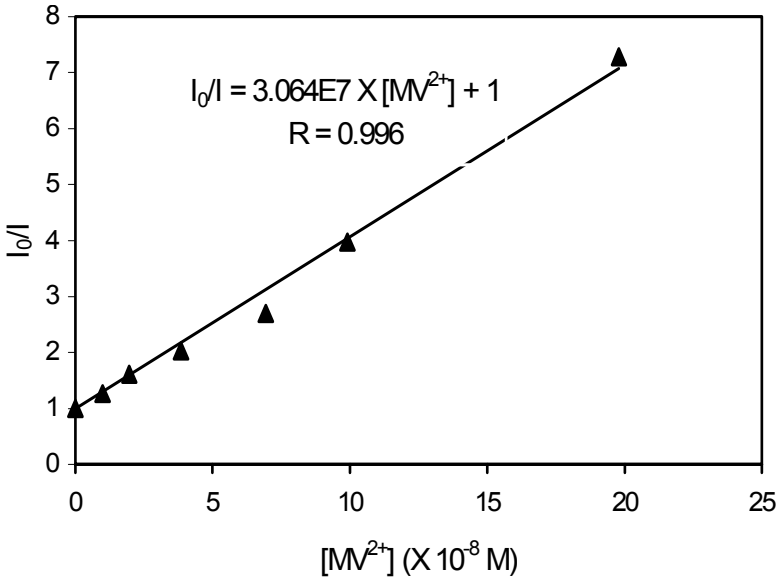

Figure 3. Stern-Volmer plot of the sensing films as a function of different quencher concentration.

Conclusions

We have successfully developed a polymer thin film optical sensor for methyl viologen (MV^{2+}) detection by combining electrospinning and electrostatic layer-by-layer self-assembly techniques for sensor fabrication. The remarkably high sensitivity of the sensor is attributed to the high surface area to volume ratio of the film and efficient interaction between the fluorescent polymer and the quencher. Further efforts will focus on the optimization of the performance of the sensor.

Acknowledgments

Financial support from the U.S. Army is acknowledged. The authors are grateful to Professor L. Chiang for discussions of optical sensing. The authors also recognize Professor C. Sung and Ms. Jamila Shawon for the SEM images and Dr. H. Schreuder-Gibson and Ms. Kris Senecal for advice and assistance with electrospinning. This work is dedicated to Professor S. K. Tripathy.

References

1.Jye-Shane Yang and Timothy M. Swager, *J. Am. Chem. Soc.*, 1998, 120, 11864.
2. Liaohai Chen, Duncan W. Mcbranch, Hsing-Lin Wang, Roger Helgeson, Fred Wudl, and David G. Whitten, *Proc. Natl. Acad. Sci.*, 1999, 96, 12287.
3. Chunhai Fan, Kevin W. Plaxco, and Alan J. Heeger, *J. Am. Chem. Soc.*, 2002, in press.
4. Wang, Xianyan; Drew, Christopher; Lee, Soo-Hyoung; Senecal, Kris J.; Kumar, Jayant; Samuelson, Lynne A., *Journal of Macromolecular Science* **2002** *In Press*.
5. K.G. Chittibabu, S. Balasubramanian, W.H. Kim, A.L. Cholli, J. Kumar and S.K. Tripathy, *J. Macro. Sci.-Pure Appl. Chem*., 1996, A33(9), 1283.
6, D.T. McQuade, A.E. Pullen, T.M. Swager, *Chem. Rev*. 2000, 100, 2537.

Xianyan Wang is a Ph. D. student at the University of Massachusetts Lowell. She received her B.S. and M.S. degrees from Tianjin Institute of Textile Science & Engineering in China. Her research interests focus on polymeric electrically active and optically active materials and their applications. She is a member of American Chemistry Society and Material Research Society.

Improving the Properties of Protective Clothing by Exposing Nanofiber Webs to a One Atmosphere Uniform Glow Discharge Plasma (OAUGDP)

Peter P. Tsai and J. Reece Roth
Textiles and Nonwovens Development Center (TANDEC), University of Tennessee

Nanofiber webs made by the electro-spinning process provide excellent protective properties against biological and aerosol particles, while maintaining a high moisture vapor transmission rate when used for protective clothing. However, the weak web strength of nanofibers presents a problem when they are worn and laundered as garments. The web strength can be improved to a level satisfactory for garments by appropriate post-treatment of the web or by laminating the web to a suitable substrate. This paper will present preliminary results on the web strength as well as the laminating strength of nanofiber webs in which the nanofiber webs or the laminate substrate were exposed to a One Atmosphere Uniform Glow Discharge Plasma (OAUGDP). The mechanisms that affect the web or the laminate strength will be discussed. The effects of the OAUGDP electrode configuration and the plasma parameters will be addressed. The following photograph shows a parallel plate OAUGDP reactor at work.

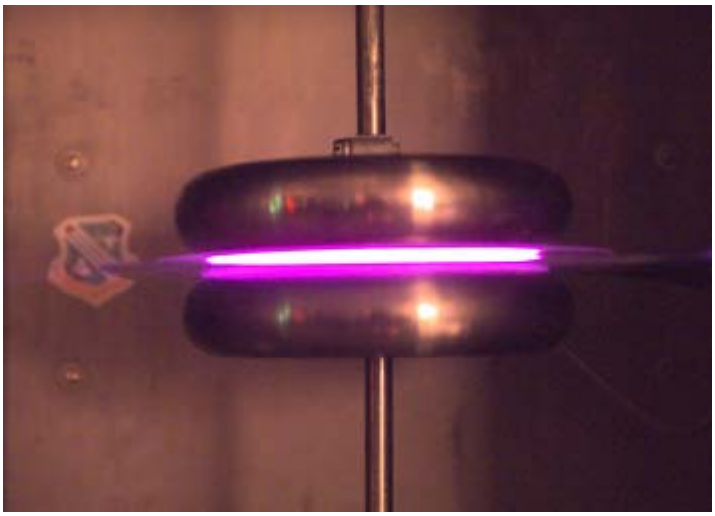

Melt Blown and Spunbond Thermoplastic Polyurethanes for Elastic Military Protective Chemical Liners and for Other Possible Military Applications

Larry C. Wadsworth[1], Youn Eung Lee[1],
Heidi L. Schreuder-Gibson[2], Phillip W. Gibson[2]
[1]Textiles and Nonwovens Development Center (TANDEC), University of Tennessee, 1321 White Avenue, Knoxville, TN 37996-1950; [2]U.S. Army Soldier Biological Chemical Command, Natick, MA 01760-5020

In light of current world events, there is increased interest in development of protective wear that provides protection against chem/bio threats while also being lightweight, comfortable, and affordable. Towards this goal, research first presented at INTC in 2001, with a follow-up paper to be presented at INTC 2002, in which melt blown (MB) thermoplastic polyurethane (TPU) nonwovens were produced and characterized has been accelerated, resulting in notable enhancements in web uniformity, strength, elasticity, controllable air permeability and barrier performance. MB TPU (Noveon Estane® 58245 and Estane® 58280) webs have been produced on the 20-inch MB line at TANDEC with nominal basis weights ranging from 29 to 494 g/m^2. Surprisingly strong MB webs with good cover have been produced with Estane 58280. Furthermore, progress has been made in producing spunbond (SB) TPUs on the 1.0 meter Reicofil 2 line at TANDEC, for applications requiring even greater strength, combined with isotropic elasticity. The SB TPUs are being evaluated for possible stand alone applications or as laminates of MB and SB TPUs for maximum strength and barrier performance. All fabrics are being tested for basis weight, thickness, air permeability, and tearing and tensile strength.

Quality Control in Manufacturing of Electrospun Nanofiber Composites

Dmitry M. Luzhansky
Donaldson Company, Inc., Minneapolis, Minnesota, USA

The extremely small fiber size and low mass of nanofiber composites renders quality control measurements very difficult. Most of the commercially available contact measurement equipment is not able to work with the nanofiber composite without altering its characteristics. Generally non-contacting optical methods suffer because the wavelength of the light used is greater than the diameter of the nanofibers and non-contact Gamma or Beta gauges lack the necessary resolution. Research methods such as Scanning Electron Microscopy (SEM) are not practical in a production setting. Large scale production of nanofiber composites requires unique quality control (QC) methods.

As Donaldson Company's nanofiber production has increased to over 10,000 m^2 per day during the last 20 years, QC methods have been developed to address these needs. Four evaluation tools that have been developed for commercial production of nanofibers will be described. These evaluation tools focus on: uniformity of nanofiber distribution, fiber size distribution, durability of fiber layer in the composite, and environmental resistance.

Uniformity of nanofibers' distribution

The layer of nanofibers in the composite has low solidity, low thickness, is extremely light weight, and has small fiber size. Conventional on-line methods employing different parts of electro-magnetic spectra (b-radiation, optical methods) measures have not worked.

To control the process and product quality on-line web filtration efficiency test method and on-line efficiency monitor (OEM) were invented. The test system uses two conventional laser particle counters with the addition of a specialized sampling head. The sampling head incorporates an air curtain effect to allow efficiency measurements at speeds up to several hundred feet per minute. This test method can be applied to nanofiber web development, manufacturing process development, and production process control. The details of the OEM and operating procedure are described elsewhere [1,2] .

The nanofiber layer accounts for most of the filtration efficiency in the nanofiber composite. Results of measurements describe the quality by assessing the uniformity of the nanofiber layer in the machine and cross machine directions.

Automated Fiber Sizing

To use the OEM as a process control monitor, one must assume that the mean fiber size and fiber size distribution are controlled within a limited range. Routine sampling and measurement of fiber size and fiber size distribution is done using SEM. Measuring nanofiber diameters usually consists of manually comparing the diameter of fibers in a photomicrograph to a known scale. The process is very time consuming and operator consistency and fatigue can be problems. Automating the fiber sizing is a natural solution to the problem.

There are several commercially available fiber sizing software packages. Many of them were analyzed but didn't meet our requirements. The automated fiber sizing method that is used here is based on a proprietary algorithm.

A computer program determines desired size and eliminates undesirable details from SEM image. On the next step it converts the image to a binary image using a gray scale function. After referencing the calibration bar from the SEM image, the program performs measurements and calculations. All fiber diameter lengths are recorded and a running histogram is generated. The process that used to take hours of painstaking measurements can be completed in seconds.

Accelerated Environmental Resistance Test

Many nanofiber composites used in filtration are exposed to hot and humid environments. Therefore, fiber resistance to such environments becomes a vital element of their performance. To perform such analysis we measure the filtration efficiency of the nanofiber filter material using ASTM test method F1215-89 [3], soak it in hot water for 5 minutes, dry, and measure the efficiency again. Likewise we can measure the resistance of composites to aggressive systems such as solvent vapors, oils, etc.

DL bending tester [4]

Understanding strain-stress characteristics is important in understanding the performance of a nanofiber composite due to dynamic stress. Due to the small size of fibers and extremely low weight of the layer, known methods do not give useful results.

The DL bending tester was developed to study strain properties and failure mechanisms of nanofibers applied to the surface of another media. A sample is secured in the tester and positioned in the optical microscope. A motor then bends and extends the sample around a cylinder with known diameter. During the movement the sample is observed on the monitor connected to the camera attached to the microscope while measuring the angle. The movement is observed in the structure of substrate, operator records what kind of movement occurred and continues stretch until the first destruction the nanofiber layer. Comparison of the angle for different composites gives the measure of stability of the structure. Angle can be recalculated into the strain measure:

$$\varepsilon = \frac{4\pi\alpha R}{360 L_0}$$

α - angle of stretch; R – cylinder diameter; L0 – initial length of the specimen.

Conclusion

Large scale production of nanofiber composites requires quality and process control. Critical parameters include the uniformity of nanofiber distribution, fiber size distribution, durability of fiber layer in the composite, and environmental resistance. Fundamentally new approaches are required due to the low solidity, low thickness, extremely low weight, and small fiber size. The methods and instruments described have shown their relevance and reliability.

1. M. A. Gogins and J. W. Schaefer, “Variability of Filter Media Efficiency”. In: Advances in Filtration and Separation Technology, vol. 8. American Filtration and Separations Society. Chicago, Illinois, 1994.
2. Gogins M. US Patent 5,203,201, assigned to Donaldson Company, Dec. 20, 1991.
3. Standard Test Method for Determining the Initial Efficiency of a Flatsheet Filter Medium in an Airflow Using Latex Spheres. ASTM F1215-89. ASTM International. Philadelphia, 1989.
4. Effort sponsored by the Natick Soldier Center, Soldier, Biological and Chemical Command, USA, under cooperative agreement number DAAD16-01-3-0001. The U.S. Government is authorized to reproduce and distribute reprints for Governmental purposes notwithstanding any copyright notation thereon. The views and conclusions contained herein are those of the authors and should not be interpreted as necessarily representing the official policies or endorsements, either expressed or implied, of the Natick Soldier Center or the U.S. Government.

Dmitry M. Luzhansky.
dmitryl@corptech.donaldson.com
Ph.: 952-887-3765

Currently Principal Engineer at Donaldson Company, Inc. B.S. in Thermal Engineering from Tashkent Polytechnic University, 1979. PhD in Chemical Engineering from Tashkent Textile Institute, 1986. Experience includes research and development in the area of heat and mass transfer in fiber spinning and non-woven webs. Published 35 articles and holds 15 patents.

Predicting Performance of Protective Clothing Systems

James J. Barry, Roger W. Hill
Creare Incorporated, P.O. Box 71, Etna Road, Hanover, NH 03755

Protective clothing provides laboratory and hazardous materials workers, fire fighters, military personnel, and others with the means to control their exposure to chemicals, biological materials, and heat sources. Depending on the specific application, the textile materials used in protective clothing must provide high performance in a number of areas, including impermeability to hazardous chemicals, breathability, light weight, low cost, and ruggedness. Models based on computational fluid dynamics (CFD) have been developed to predict the performance of protective clothing. Such models complement testing by enabling property data from tests of textile swatches to be used in predictions of integrated multilayer garments under varying environmental conditions.

The modeling software computes the diffusive and convective transport of heat and gases/vapors; capillary transport of liquids; vapor and liquid sorption phenomena and phase change; and the variable properties of the various clothing layers. It can also model the effects of sweating and humidity transport on the thermal stress imposed on the wearer of the clothing. The basis for our models is the FLUENT code, a leading commercial CFD software package. To simulate the physics of transport in textiles, new models and capabilities have been added via the software's "user-defined function" interface:

- Vapor phase transport (permeability)
- Liquid phase transport (wicking)
- Fabric property dependence on moisture content
- Vapor/liquid phase change (evaporation/condensation)
- Sorption to fabric fibers

Using the software with the additional fabric capabilities, two- and three-dimensional representations of clothed humans are built and used to compute the transport of chemical agents (e.g., deposition, transfer through clothing materials) and the thermal comfort properties (e.g., diffusive and convective heat transfer, moisture transport, and phase change at various workloads and sweating rates) both for steady-state and time-varying situations. Multilayer clothing can be modeled including the presence of air gaps. Properties of the textile materials (woven or nonwoven) are represented on a volume-average basis in each computational cell in the fabric layers making up the clothing.

Comparisons with experimental data show good agreement in predicting the effects of fiber swell due to transients in humidity, and the models have been used to predict the sensitivity of clothing performance to material properties such as permeability under varying environmental conditions. Applications of the models include analysis of chemical protective garment design for military and emergency response personnel, comparisons of thermally protective materials for steam or fire protection, and evaluation of textile material test data. The models also have potential broad application in design of outdoor clothing and other woven/nonwoven products.

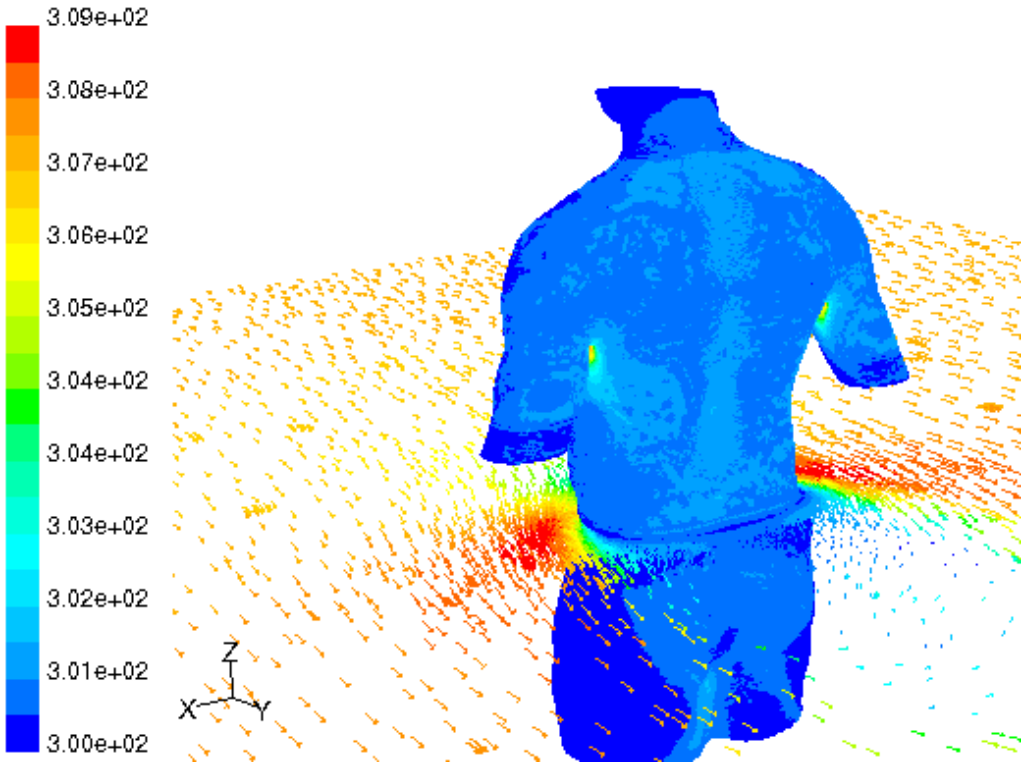

Figure 1. Model of Torso Clad in T-Shirt: 5 mph Wind from Front at 27 C and 70% Humidity, Resting Workload, Temperature Contours on Surface, Air Velocity Field Shown at Waist-Level Slice

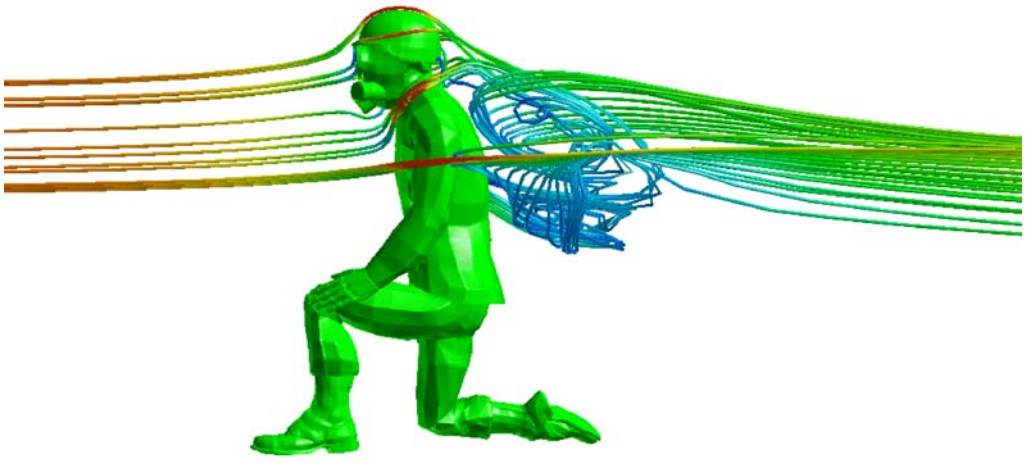

Figure 2. External Flowfield Over Soldier: Wind Speed 10 mph

Application of Electrospinning to the Reinforcement and Fabrication of Gossamer Space Structures

Kevin White, John Lennhoff, Edward Salley, Karen Jayne
Physical Sciences Inc., 20 New England Business Center, Andover, MA 01810

Physical Sciences Inc. (PSI) has demonstrated the application of the electrospinning technique to fabrication and reinforcement of Gossamer structures (thin, lightweight membranes for space applications). PSI has shown the ability to apply electrospun rip-stop patterns to traditional Gossamer films through a newly developed technique referred to as *Patterned Electrospinning*. In addition we have developed techniques intended for the on-orbit production of electrospun Gossamer membranes based on traditional melt electrospinning techniques. The results of these NASA funded efforts will be presented.

The common goal of Gossamer structures is function at reduced mass. When dealing with large area polymeric films, mass reduction is obtained by decreasing the thickness of the film. The obvious trade off in this situation is a concurrent reduction in the strength of the film, increasing the probability of damage during deployment or during operation (by micro-meteorites for example). Substantial increase in tear strength with negligible increase in mass can be engineered into a film through the addition of rip-stop features. Conventional thick film rip-stop reinforcement is accomplished by imbedding fibers in the film that terminate film tear propagation. This approach is difficult to execute for Gossamer films because conventional fiber diameters are significantly larger (>15 μm) than the films, adversely impacting film modulus. Figure 1 shows a schematic of conventional and electrospun fiber reinforcement of Gossamer films. Patterned Electrospun reinforcing Gossamer films with nanofibers have been shown in our labs to be an effective way to provide rip-stop without weight or modulus penalty.

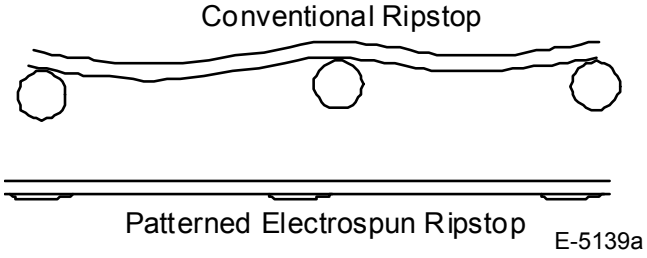

Figure 9. Schematic comparison of large diameter rip stop fibers with an electrospun rip stop deposit.

PSI has developed a variation of the electrospinning technique termed Patterned Electrospinning which was used to produce rip-stop features on space durable polymer films suitable for Gossamer structures. Patterned Electrospinning utilizes a grounded template, in a user specified pattern, that promotes selective electrospinning deposition and, under proper conditions, sharp reproduction of the template (see Figure 2). When an insulating thin film (such as those used in Gossamer structures) is placed between the template and the spinning nozzle, deposition occurs on its surface. Templates from complex grid patterns to simple spots have been demonstrated in our labs. This presentation will demonstrate the adaptation of Patterned Electrospinning to the rip-stop problem with special emphasis on using basic electrospinning knowledge to solve complex problems.

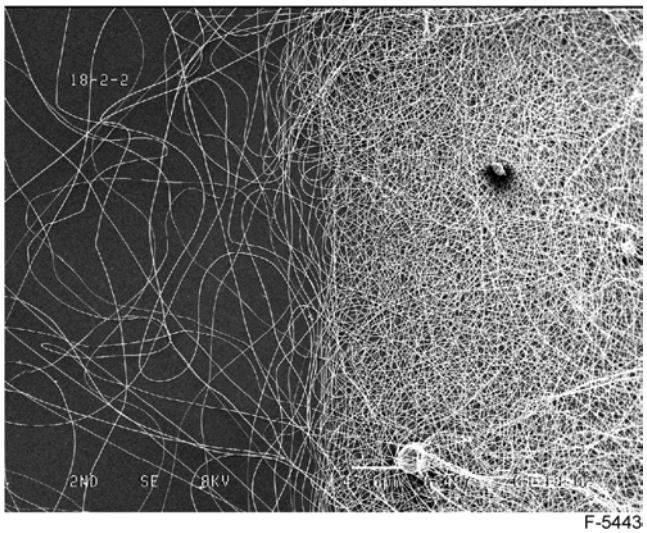

Figure 10. Scanning Electron Microscope image at the edge of a Patterned Electrospun reinforcement deposit showing selective deposition of fibers over the template.
The sample is CP-1 fibers on CP-1 film.

The SRS Technologies (Huntsville, AL) space durable polymer CP-1 (Colorless Polyimide 1) was electrospun as rip-stop reinforcement on thin films of the same from various solvent combinations of dimethylformamide and N-methylpyrrolidone. The parameter space investigated (with the goal of optimizing the tear resistance of the rip-stop deposit) included solvent composition, spinning distance, the effects of static charge, field strength, polymer delivery rate, relative humidity and deposition areal density. Primary analysis tools included scanning electron microscopy and tensile testing. Increases in tear strength up to 7 times the associated film strength have been demonstrated.

The need for thin polymeric films with low areal densities for ultra-lightweight space propulsion is at the forefront of reduced cost space exploration. This propulsion method, termed solar sailing, utilizes a large area (thousands of square meters) reflective membrane to harness the energy of incident photons for forward motion. The acceleration (and therefore velocity) is determined by the reflectivity of the surface and the areal density of the material, with high reflectivity and low areal density being desired. Current state of the art solar sail is aluminized, 0.2 mil Mylar which has an areal density of 6.5 g/m^2 and reflectivity in the visible spectrum of 98%.

PSI has developed a method, suitable for scale-up to large areas, for electrospinning membranes from melt processable, space qualified polymers. These membranes have been shown to exhibit reflectivity in excess of 80% at areal densities of 2.5 g/m^2. These data equate to a two fold improvement in acceleration over state of the art from a film that is more durable and can be fabricated on orbit. The SRS Technologies space durable polymer CP-2 (Colorless Polyimide 2) was electrospun from dimethylformamide (DMF) solution on a variety of substrates to facilitate evaluation by several methods. The non-woven deposits were optimized for areal density, reflectivity, and strength through manipulation of fiber diameter, and deposition time. Ultraviolet-visible reflectance spectroscopy, scanning electron microscopy and tensile testing were used to quantify the optimization progress. These results will be discussed.

Presenting Author:

Kevin White
Physical Sciences Inc.
20 New England Business Center
Andover, MA 01810
Tel.: (978) 689-3232
Fax: (978) 687-7211
e-mail: kwhite@psicorp.com
http://www.psicorp.com

Kevin White received a bachelors degree in chemistry from Michigan State University and a Ph.D. in electrochemistry from the University of Wyoming. While at the University of Wyoming Dr. White participated in an international scholar exchange with the Universidade de Sao Paulo, Brazil and was honored as a NASA fellow. As a Principal Scientist at Physical Sciences Inc., Dr. White is a member of the Materials Science group and focuses on novel applications for electrospinning and lithium ion battery cathode development. Dr. White is a member of the Materials Research Society and the Electrochemical Society.

Nanofiber Garlands of Polycaprolactone by Electrospinning

D.H. Reneker [1], W. Kataphinan [1], A. Theron [2], E. Zussman [2], and A.L. Yarin [2]
[1]Department of Polymer Science, The University of Akron, Akron, Ohio;
[2]Department of Mechanical Engineering, The Technion, Haifa, Israel

Abstract

Over a period of time, the typical path of a single jet of polymer solution in the electrospinning process follows the nearly straight electric field lines for a certain distance away from the tip, and then develops a series of electrically driven bending instabilities that cause the path of the jet to explore a cone shaped envelope as the jet elongates and dries into a nanofiber. The multitudes of open loops that are formed are rarely observed to come into contact with each other until the dry nanofiber is collected at the end of the process.

A new phenomenon is reported in this paper. Electrospinning a solution of polycaprolactone in acetone caused the dramatic appearance of a fluffy, columnar network of fibers that moved slowly in large loops and long curves. The name "garland" was given to the columnar network.

Open loops of the single jet came into contact just after the onset of the bending instability and then merged into a cross-linked network that created and maintained the garland. Contacts between loops occurred when the plane of some of the leading loops of the jet rotated around a radius of the loop. Then a small following loop, expanding in a different plane, intersected a leading loop that was as many as several turns ahead. Mechanical forces overcame the repulsive forces from the charge carried by the jet, the open loops made contact in flight and merged at the contact point, to form closed loops.

The closed loops constrained the motion to form a fluffy network that stretched and became a long, roughly cylindrical column a few millimeters in diameter. This garland never traveled outside a conical envelope similar to, but larger than, the conical envelope associated with the bending instability of a single jet.

Biographical sketch

Darrell Reneker has a B.Sc. in Electrical Engineering from Iowa State University and a Ph. D. in Physics from the University of Chicago (1959). He was a research physicist at Dupont for one decade, a scientist and manager at the National Institutes of Science and Technology for two decades, and since 1989 has been a Professor of Polymer Science at the University of Akron. For three years, he was the executive secretary of the Interagency Committee on Materials in the White House Science Office. His research interests include nanotechnology, morphology, electron microscopy, crystallographic defects in polymer crystals, polymer nanofibers, electrospinning, and the electronic, photonic, and ionic properties of polymers.